Title

Application of enhanced methods of microbial assessment in piped drinking water, wastewater, and recycled water systems

Author

Kennedy, Lauren Catherine

Publication Date

2021

Peer reviewed|Thesis/dissertation

Application of enhanced methods of microbial assessment in piped drinking water, wastewater, and recycled water systems

by

Lauren Catherine Kennedy

A dissertation submitted in partial satisfaction of the

requirements for the degree of

Doctor of Philosophy

in

Engineering- Civil and Environmental Engineering

in the

Graduate Division

of the

University of California, Berkeley

Committee in charge:

Professor Kara Nelson, Chair
Professor Lisa Alvarez-Cohen
Professor Jill Banfield

Spring 2021

Application of enhanced methods of microbial assessment in piped drinking water, wastewater, and recycled water systems

Abstract

Application of enhanced methods of microbial assessment in piped drinking water, wastewater, and recycled water systems

by

Lauren Catherine Kennedy

Doctor of Philosophy in Engineering- Civil and Environmental Engineering

University of California, Berkeley

Professor Kara Nelson, Chair

A primary goal of microbial monitoring in piped water systems is to ensure an acceptably low risk of ingesting enteric pathogens from contact with treated water. Microbial monitoring strategies in piped water systems are generally based on the type of water being treated and the intended use, but strategies that are developed with a narrow focus on each type of water system could disincentivize some beneficial monitoring targets. For example, raw wastewater contains genetic material from pathogens that does not pose a risk public health from the perspective of water treatment but could be monitored to assess the disease burden in the contributing population (e.g., severe acute respiratory syndrome coronavirus 2; SARS-CoV-2). Developing integrated microbial monitoring strategies in water systems could produce data that are beneficial for drinking water providers, wastewater treatment service providers, and public health departments.

The overall goal of this work was to apply enhanced methods of microbial assessment in piped water systems and to identify integrated microbial monitoring strategies with the potential to benefit public health. Enhanced methods of microbial assessment include methods to assess microbial abundance (e.g., intact cell counts, total cell counts, intracellular ATP, and total ATP), microbial community composition (e.g., 16S rRNA gene amplicon sequencing), and specific microbial targets (e.g., quantitative polymerase chain reaction; qPCR). Applications for enhanced microbial assessment include (i) routine assessment such as monitoring impacts of local-scale water quality conditions on microbial abundance in drinking water distribution systems (e.g., disinfectant concentration); (ii.) diagnostic or preventative assessment such as monitoring impacts of system-scale changes on microbial communities in drinking water distribution systems (e.g., transition to direct potable reuse); and (iii) public health surveillance such as monitoring pathogens in community sewersheds during disease outbreaks.

First, five measures of microbial abundance were applied in six chlorinated and chlorami-

nated drinking water distribution systems and enhanced methods of microbial assessment (i.e., total and intact cell counts and total and intracellular ATP concentrations), were compared with heterotrophic plate counts. Flow cytometry-based intact cell counts were the least variable (intraassay coefficient of variation = 16.9%) and most quantifiable (97.6%) of the viability assays tested. Therefore, intact cell counts may be promising monitoring targets for diagnostic or preventative monitoring in drinking water distribution systems and in low microbial abundance conditions (i.e., monitoring advanced-treated wastewater). In one chloraminated distribution system, a generalized linear mixed model was used to asssess the effect of physicochemical water quality conditions on intact cell counts, and total chlorine had the greatest inverse effect on intact cells with a greater positive effect of temperature at lower levels of total chlorine.

Next, preventative monitoring of simulated distribution systems was completed during augmentation of conventional drinking water with advanced-treated wastewater. The five pipe loop rigs used to simulate this event were sampled over 21 weeks using 16S rRNA gene amplicon sequencing and total cell counts. While this simulation study may not accurately represent a full-scale direct potable reuse system, the experiments demonstrate the enhanced microbial monitoring that could be completed during full-scale implementation. It was observed that despite advanced-treated wastewater having high water quality (e.g., low concentrations of organic carbon and nutrients) and low cell counts, microorganisms were seeded and grew in reverse osmosis permeate. Furthermore, the pipe loop bulk water and biofilm bacterial community profiles shifted with introduction of the advanced-feedwater that had been seeded with microorganisms and nutrients.

Finally, the value of wastewater as a source of information to assess the health of the contributing population was investigated. Raw wastewater was collected from five locations in the San Francisco Bay Area during the coronavirus infectious disease 2019 (COVID-19) pandemic. For these samples, SARS-CoV-2 wastewater testing results were compared to geocoded COVID-19 clinical testing results. Findings include that SARS-CoV-2 was reliably detected (95% positivity) in frozen wastewater samples when reported daily new COVID-19 cases were 2.4 or more per 100,000 people. Additionally, spatio-temporal trends in wastewater SARS-CoV-2 signal and daily per capita COVID-19 cases were generally consistent with each other, with a few exceptions that could indicate clinical undertesting at some locations.

This research is useful to academics as well as practitioners considering or implementing management practices for integrated water systems. This dissertation includes one of very few studies on drinking water distribution system microbial impacts from direct potable reuse, which also provides recommendations for future microbial assessments in simulated direct potable reuse distribution systems. More work is needed applying DNA sequencing methods in full-scale systems as part of diagnostic or preventative monitoring and applying integrated monitoring methods in full-scale water systems. Additionally, while SARS-CoV-2 wastewater testing is a promising public health surveillance strategy, it is a relatively new application that requires more research and development. With these advancements

to the field of wastewater-based epidemiology, pathogen targets in raw wastewater could be expanded to include enteric pathogens. Particularly as more full-scale direct potable reuse systems come online, these methods with other public health surveillance campaigns can be used to verify that consumption of advanced-treated wastewater does not result in transmission of pathogens back to the contributing population.

Contents

List of Figures

List of Tables

Acknowledgments

The work in this dissertation could not have been possible without the academic and emotional support from my mentors, peers, family, and friends. First, I am grateful to my advisor and committee chair, Prof. Kara Nelson. Thank you for showing me the ropes of academia, encouraging me to follow my scientific interests, as well as holding steadfast, high standards and an optimistic outlook through it all. I thank the other members of my committee, Prof. Jill Banfield and Prof. Lisa Alvarez-Cohen, for asking difficult and constructive questions early on, providing keen insights that made my dissertation research more robust, and staying supportive as my dissertation work adapted during the COVID-19 pandemic. Also, I am grateful to the mentors I had as an undergraduate student for their academic and professional guidance: Prof. Carlos Martinez, Prof. Chad Jafvert, Prof. Larry Nies, Dr. Lindsey Payne, Prof. Kris McNeill, Dr. Chiheng Chu, Prof. Scot Martin, and Dr. Adam Bateman.

I am deeply grateful to my co-authors and Nelson-lab mates: Dr. Scott Miller, Dr. Rose Kantor, Hannah Greenwald, and Adrian Hinkle. These projects have truly been epic, and I am so lucky to have teamed up with you for this odyssey! I would also like to thank the other graduate students and postdocs who I overlapped with in the environmental engineering program for the academic, professional, as well as much broader discussions: especially, Dr. Aidan Cecchetti, Casey Finnerty, Emily Cook, Dr. Erica Fuhrmeister, Ileana Wald, Karina Chavarria, Dr. Kevin Orner, Kim Huynh, Liya Weldegebriel, Luis Anaya, Soliver Fusi, and Prof. Will Tarpeh. I wish to acknowledge the stellar undergraduate students who helped with sample collection, lab work, and methods development and are now tackling their own research projects in graduate school: Lorelay Mendoza and Mira Chaplin.

I would like to express my gratitude to my family. My partner, Obed Hernández-Gómez has provided me with so much love and support throughout this process. In particular, thank you for your unwavering ability to make me laugh, the late night chats about your or my latest idea, and the urban foraging random walks. I am so excited for our future together! I am grateful to my parents for encouraging me to take the opportunities they did not have: James, Donna, and Steve. I want to thank the Tratar family (Terri, John, and Jon), my siblings (Jacob and Linzy), and my grandparents (Mary, Dale, Lyra, and James) for providing me with unwavering support and encouragement. To the Hernández family: thank you for lovingly accepting me into your family.

Finally, the research in this dissertation was possible because of utility and consulting partners and financial support from a Civil and Environmental Engineering Departmental Fellowship, a National Science Foundation Graduate Research Fellowship, the Engineering Research Center for Reinventing the Nation's Urban Water Infrastructure (ReNUWIt), and American Water Works Association scholarships.

Chapter 1

Introduction

1.1 An integrated approach to microbial monitoring in piped water systems

Society is continuing to face the consequences of increased human activity, including climate change and biodiversity loss [1]. Environmental Engineering and Science is a field actively evolving to address these challenges using integrated solutions from multiple fields of expertise [2]. This approach is exemplified through the concept of one water for which all forms of water (e.g., wastewater, stormwater, irrigation water, drinking water, etc.) are managed together [2, 3, 4]. The one water concept can help cities become more sustainable by developing integrated urban water management for water that is linked through the same water cycle [4]. As water management becomes more integrated, the microbial monitoring strategies applied in water systems will also require integration. For example, ingesting pathogens from wastewater represents the greatest microbial risk of drinking water to public health [5], but wastewater can also serve as a supplemental water source [6, 7, 8, 9] and a valuable tool for understanding and mitigating the circulation of pathogens in the contributing population [10]. Designing integrated microbial monitoring strategies could benefit public health and make the resulting data of greater use to both utilities and public health departments than current monitoring strategies alone Figure 1.1.

Microbial monitoring in piped drinking water systems is one of multiple barriers designed to minimize the risk of ingesting feces or water contaminated by fecal pollution [11]. Specific microorganisms that indicate fecal contamination could have occurred are monitored, which ideally are similar in behavior to pathogens of concern, are sourced from feces, are relatively easy to detect, and are not pathogenic themselves [12, 11]. Usually, only bacteria are regulated, monitored, and expected to result in non-detects, such as total coliform bacteria and *Escherichia coli* [5, 12, 13, 14, 11, 15]. While monitoring these indicator microorganisms is necessary to diminish the risk of fecal pathogens to public health, relying on a microbial monitoring strategy that only includes fecal indicator bacteria has several disadvantages. First, results are limited to whether fecal contamination could have occurred, and

for that reason, positives should be extremely rare because multiple barriers of protection are in place to prevent fecal contamination of drinking water. Additionally, assessment of fecal contamination potential does not cover environmental opportunistic pathogens that are found in drinking water (e.g., non-tuberculous mycobacteria [16]) or common microbial issues in drinking water distribution systems (e.g., microbially-induced corrosion [17, 18, 19, 20] or nitrification [21, 22, 20, 23]). Furthermore, fecal indicator bacteria in particular are imperfect representations of enteric pathogens because they are readily susceptible to disinfectants [24], can have non-fecal origins [25, 11, 15], and do not always correlate with pathogens of concern [26, 27].

Microbial monitoring strategies that integrate drinking water quality targets and broader health outcome targets could increase the value and performance of centralized drinking water and wastewater treatment systems. In drinking water, monitoring could be expanded to include non-enteric microorganisms that are more commonly present in drinking water distribution systems, including opportunistic pathogens and broad measures of microbial abundance. Similarly, raw municipal wastewater contains information not commonly monitored that could be relevant to public health. Monitoring pathogens of concern in raw wastewater could help characteize the variation in concentration expected for a given sewershed, and, for potable reuse applications in particular, ensure that the risk of infection from finished water is sufficiently low [28, 6, 29, 30]. Additionally, through wastewater-based epidemiology, wastewater can be used to monitor the sewersheds of communities for pathogens that are shed in feces [10] but do not necessairily present a safety concern from a wastewater treatment performance perspective, such as severe acute respiratory syndrome coronavirus 2 (SARS-CoV-2) [31, 32, 33, 34, 35, 36]. Particularly, in the midst of the coronavirus infectious disease 2019 (COVID-19) pandemic, the applicability of wastewater-based epidemiology to assist with pandemic response has become of great interest to the environmental engineering community [37]. Thus, integrating enhanced monitoring methods in centralized water treatment systems could improve both water treatment performance and public health in communities.

In this introduction, foundational concepts for the research presented in this dissertation are summarized. First, microbial communities in disinfected drinking water systems and their importance for these systems are discussed. Next, wastewater is presented as a resource in two ways: as a source of drinking water and as a resource for public health surveillance. Afterward, strategies for enhanced assessment of microorganisms in disinfected drinking water systems and in raw wastewater are summarized. Finally, the objectives of the research in this dissertation are presented.

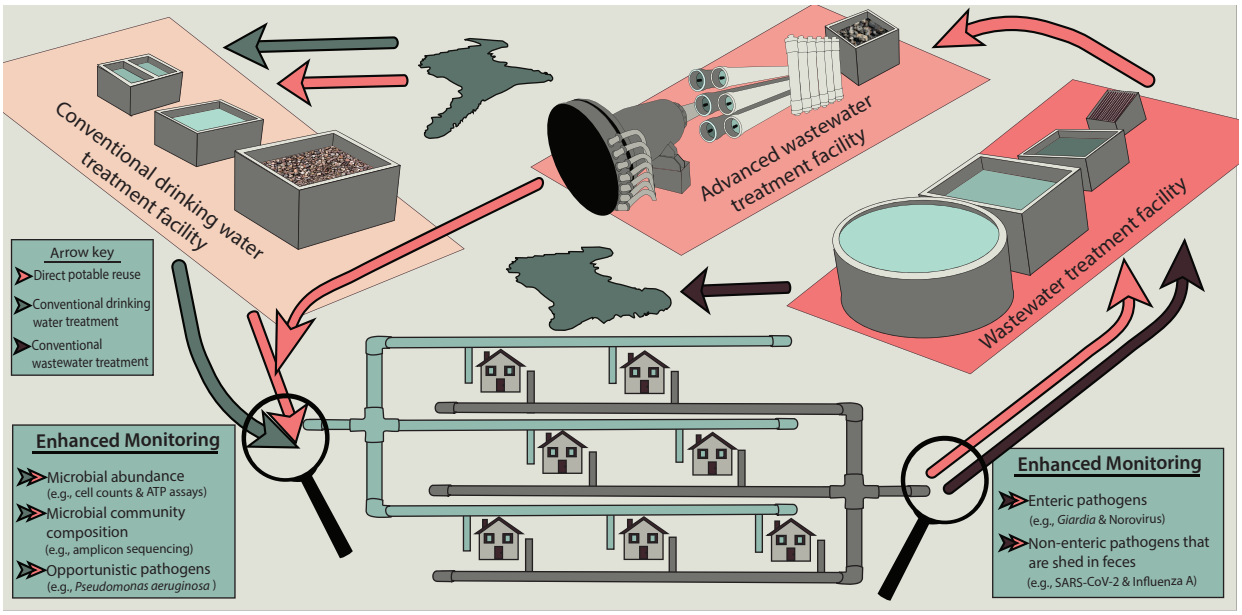

Figure 1.1: Examples of enhanced methods of microbial assessment in drinking water (left) and wastewater (right) systems that together depict an integrated microbial monitoring strategy for the direct potable reuse system shown.

1.2 Microbial communities in disinfected drinking water distribution systems and risks to public health

Drinking water distribution systems host microbial communities that respond to physicochemical water quality changes and infrastructural changes, such as upgraded treatment systems. Large shifts in the abundance of microorganisms or composition of microbial communities do not inherently pose risks to public health, but may signal that water is of low quality. Notably, these shifts are often not detected by conventional monitoring methods [38, 39, 40]. Currently, only a subset of microorganisms present in drinking water distribution systems is monitored in the United States (i.e. total coliform bacteria, *Escherichia coli*, and sometimes heterotrophic plate counts; HPC). Thus, physicochemical parameters are applied to assess and control threats to water quality from microorganisms not commonly monitored. For example, to control and prevent nitrification in chloraminated drinking water systems, drinking water providers have been advised to monitor disinfectant residuals, pH, nitrite, ammonia, and nitrate [41]. However, accessible physicochemical water quality parameters cannot always be used to preemptively detect microbial water quality issues arising from specific microorganisms (e.g., nitrification [21, 22]). Furthermore, when repetitive microbial issues arise in drinking water distribution systems, a deeper understanding of the micro-

bial communities associated with the issue may elucidate new approaches for rectification. Research on microbial water quality assessment techniques is needed to diversify microbial monitoring strategies for drinking water providers, to explore drinking water distribution system issues caused by commonly undetected microorganisms, and to confirm that changes to source water quality will not adversely affect finished drinking water quality.

In particular, the origin of and the selection pressures on microbial communities in drinking water distribution system bulk water have implications for engineering applications. Researchers have found evidence that microorganisms in drinking water distribution systems originate from source water [42, 43, 44, 45] and from intrusion during low pressure events [46, 47]. Microorganisms respond to selection pressures imposed within in drinking water systems, such as the treatment process [48, 49, 45, 50, 43, 44] and application of residual disinfectant [51, 48, 52, 49]. For example, drinking water distribution systems with chlorine or chloramine residuals had significantly lower alpha-diversity, lower relative abundance of *Legionella*-classified sequences[1], and higher relative abundance of both *Mycobacterium*- and *Pseudomonas*-classified sequences compared to systems without residual disinfection processes [51]. Selection pressures in drinking water distribution systems that induce shifts in microbial community composition are concerning when the shift reflects an increase in opportunistic pathogens [49, 53, 16] or in microorganisms with unwanted functionality (e.g., microorganisms that cause pipe corrosion [17, 18, 19, 20], nitrification [21, 22, 20, 23], or finished water aesthetic deterioration [54]). An unexpected increase in the abundance of microorganisms or shift in microbial community composition could indicate an unidentified issue occurred in a drinking water distribution system, even without knowledge that the shift reflected an increase in concerning microorganisms. More research is needed to explore the utility of advanced microbial water quality monitoring techniques in drinking water distribution systems.

Enhanced monitoring techniques are needed to characterize shifts in microbial water quality resulting from perturbations in drinking water distribution systems both at local scale (i.e., site-to-site within a distribution system) and system scale (i.e., full distribution system). At local scale, residual disinfectant concentration is a key parameter that interacts with other characteristics of the distribution system, such as water age, pipe material, and pipe age. In the United States, drinking water providers apply residual disinfectants (e.g., free chlorine or chloramine) in an effort to prevent microbial growth during distribution, but disinfectant concentrations decrease with water age, which can be exacerbated by pipe characteristics. For example, tuberculated cast iron pipes are known to exert a demand on disinfectant residual [55, 56] that is higher in older pipes [57]. In general, higher disinfectant residual concentrations are associated with lower microbial abundance [58, 59, 60, 61, 62]. The impacts of local-scale changes on microbial community composition are contradictory. Researchers have proposed that disinfection concentration explained spatial [62] and temporal [63] shifts in microbial community composition in drinking water distribution

[1]In this chapter, amplicon sequence varients or operational taxonomic units are referred to as the Genera followed by "-classified sequences"

systems. However, in a full-scale distribution system with a low disinfectant residual, Perrin et al. (2019) found that the most abundant taxa were positively correlated with nitrate concentration, conductivity, and temperature, but not disinfectant residual. Some researchers observed spatial differences within bulk water microbial communities that were not discussed in relation to local water quality parameters [65, 66], while others did not observe spatial or short-term temporal differences [48, 67, 68, 69, 44].

System-scale changes that affect the whole distribution system (e.g., natural events, treatment upgrades, and source water switches) also influence microbial water quality. Researchers have observed increases in abundance or shifts in microbial communities after natural events such as changes in season [70, 67, 51, 66, 68] and flooding [64]. However, studies of operational changes are less common. Chen et al. (2020) found that the overall microbial water quality six months after a treatment upgrade to include filtration and softening was higher than before the upgrade; however, there was a transition period three weeks after the upgrade during which biofilm sloughing likely occurred and the bacterial community profile shifted (for example, the genera *Legionella*-classified sequences represented the largest relative abundance in bulk water, only during the transition period) [71]. Similarly, Chan et al. (2019) found that when a full-scale system upgraded treatment to include ultrafiltration, pipe biofilm that sloughed into the bulk water and represented most of the bulk water community over five weeks after the transition, but they did not sample at a later time point (i.e., more than six months after the upgrade). Research at lab scale has focused on implications of switching source water supply, and findings have included higher relative abundances of sulfate reducing bacteria after switching to source water with a higher sulfate concentration [73, 74] and lower microbial abundance in bulk water after switching to source water with higher overall quality [75]. The Flint, Michigan Water Crisis exemplifies the importance of understanding the impacts of switching source water on the microbial water quality in addition to chemical water quality. Following the change in source water from Lake Huron to the Flint River, an outbreak of Legionellosis occurred that accompanied elevated lead levels (up to 100 µg/L [76]). Researchers have proposed that proliferation of *Legionella pneumophila* stemmed from a lack of residual disinfectant and an increase in assimilable organic carbon in the drinking water distribution system [77]. Shifts in microbial communities are expected but understudied for some applications that are currently uncommon, such as in drinking water systems that augment conventionally-treated drinking water with advanced-treated wastewater.

1.3 Piped wastewater: an undervalued resource

In this section, I will discuss two applications for piped wastewater 1. Wastewater as a source of drinking water and 2. Wastewater as a resource for public health surveillance.

Wastewater as a source of drinking water

While wastewater is commonly treated to a quality that is acceptable for environmental discharge, it would be concerning for human health if used directly as a conventional drinking water source. Thus, advanced treatment (typically consisting of microfiltration, reverse osmosis, and advanced oxidation processes) can be applied to further treat wastewater to meet and often exceed drinking water quality standards for conventional systems (i.e., those that treat surface water or groundwater) [78, 79]. Through direct potable reuse (DPR), this advanced-treated wastewater may be blended with conventional surface water prior to treatment, resulting in raw water augmentation, or with finished conventional drinking water resulting in treated water augmentation [80]. Treated water augmentation has been applied in Windhoek, Namibia since 1968 [81, 82], but the United States has been slow to adopt this practice, with El Paso, Texas planning to build the first treated water augmentation system in the United States [82]. Previous studies have focused on reduction of pathogens following advanced treatment of wastewater [78], the effect of advanced treatment on microbial water quality [83, 84, 85, 86, 87], and the potential for antibiotic resistance in finished water [88, 87]. However, implementation of DPR will require that existing drinking water distribution systems undergo a system-scale change in operation that could impact microbial water quality. Research focusing on the microbial impact of introducing advanced-treated wastewater to drinking water distribution systems and premise plumbing is limited [6, 89, 84, 85]. Garner et. al (2019) found that introduction of advanced-treated wastewater to simulated premise plumbing rigs did not increase potential of antimicrobial resistance, quantity of opportunistic pathogens, or absolute abundance of bacteria relative to the finished water. More research is needed to characterize the impacts of treated water augmentation on drinking water distribution system microbial water quality and to anticipate issues that might arise in full-scale DPR systems.

To safely use wastewater as a source of drinking water, pathogens need to be adequately removed through advanced treatment processes. Wastewater contains enteric pathogens that cause gastrointestinal disease and are transmitted through a fecal-oral route [7, 6, 90]. The pathogens that are of primary concern for DPR include Adenovirus, Norovirus, *Giardia*, and *Cryptosporidium* [7]. It is not feasible to ensure that each individual pathogen is removed, but instead they are grouped into categories of viruses, bacteria, and protozoa that require certain log_{10} reduction values to be achieved through treatment [6, 91]. In California, potable reuse systems require 12 log_{10} reduction of enteric viruses and 10 log_{10} reduction of *Giardia* and *Cryptosporidium*, which is higher than that for conventional drinking water sources (4 log_{10} reduction of enteric viruses, 3 log_{10} reduction of *Giardia*, and 2 log_{10} reduction of *Cryptosporidium*) [6, 91, 92, 93]. A recent draft proposed framework for regulating DPR in California suggests that even higher log_{10} reduction targets will be required for both treated water and raw water augmentation (e.g., 20 log_{10} reduction of viruses) [94]. The higher virus log_{10} reduction targets proposed could be partially because enteric viruses are of particular concern for DPR as they occur in higher concentrations in wastewater and have greater infectivity than protozoa or bacteria [95]. Furthermore, enteric virus concentrations

in wastewater can be higher (i.e., 10^7 to 10^9 viral particles per L) than the concentrations used to determine the log_{10} reduction targets for potable reuse in California (i.e., 10^5 to 10^6 viral particles per L) [28]. Also, compared to bacteria and protozoa, viruses generally are more difficult to inactivate (especially non-enveloped viruses) and remove [90].

Similar to conventional drinking water systems, DPR systems should have microbial monitoring plans for source water, treatment processes, final effluent, and drinking water distribution systems [6]. Ideally pathogens of concern would be monitored, but maintaining a risk of infection less than or equal to 10^{-4} /person/year requires monitoring pathogens quickly and at a much lower concentration than can be reliably measured in the final effluent (e.g., $2.2\text{x}10^{-7}$ viral particles/L) [6, 96]. Instead, surrogate microorganisms (e.g., *Escherichia coli*) or related physicochemical parameters (e.g., turbidity) are monitored [6, 7, 8, 9]. First, raw wastewater is variable in flow and composition compared to conventional drinking water sources, and physicochemical parameters (e.g., total organic carbon) are often monitored to help ensure treatment trains meet performance goals [7]. Monitoring the variation of pathogens in raw wastewater is not common but has been recommended to help ensure that the risk of infection is sufficiently low [28, 6, 29, 30] by providing data for quantitative microbial risk assessments and to ensure that outbreaks are not occurring in a sewershed [6] by providing routine concentrations of pathogens that can be used to to establish a baseline or seasonal trends in pathogen concentration by location. Furthermore, these data could become an additional part of the recommended public health surveillance for DPR systems [6] to ensure ingestion of recycled water does not result in adverse health conditions. Next, in addition to raw wastewater, treatment train unit processes are monitored through process monitoring to ensure regulations are continuously met [7, 8, 9]. Through process monitoring, physicochemical parameters that are easily measured online, such as turbidity or disinfectant concentration, are continuously monitored during operation to ensure the barrier is operational and to catch issues before potentially compromised water is conveyed [8]. Finally, finished water and distribution system monitoring is similar to that in conventional drinking water systems and relies on indicator microorganisms, such as *Escherichia coli*, and disinfectant residual monitoring [7, 6, 8]. However, for DPR systems specifically, additional monitoring of drinking water distribution systems beyond what is commonly done in conventional systems has been recommended [6].

Wastewater as a resource for public health surveillance

Physicochemical conditions (e.g., total organic carbon) are commonly monitored at wastewatertreatment facilities to ensure consistent treatment efficiency, but monitoring efforts could expand to include public health surveillance targets that provide insight into the health of the contributing community through wastewater-based epidemiology (WBE). In general, the field of WBE has focused on assessing the impact of pharmaceuticals, illicit drugs, tobacco, and alcohol in wastewater catchment areas [10]. Research assessing disease burden in communities has been founded on early work monitoring poliovirus, which includes evidence that WBE has been helpful in global efforts to eradicate poliovirus [97, 98, 99, 100]. From

an integrated monitoring perspective, the pathogens monitored in raw wastewater could expand beyond those that present the highest risk from a treatment breakthrough perspective to include those that present the highest risk from a general public health perspective. For instance, pathogens detectable in wastewater that present a low risk of transmission through wastewater directly but a high risk to public health include Ebola virus [7, 5] and SARS-CoV-2 [101, 102].

Supplementing clinical public health surveillance strategies with WBE could be beneficial for society. Correlations between clinical data and wastewater data can help validate WBE methodologies [103]. While researchers have observed statistical correlations between wastewater and clinical data for norovirus [104], poliovirus [98], and SARS-CoV-2 [105, 106, 107, 108, 109], others only observed visual trends [110, 111, 112, 113, 114, 115]. Situations where correlation was not significant or the pathogen was detected in wastewater but not in clinical data could be the result of sampling bias associated with clinical testing, clinical undertesting, or high proportions of asymptomatic carriers [112, 116, 113]. Because WBE methods aggregate results from anyone who sheds the virus in stool, not just symptomatic individuals, early detection of outbreaks in wastewater compared to clinical data is possible [117]. Lead time in the wastewater signal has been observed for poliovirus [97], norovirus [111], and SARS-CoV-2 [105, 107, 118, 106, 114, 119, 115, 109]. In addition, WBE could help overcome selection bias and stigma associated with individual clinical testing [120, 121] that can lead to underreporting of disease occurrence [122, 123]. WBE is completed at population-level rather than individual-level to compare across communities, which also anonymizes data [124, 125]. Concerns with WBE include that, as with any type of public health surveillance, the monitoring could become invasive or result in stigmatization, especially if surveillance occurs on a small enough basis (i.e., household level) [124, 121, 126, 125]. Additionally, sewer system conditions might influence quantification of pathogens and respective interpretation of disease burden. For example, wastewater is an inhospitable environment and can degrade genetic material too quickly to be accurately quantified, especially in warm conditions [127, 128]. Thus, the detection of a pathogen could vary seasonally or with other physicochemical changes in wastewater [127, 129, 117].

Recently, WBE has been applied to aid with testing efforts of the COVID-19 pandemic [130, 131, 125, 108, 121, 105, 132, 133, 106, 107, 118, 114, 119, 134, 115, 109]. SARS-CoV-2 is an enveloped, single-stranded RNA virus that is primarily transmitted through respiratory pathways [32]. However, SARS-CoV-2 is shed in feces [32, 31, 33, 36, 130] and possibly transmitted through fecal-oral routes [33, 135]. Not all individuals with COVID-19 shed SARS-CoV-2 in feces, and the shedding rate and duration is still unclear and possibly erratic [129, 34, 136]. For successful application of WBE, SARS-CoV-2 or its RNA needs to persist in the sewer system long enough for detection and accurate quantification. While there is evidence that high temperatures degrade the SARS-CoV-2 signal [137, 127, 128, 102], globally, researchers have detected SARS-CoV-2 in wastewater and sludge [130, 108, 134]. These data are promising, but more research is needed to determine the applicability of WBE during the COVID-19 pandemic.

1.4 Strategies to enhance assessment of microorganisms in piped water systems

Applying enhanced methods to assess microorganisms in piped water systems could benefit public health by expanding on the commonly assessed and often regulated monitoring target, fecal indicator bacteria [5, 12, 13, 14, 11, 15], to include microbial abundance, bacterial community composition, and targeted pathogens. Microbial abundance can be incorporated into routine or diagnostic monitoring and can help providers understand day to day fluctuations in water systems [138, 139, 140, 39, 40, 141, 142, 143, 144, 145]. Additionally, in anticipation of major changes in water quality, characterizing bacterial community composition can add to the insights gained from real-time monitoring. For example, broad assessment of bacterial community profiles could reveal specific taxa to target with more specific methods such as quantitative polymerase chain reaction (qPCR). Additionally, qPCR can be applied to monitor pathogen concentrations in raw wastewater for applications in direct potable reuse or WBE. Four emerging methods to monitor microorganisms in piped water systems are discussed in this section: adenosine triphosphate (ATP) quantification, flow cytometry-based cell counts, qPCR and 16S rRNA gene amplicon sequencing. None of these methods assess viability directly, and, for some applications, such as early detection of disease outbreaks using wastewater, viability is not as important to assess, but for others, such as determining risk of infection from ingesting pathogens, quantifying viable pathogens is ideal.

Drinking water treatment facilities can supplement routine and diagnostic monitoring with assessment of microbial water quality. The most common and well-known option for assessing microbial abundance is a culturing method that quantifies only a subset of the microorganisms known to inhabit drinking water systems, HPC [146]. Comparatively, flow cytometric cell counts and ATP assays are much faster to quantify and are inclusive of all microorganisms as opposed to only heterotrophic microorganisms [147, 148, 143, 144]. While these methods are not routinely applied in drinking water facilities in the United States, they have most commonly been applied in systems with no or low residual disinfectant concentrations [39, 61, 149, 150, 151, 58, 144] and might be useful in systems with high disinfectant residuals, such as those in the United States. Assessing microbial abundance provides a quick but broad snapshot of microorganisms in water systems, but this type of assessment cannot distinguish which types of microorganisms are present.

Methods that require polymerase chain reaction (PCR) can be specific, to quantify targeted microorganisms, or broad, to characterize bacterial community profiles in water systems. When monitoring a specific pathogen, most water treatment facilities currently use culturing methods for fecal indicator bacteria [5, 12, 13, 14, 11, 15] and sometimes for culturable pathogens of interest such as *Legionella pneumophila* [152]. These methods apply to only culturable microorganisms, require time for microorganisms to replicate before quantification, and quantify only a fraction of the viable portion of the cultured microorganism [153, 154, 155]. Furthermore, by design, cultured microorganisms grow in number, and, therefore, the culture can be more dangerous than the sample itself when working with pathogens.

Alternatively, specific pathogens can be sensitively quantified in water using qPCR (DNA targets) or reverse-transcription qPCR (RNA targets), which might be useful for retrospective pathogen monitoring in water systems [153, 155]. In addition, the application of 16S rRNA gene amplicon sequencing shows promise for retrospective monitoring applications in water systems [38, 44, 156], especially because the cost of nucleotide sequencing has rapidly decreased [157]. However, limitations to any method that utilizes PCR, including amplicon sequencing and qPCR, include well-known biases [158, 159, 160, 161, 162], contamination issues [153, 163, 164, 165], PCR inhibition [166, 167, 168, 169, 170], and that viability can only be assessed using a modified assay [171, 172, 173, 174].

In drinking water distribution systems, there are several challenges to characterizing microbial communities with enhanced methods. First, for methods targeting genetic material, disinfectant residuals lyse microorganisms relatively quickly compared to the time it takes to completely degrade genetic material [175, 176], therefore, disinfected drinking water often contains an abundance of genetic material from nonviable organisms that pose no public health risk. Thus, if viability is important to an assessment, a separate assay is often required (e.g., intact vs total cell counts) [177, 171, 178]. Another challenge is concentration of enough biomass to quantify or detect changes in microbial water quality throughout drinking water systems, particularly in systems that have low biomass because of high residual disinfectant concentrations or advanced treatment processes (e.g., reverse osmosis [83, 84]). While microbial abundance measures can rely on grab samples, nucleotide sequencing and qPCR methods require filtering large quantities of water to increase chances of detection [167, 179]. The fluctuations in water quality throughout the range of distribution systems may also impact PCR inhibition, which occurs as a result of some components in drinking water, such as organic material [168, 169, 170]. In addition, for 16S rRNA gene amplicon sequencing, comparisons across different systems is difficult because lab methods are not standardized and have large impacts on results, including the hypervariable region of the 16S rRNA gene targeted, the library preparation protocol, and the use of both negative and positive controls [180, 159, 161, 162, 164].

Challenges to monitoring pathogens as part of WBE begin with collecting a representative sample from a sewer system. One benefit to working with raw wastewater compared to sludge is that it can be collected upstream of a wastewater treatment plant and specific wastewater catchment areas can be selected by sampling at different locations in the sewer system. However, this approach requires effort from the wastewater treatment facility to determine where to sample and then verify that the sewage being sampled represents a known population [10, 181]. Once the sampling locations are selected, a method to collect the samples must be determined. There are two methods that have been applied in COVID-19 WBE: collection of a grab sample, which is a sample taken at one point in time that could miss the peak signal of the pathogen of interest, or collection of a composite sample, which is a combination of smaller subsamples collected at regular intervals over a long time period (e.g., 12 or 24 hours) that could dilute the signal to a value below the detection limit [182, 183, 184] and could be too little volume to capture the heterogeneity of wastewater over the collection period. Once the sample is collected, preservation of the genetic material becomes

a concern. If the target is RNA, it is pivotal to keep the sample cold and preserve the RNA as quickly as possible. For example, in the case of SARS-CoV-2 it is likely that the signal detected in wastewater is largely from free RNA and that temperature and storage conditions impact quantification [102, 185, 186, 187]. Once the genetic material is transported back to lab, accurate quantification is pivotal. While wastewater contains more biomass compared to drinking water, it also has higher concentrations of the components that contribute to PCR inhibition [168, 169, 170, 188], which makes accurate quantification more challenging. Lastly, all of these challenges contribute to difficulties in interpreting the concentration of a pathogen in wastewater for public health decision-making.

1.5 Research objectives

The goal of this research was to apply enhanced methods of microbial assessment in piped water systems and to identify integrated monitoring strategies that benefit public health. Current microbial monitoring strategies in piped water systems are applied to address the specific problem of fecal contamination. Enhanced microbial monitoring methods could be integrated into current strategies to provide data that are of greater use to both utilities and public health departments. Applications for enhanced microbial assessment include 1. routine assessment such as monitoring impacts of local-scale water quality conditions (e.g., residual disinfectant) on microbial abundance in drinking water distribution systems (Chapter 2), 2. diagnostic or preventative assessment such as monitoring impacts of system-scale changes (e.g., transition to direct potable reuse) on drinking water distribution system microbial communities (Chapter 3), and 3. public health surveillance such as monitoring pathogens in community sewersheds during outbreaks (Chapter 4). The following objectives are addressed:

Objective 1: Evaluate enhanced microbial monitoring strategies for disinfected, piped drinking water

Six full-scale chlorinated and chloraminated distribution systems were sampled and five measures of microbial abundance were compared for quantifiability and variability throughout distribution: total cell counts, intact cell counts, total ATP, intracellular ATP, and heterotrophic plate counts.

Objective 2: Characterize the impact on bacterial community composition from transitioning a piped distribution system fed with surface water to a treated water augmentation system.

Five pipe loop rigs that circulated 100-L of water each were used to simulate transition from conventional drinking water to augmentation with advanced-treated wastewater. The impact

of the transition on biofilm and bulk water microbial communities in the pipe loop rigs was assessed using flow cytometry-based cell counts and 16S rRNA gene amplicon sequencing.

Objective 3: Assess SARS-CoV-2 wastewater testing as a public health surveillance strategy during the COVID-19 pandemic

SARS-CoV-2 was measured weekly in raw wastewater from five locations in the San Francisco Bay Area during the COVID-19 pandemic (April - September 2020). Daily per capita COVID-19 cases were geocoded to each sewershed and used to interpret spatial and temporal trends in SARS-CoV-2 measured in wastewater.

Conclusions

The implications of this work and methods to develop an integrated approach to microbial monitoring that benefits public health are discussed in the final chapter of this dissertation (Chapter 5).

Chapter 2

Evaluation of enhanced microbial monitoring strategies for disinfected, piped drinking water

The following chapter is adapted from Kennedy et al. (2020). Effect of disinfectant residual, pH, and temperature on microbial abundance in disinfected drinking water distribution systems. Environmental Science Water Research & Technology 7, 78–92, with permission from Scott E. Miller, Rose S. Kantor, and Kara L. Nelson.

2.1 Introduction

Microbial water quality in piped drinking water distribution systems depends on complex interactions between the microbial community (composition, abundance, and growth rates of microorganisms) and chemical and physical conditions. Over the last five years, researchers have made great progress to better understand these interactions with the common goal of guiding drinking water providers toward more efficient management of microbial water quality in piped drinking water systems with continuous or intermittent flow [190, 51, 52, 62, 191, 192, 193, 150, 64, 194, 43]. Advances in meta-omics techniques allow researchers to characterize changes in the microbial community composition throughout piped distribution [195, 196], but these techniques often do not quantify absolute microbial abundance. Increases in microbial abundance in piped drinking water distribution systems can signal mobilization of loose deposits [197, 71], loss of disinfectant residual [61, 59, 58], treatment breakthrough [198], nitrification [199, 200], stagnation [201, 202], and intrusion or backflow [190]. It is important to pair measures of microbial abundance with compositional data to better characterize microbial water quality in drinking water systems.

In the United States, total coliform bacteria are the only regulated parameter for microbial abundance, but because levels are required to be maintained below the quantification

limit, this parameter provides little insight into the total microbial abundance. Given this limitation, other measures of microbial abundance have been used that include heterotrophic plate counts (HPC), which are the most common [203, 64], and newer methods that aim to capture the entire microbial community such as adenosine triphosphate (ATP) assays [204, 205] and flow cytometry-based assays [206, 70]. Each assay has its limitations. The World Health Organization recommends HPC for monitoring the "general bacterial content" of water [203], but the HPC assay has been shown to quantify a varied fraction of total bacteria in drinking water [146] that can be several orders of magnitude smaller than total cell counts and usually requires two days to complete [148]. However, HPC may require less technical skill than ATP or cell counts if user-friendly proprietary HPC kits are used. As an alternative to HPC, the quantification of intracellular ATP has been used to estimate the viable biomass in water samples [207, 208, 209]. However, ATP concentration depends on the types of microorganisms present [210] and local conditions [211, 212], which hinders accurate quantification of microbial abundance. In addition, ATP assays require an extra filtration step during sample processing to measure total ATP (both intracellular and extracellular) as well as extracellular ATP (ATP in 0.1 µm filtered sample), which is subtracted from total ATP to obtain intracellular ATP [204]. In contrast, flow cytometry-based methods can be used to quantify microbial cells [213, 147] with high reproducibility (<5% error [38]), low limits of quantification (<25 cells/mL [85]), and rapid sample turnaround. Flow cytometry-based monitoring has been estimated to cost twice that of standard monitoring methods using HPC [214], and that cost does not include the cost of instruments needed, which for flow cytometry are currently more expensive than for HPC. For flow cytometry-based monitoring, an assessment of viability can be included by distinguishing between total cells and intact cells through staining procedures.

Drinking water distribution systems are dynamic, and changes in physical and chemical conditions in full-scale systems also influence the microbial abundance. For example, seasonal variations in drinking water quality have been linked to changes in intact cell count in a full-scale system without disinfectant residual [70]. In drinking water systems with residual disinfectants, characterizing these impacts can be difficult because environmental factors that can impact microorganisms can also impact the efficacy of disinfection (e.g., temperature, pH) [215]. In addition, high levels of residual disinfectant can make microbial abundance difficult to quantify because they might drive the quantity of microorganisms below the quantification limit of the assay. For instance, flow cytometry-based methods have only been applied in full-scale systems with relatively low residual concentrations (<0.9 mg/L free chlorine and <1.8 mg/L combined chlorine) [39, 61, 149, 150, 151, 58], while drinking water systems in the United States have reported free chlorine concentrations of up to 4 mg/L as Cl_2 after primary disinfection [216]. The understanding of disinfectant residual, and its interaction with other physical and chemical parameters, on total microbial abundance is still far from complete. Nonetheless, measures of microbial abundance that better reflect the entire microbial community, rather than a small fraction, and that are quantifiable throughout the range of conditions encountered in piped drinking water distribution systems, have the potential to provide more insight to guide the safe management of drinking water.

In this study, five measures of microbial abundance were compared (total and intact cell counts, total and intracellular ATP, and HPC) in six piped drinking water distribution systems. The drinking water systems had different treatment trains and used either free chlorine or chloramine as a residual disinfectant. These systems were surveyed to: (1) assess the impact of commonly measured parameters (disinfectant concentration, pH, and temperature) on microbial abundance, including statistical approaches to account for interactions between parameters; and (2) compare the quantifiability and variability of five measures of microbial abundance under the conditions of distribution. This study may be the first to apply flow cytometry-based total and intact cell counts in drinking water distribution systems with high disinfectant residual concentrations (>0.9 mg/L free chlorine and >1.8 mg/L total chlorine). These data will serve as points of comparison for future studies applying these methods in similar water systems.

2.2 Methods

Sampling Locations

Piped drinking water distribution systems in California and Texas were sampled as indicated in Table A.1. Treatment processes and other metadata for these systems are shown in Table 2.1. Sampling efforts were coordinated with drinking water providers, and samples were collected from a subset of their routine monitoring locations. Systems A and B were sampled one time each in both 2016 and 2018. Systems C, D, and E were sampled one time in 2016. System F was sampled six times in 2018 (Table A.1). Prior to bulk water grab sampling, drinking water distribution system site taps were flushed for 10 minutes and 500-mL grab samples of bulk water were aseptically collected in autoclaved-sterilized glass bottles. pH (Electrode Sealed SJ F; Fisher Scientific) was determined within eight hours of sampling. Temperature (Electrode Sealed SJ F; Fisher Scientific) and free and total chlorine measurements (HACH pocket colorimeter II) were determined onsite at the time of sampling. Samples for quantification of microbial abundance were treated with sodium thiosulfate in excess to quench disinfectant residual and kept at 4°C until processing within 24 hours of sampling. For DWDS F, water ages for each site were provided by the utility based on an internal model of the full distribution system developed using SynerGEE Water (v4.7.0). Consumables, including filtered pipette tips (RAININ TerraRack or Finntip Flex) and 2-mL microcentrifuge tubes (Thermo Scientific) used for microbial analyses were purchased presterilized and free of DNA, DNase, and RNase as well as of ATP when available.

Cell counts by fluorescent staining and flow cytometry

Total and intact cell concentrations were measured following the methods of Miller et al. (2020). Briefly, cell concentrations were measured using flow cytometry with SYBR Green I (S9430; Sigma-Aldrich, St. Louis, MO) and propidium iodide (30 mM P1304MP; Life

System	Source water type	Maximum capacity (million gallons per day)	Treatment Process										Secondary disinfectant
			free chlorine	coagulation, flocculation, sedimentation	ozone	free chlorine	filtration (anthracite & sand)	filtration (granular activated carbon & sand)	filtration (granular activated carbon)	membrane filtration (ultrafiltration)	chlorine dioxide	free chlorine	ammonia	
A	S	12		X		X		X				X		free chlorine
B1	S	5.5		X			X					X		free chlorine
B2	S	5.5		X						X		X		free chlorine
C	S	200	X	X			X					X	X	chloramine
D	S/G	40		X					X		X	X		free chlorine
E	G	30		X					X			X		free chlorine
F	S	144		X	X	X	X					X	X	chloramine

Table 2.1: Treatment processes for each drinking water distribution system sampled in this study, presented in their sequential order at the treatment plant, where source water type is either surface water (S) and/or ground water (G). System B had two parallel trains (B1 & B2). Systems D and E had free chlorine added throughout the distribution system. System D used both chlorine dioxide and free chlorine as primary disinfectants.

Technologies, Carlsbad, CA) to distinguish cells with intact membranes. From each bulk water grab sample, a 1000-μL aliquot of each triplicate was processed and the geometric mean and geometric standard deviation were calculated. Measurements were performed on two separate flow cytometers, an Accuri C6 flow cytometer (Accuri; BD Biosciences, San Jose, CA) and a BD FACSCanto cell analyzer (Canto; BD Biosciences, San Jose, CA). The Accuri was used to sample all locations but had to be sent in for repair during field sampling at DWDS F. While the Accuri was not available the Canto was used, which was during sampling of DWDS F (more information can be found in the Appendix A). The Accuri was equipped with a 50 mW laser emitting a fixed wavelength of 488 nm, and measurements were performed at the "fast" flow rate of 66 µL minute^{-1} on sample volumes of 50 µL. Microbial cell signals were distinguished and enumerated from background and instrument noise on density plots of green (FL1; 533 ± 30 nm) and red (FL3; >670 nm) fluorescence using FlowJo gating software (v10.5.3). Gate positions were modified slightly from a template publicly available for the BD Accuri C6 [147] to adapt for FlowJo software. The Canto was equipped with a 20 mW laser emitting a fixed wavelength of 488 nm, and measurements were performed at a flow rate of 1 µL s^{-1} for 50 seconds. Microbial cell signals were distinguished and enumerated from background and instrument noise on density plots of green (FTIC; 530 ± 30 nm) and red (PerCP; 695 ± 40 nm) fluorescence using FlowJo gating software. Gate positions were modified slightly compared to BD Accuri C6 gating based on calibration beads (Spherotech, Catalog # NFPPS-52-4K, Lake Forest, IL). For the Accuri, the lower quantification limits were determined for intact cell count (22 cells per mL) and total cell count (12 cells per mL) by Miller et al. (2020) using the same instrument used in this study. All data from the Canto were deemed detectable based on the recommended lower quantification limit ($> 10^2$ cells per mL [147]) after gate adjustment (more information can be found in the Appendix A). All of the flow cytometric measurements in this study were at least an order of magnitude lower than the upper recommended upper quantification limit ($< 10^7$ cells per mL [147]). For a negative control, 0.22 μm filtered, Millipore Milli-Q water was used.

Adenosine tri-phosphate concentrations

Total and intracellular ATP concentrations were measured following the methods of Miller et al. (2020). Briefly, ATP concentrations were measured using the BacTiter-GloTM Microbial Cell Viability Assay (G8231, Promega Corporation, Madison, WI) and GloMaxR 20/20 Luminometer (Turner BioSystems, Sunnyvale, CA). From each bulk water grab sample, a 500-µL aliquot of each triplicate was processed and the geometric mean and geometric standard deviation were calculated. Relative light units from the luminometer were converted to ATP concentrations using calibration curves made with a pure ATP standard (P1132; Promega Corporation, Madison, WI). Extracellular ATP was separated from total ATP prior to sample incubation through removal of microbial cells by filtration (0.1 µm, Millex-VV Syringe Filter Unit; Millipore, Billerica, MA). For total and extracellular ATP, the quantification limits were set by the standard curve, which ranged from 1x10^{-4} nM to 10

nM. No total or extracellular ATP measurement was higher than the upper quantification limit. The lower quantification limit for intracellular ATP was determined by Miller et al. (2020) as $1.83\text{x}10^{-5}$ nM. Empty tube measurements and reagent-only measurements were used as negative controls and reagent controls respectfully.

Heterotrophic plate counts

Heterotrophic plate counts (HPC) were determined using Quanti-Tray 2000 (IDEXX US; Westbrook, Maine) with HPC for Quanti-Tray media (IDEXX US; Westbrook, Maine) following the manufacturer's instructions with the trays incubated at 37°C for 44-72 hours. 100 mL of bulk water grab sample was transferred to autoclave-sterilized bottles for each replicate and the geometric mean and geometric standard deviation were calculated. Technical duplicates of all samples were completed except samples from distribution system B in 2016, for which there were no replicates. The lower limit of quantification was set using the IDEXX Quanti-Tray format at a most probable number of one cell per 100 mL. The upper limit of quantification was set at a most probable number of 2419.6 cells per 100 mL (a fully positive IDEXX tray).

Statistical Analyses

This dataset had inherent dependencies that needed to be considered in the analysis, including dependent variables that may be correlated with each other (e.g., pH, temperature, chlorine residual), samples collected from the same drinking water distribution system on the same day, or at the same location within a distribution system over time. Thus, relationships between microbial abundance and water quality parameters were assessed via correlation analyses and generalized linear mixed models using R (3.6.2) [217]. To investigate potential multicollinearity, Spearman's Correlation values of all chemical and microbial water quality parameters were determined using Hmisc (4.3-0) [218] and GGgally (1.4.0) [219]. Data exploration was completed following Zuur et al. (2009) using Cleveland dot plots to detect outliers, GGgally to assess colinearity, and scatter plots of all covariates to visualize relationships [220, 221]. Outliers and collinearity between covariates were not detected. Generalized linear mixed model (GLMM) analysis and validation was completed following the methods of Zuur et al. (2013, 2016). Prior to analysis, microbial abundance metrics were tested for goodness of fit to a normal distribution, log-normal distribution, and gamma distribution [223] using goft (1.3.4) [224]. The GLMM was fitted to raw intact cell counts from distribution system F with centered and scaled predictors (to improve the parameter optimization process) using lme4 (1.1-23) [225] with site as a random variable. The most optimal model was selected based on minimizing conditional Akaike information criterion with MuMIn (1.43.15) [226] through backward stepwise model selection. Wald confidence intervals for fixed effects were calculated using lme4. For correlation, GLMM, and summary statistic calculations, values below the quantification limit of intracellular ATP, total ATP, intact cell counts, total cell counts, HPC, free chlorine and total chlorine were replaced with

the respective lower quantification limit for the assay to be conservative. However, for calculations of the coefficient of variation, only the quantifiable samples were used (Table 2.4). In figures, these data were plotted at a value below the quantification limit for visualization. Four HPC samples were above the quantification limit and were removed from all statistical analyses and figures. Plotting was completed using ggplot2 (3.2.1) [227], tables were generated using stargazer (5.2.2) [228], plot fonts were set using extrafont (0.17) [229], figures with multiple plots were generated using ggpubr (0.4.0) [230], and color palettes were chosen from viridis (0.5.1) [231]. The full reproducible code and csv files that have all data used in this paper are available in GitHub (`https://zenodo.org/record/3993877#.X5n0Qy9h1TZ`).

2.3 Results

Impacts of physicochemical parameters on microbial abundance

Disinfectant residual concentration was expected to be a master variable affecting microbial abundance across the various the drinking water distribution systems that were sampled. Thus, all data were plotted for each measure of microbial abundance as a function of disinfectant residual concentration. Of the five measurements of microbial abundance applied, inverse trends were observed for two of them: intact cell counts (Figures 2.1A and 2.1D) and intracellular ATP (2.1B and 2.1E). The trends for HPC (Figures 2.1C and 2.1F), total cell counts in chloraminated systems (Figure A.1A), and total ATP (Figure A.1C and A.1D) were less clear. In free chlorinated systems, a similar trend was observed for total cell count (Figure A.1B) as for intact cell count (Figure 2.1D), likely because chlorine is a stronger disinfectant than chloramine [215]. Thus, signal from non-viable cells and free DNA likely decreases more rapidly than in chlorinated systems. A trend was not observed for proportion of potentially viable cells (intact:total cells) (Figure A.2).

In addition to disinfectant residual concentration, temperature and pH might influence microbial abundance. To explore these relationships statistically, Spearman's correlation coefficients (r_s) were used to assess the strength of correlation between the various microbial abundance metrics, disinfectant concentration, temperature, and pH (Figures 2.2A and 2.2B). The correlation between microbial abundance metrics and residual disinfectant concentration is discussed first. In both chloraminated and chlorinated systems, total chlorine concentration was significantly and inversely correlated with both intracellular ATP and intact cell counts (r_s values between -0.65 and -0.85 ; p-values <0.001; Figures 2.2A and 2.2B), consistent with the visual trends in Figure 2.1. HPC were only significantly correlated with disinfectant residual in chloraminated systems (r_s -0.45; p <0.001; 2.2A). In contrast, intracellular ATP was more strongly correlated with disinfectant concentration in chlorinated systems (r_s= -0.77 ; p <0.001; Figure 2.2B) compared to chloraminated systems (r_s= -0.65 ; p <0.001; Figure 2.2A), but intact cell count was similar in both chlorinated (r_s= -0.63; p <0.01; Figure 2.2B) and chloraminated (r_s= -0.67; p <0.001; Figure 2.2A) systems. In chlorinated systems, the majority of the total chlorine concentration consisted of free chlo-

rine except for in two cases for which total chlorine concentrations were <0.3 mg/L as Cl_2. Thus free and total chlorine concentrations were strongly correlated and appear to have similar impacts on measures of microbial abundance (Figure 2.2B). However, in chloraminated systems free chlorine concentration varied and was not significantly correlated with any microbial abundance parameters (Figure 2.2A).

In terms of the other two commonly monitored water quality variables, significant correlations were observed in chloraminated systems of temperature with intact cell counts (rs = 0.44; p < 0.001) and with intracellular ATP (rs = 0.48; p <0.001), but temperature was not correlated with any measures of microbial abundance in chlorinated systems (Figures 2.2A and 2.2B). pH was not significantly correlated with any measure of microbial abundance. It should be noted that this dataset included ranges for disinfectant residual, temperature, and pH that are typical of drinking water distribution systems located in the western/ southwestern United States (Table A.2).

In the chloraminated distribution system, microbial abundance measures were strongly correlated with both disinfect residual and temperature, and pH was strongly correlated with disinfectant residual. To assess relationships between these variables using a model, interactions between variables and measurements from the same location that were not independent needed to be considered. For this approach, intact cell counts were the focus and a mixed model was developed using data from distribution system F (n=80). Raw intact cell counts were not normally or log normally distributed, but the fit to a gamma distribution was not rejected [223]. Thus, scaled and centered predictor variables (pH, temperature, free and total chlorine) and raw intact cell counts were used in a generalized linear mixed model with log link function (Equation 2.1). The log link function was chosen because it requires positive fitted values. Sampling location within distribution system F ("site") was used as a random intercept to account for dependency associated with samples taken from the same site.

$$\begin{aligned} ICC_{ij} &\sim Gamma(\mu_{ij}, \tau) \\ log(\mu_{ij}) = total\ chlorine_{ij} &+ free\ chlorine_{ij} + pH_{ij} + temperature_{ij} \\ &+ total\ chlorine_{ij}\ X\ pH_{ij} + free\ chlorine_{ij}\ X\ pH_{ij} \\ &+ free\ chlorine_{ij}\ X\ temperature_{ij} \\ &+ total\ chlorine_{ij}\ X\ temperature_{ij} + site_i \\ site_i &\sim N(0, \sigma^2_{site}) \end{aligned} \tag{2.1}$$

In Equation 2.1, ICC_{ij} is the intact cell count (with mean μ_{ij}) for the jth observation of $site_i$. ICC_{ij} is assumed to follow a gamma distribution with scale parameter, μ_{ij}, and shape parameter, τ. The random intercept, $site_i$, is assumed to be normally distributed with mean of 0 and variance of σ^2_{site}. Fixed effects include total chlorine, free chlorine, pH, temperature, and their interactions (included as interaction terms). Stepwise model selection was applied (Table A.3) to determine the most optimal model (Equation 2.2) with parameter estimates in Table 2.2.

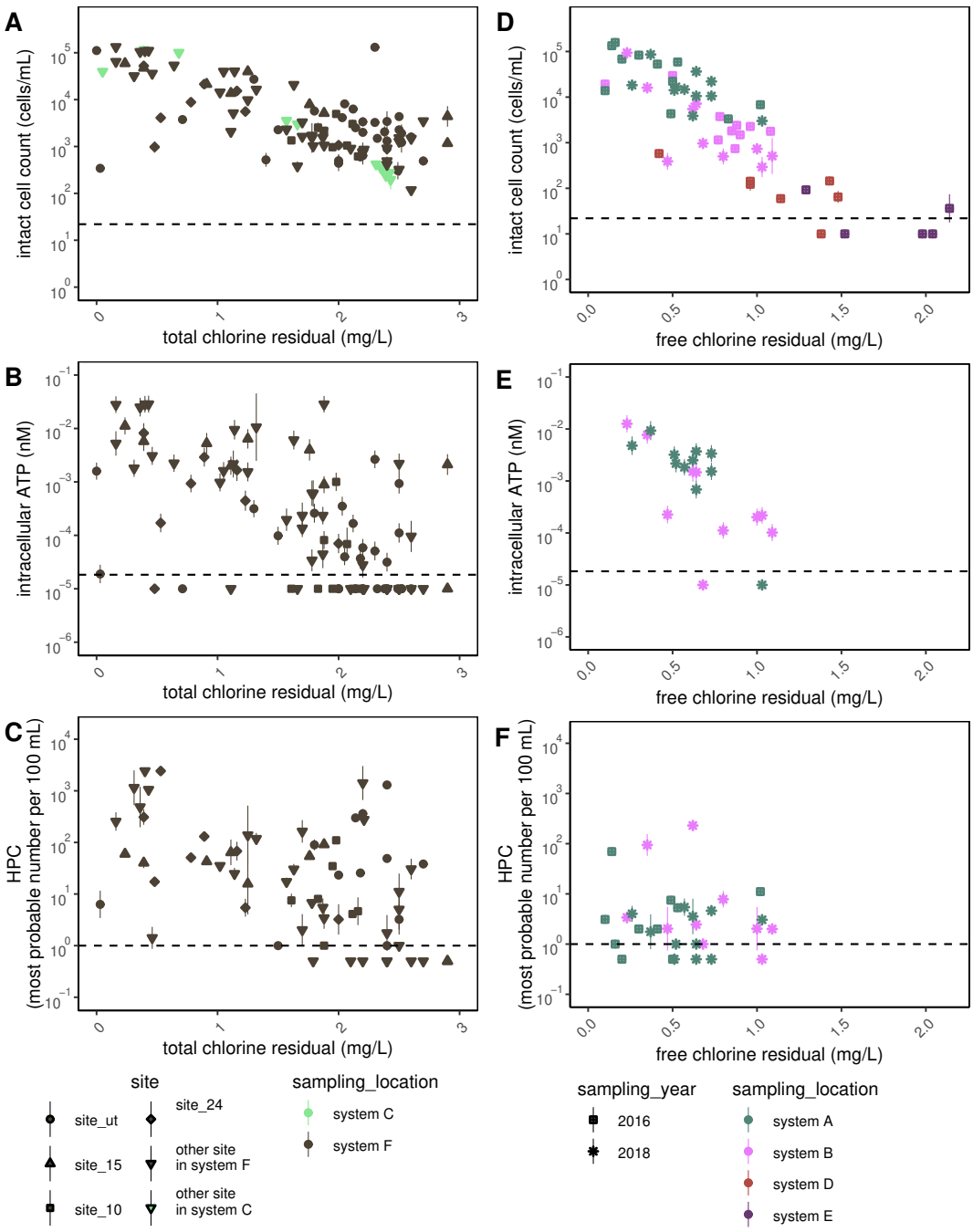

Figure 2.1: intact cell counts (A & D), intracellular ATP (B & E), and HPC (C & F). **Left (chloraminated systems):** Shapes denote sites in system F that were sampled at least six times between August 2017 and April 2018. **Right (chlorinated systems):** Shapes denote locations in systems A and B that were sampled in 2016 and 2018. Dashed lines denote quantification limits for each assay. Points are the geometric mean of the technical replicates and error bars represent the geometric standard deviation.

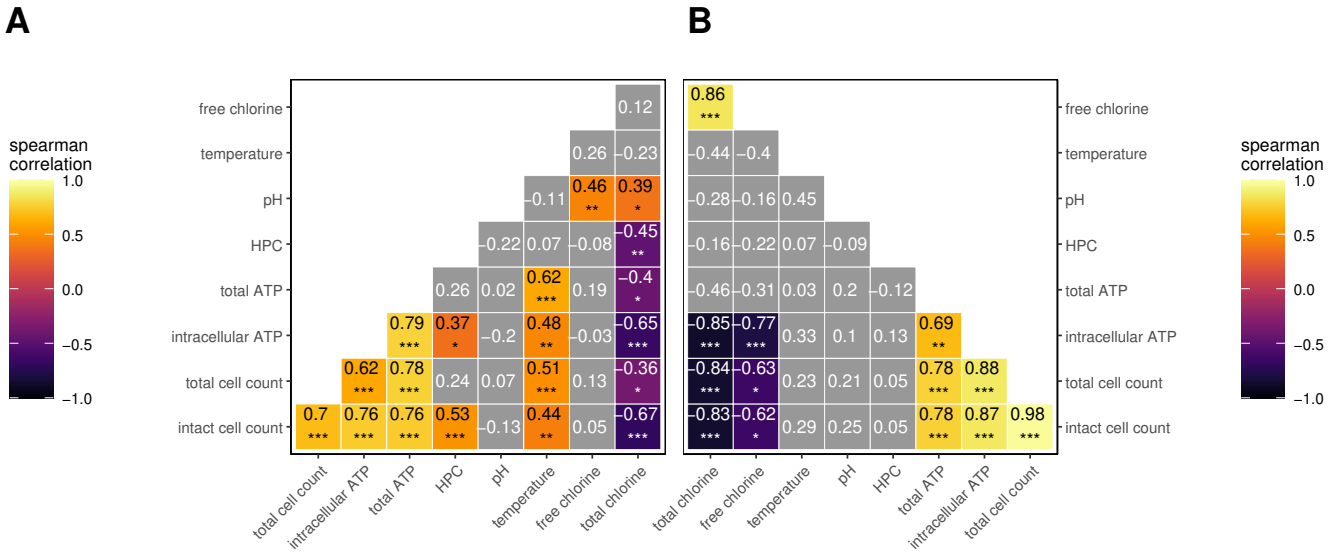

Figure 2.2: (A) Spearman's correlation coefficient heat map for all samples with complete water quality data collected from a chloraminated drinking water distribution system (n= 61) (B) Spearman's correlation coefficient heat map for all samples with complete water quality data collected from chlorinated drinking water distribution systems (n= 21). Insignificant coefficients are shown in grey where significance is coded as * p< 0.01; ** p<0.001; *** p<0.0001.

$$
\begin{aligned}
ICC_{ij} &\sim Gamma(\mu_{ij}, \tau) \\
log(\mu_{ij}) = total\ chlorine_{ij} \ + \ pH_{ij} \ + \ temperature_{ij} \ + \ free\ chlorine_{ij}\ X\ pH_{ij} \\
&+ total\ chlorine_{ij}\ X\ temperature_{ij} \ + \ site_i \\
site_i &\sim N(0, \sigma^2_{site})
\end{aligned}
\tag{2.2}
$$

The most optimal model shows that lower total chlorine concentrations resulted in higher intact cell counts; as expected, there was also an interaction with temperature that could result in higher intact cell counts at lower total chlorine values and higher temperatures (Figure 2.3). In Figure 2.3, quantiles of temperature, from lowest (purple line) to highest (yellow line), are used in Equation 2.2 at a range of total chlorine concentrations. The total chlorine term was the largest parameter estimate for a fixed effect in this model (Table 2.2), which indicates that total chlorine had a large inverse effect on intact cell counts. In addition, higher pH and temperature values resulted in higher intact cell counts (Figure A.3 and Table 2.2). However, the effect of temperature and pH on intact cell counts was smaller than that of total chlorine (Table 2.2). In addition, the interaction between pH and free chlorine in the optimized model was indistinguishable from 0 (0 falls within the confidence intervals shown in Table 2.2). It is known that free chlorine disinfection is more effective at pH values below

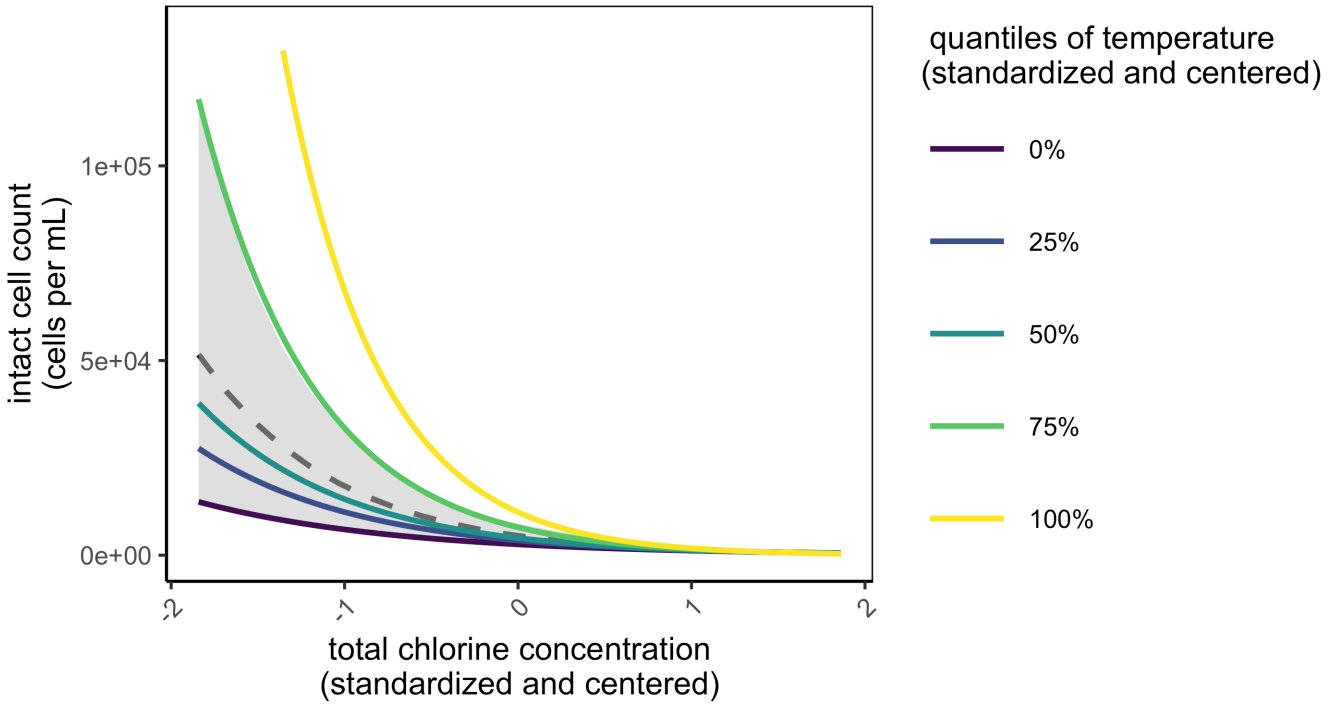

Figure 2.3: Visual representation of the most optimal model of intact cell counts in distribution system F (Equation 2). To generate dashed grey line, all fixed effects were held constant at their average value except for total chlorine (with bootstrapped 95% confidence intervals are shown in grey). To generate other lines, temperature was varied in the model at each quantile value (-1.9, -0.10, -0.53, 0.87, and 2.1). In Figure A.3, other fixed effects are shown.

7.5 [215], but the minimum pH value in system F was 7.67 (Table A.4). Thus, the pH in this system likely did not vary enough to produce an accurate estimate for this interaction term (Table A.4).

Another variable in drinking water distribution systems that may correlate with microbial abundance is water age, given that the concentration of chlorine residual is known to diminish with water age, which could have substantial impacts on microbial abundance [232]. To investigate the impacts of water age on water quality, water age was compared with with intact cell counts, intracellular ATP, HPC, and total chlorine concentration in distribution system F (Figure 2.4). Surprisingly, the measures of microbial abundance generally did not trend with water age (Figure 2.4 A-C). However, total chlorine generally decreased with water age during each specific sampling event (Figure A.4). To investigate the variability in chlorine residual at individual sampling sites, data from a year of sampling at 21 sites were aggregated in distribution system F (Figure A.5). Total chlorine at each sited varied over the course of a year depending on the location sampled and was not directly correlated with the water age at that site (Figure A.5). These results suggest that total chlorine had a large

Table 2.2: Estimated parameters, standard errors, and confidence intervals for each covariate of the most optimal model of intact cell counts in distribution system F (Equation 2.1). Generalized linear mixed model for intact cell counts with sampling location ("site") as a random variable, where $\sigma^2_{site} = 0.26$ and $\tau = 1.72$.

parameter	estimate	standard error	lower confidence interval (5%)	upper confidence interval (95%)
intercept	8.6	0.19	8.3	9.0
total chlorine	-1.3	0.13	-1.6	-1.1
pH	0.40	0.17	0.062	0.73
temperature	0.35	0.097	0.16	0.54
pH X free chlorine	0.39	0.23	-0.066	0.84
total chlorine X temperature	-0.24	0.12	-0.47	-0.0087

impact on microbial abundance that was independent of water age in distribution system F.

Quantifiability and variability of five measures of microbial abundance

To evaluate the utility of the microbial abundance assays, the measures of microbial abundance that were most frequently quantifiable in disinfected drinking water systems were determined. Intact cell counts yielded the highest percentage of results that were above lower quantification limits (97.6% of samples, n= 166; Table 2.3). In contrast, intracellular ATP was quantifiable in only 69.6% of samples (n= 115), and HPC were quantifiable in only 81.4% of samples (n= 102; 18.6% of samples either above or below limits of quantification). Total ATP and total cell counts were quantifiable in 100% of samples, as no samples were below the limit of quantification (Table 2.3). Interestingly, quantifiability of intracellular ATP was dependent on the system sampled (Table A.5). In particular, a greater fraction of samples was observed with concentrations of intracellular ATP above lower quantification limits from distribution system A (90.9% of samples with n= 11; Table A.5) and distribution system B (90% of samples with n= 10; Table A.5) and lower quantifiability was observed in samples from distribution system F (64.9% of samples with n= 94; Table A.5).

To evaluate the variability of the microbial abundance assays, the measures of microbial abundance that had the lowest average coefficients of variation were determined. The coefficient of variation is commonly used to assess variability in quantitative bioassays and is reported as a percentage with a higher percentage indicating more variation among replicates [233]. To summarize the variability across all samples taken in this study, an average coefficient of variation was calculated for each of the measures of microbial abundance by taking

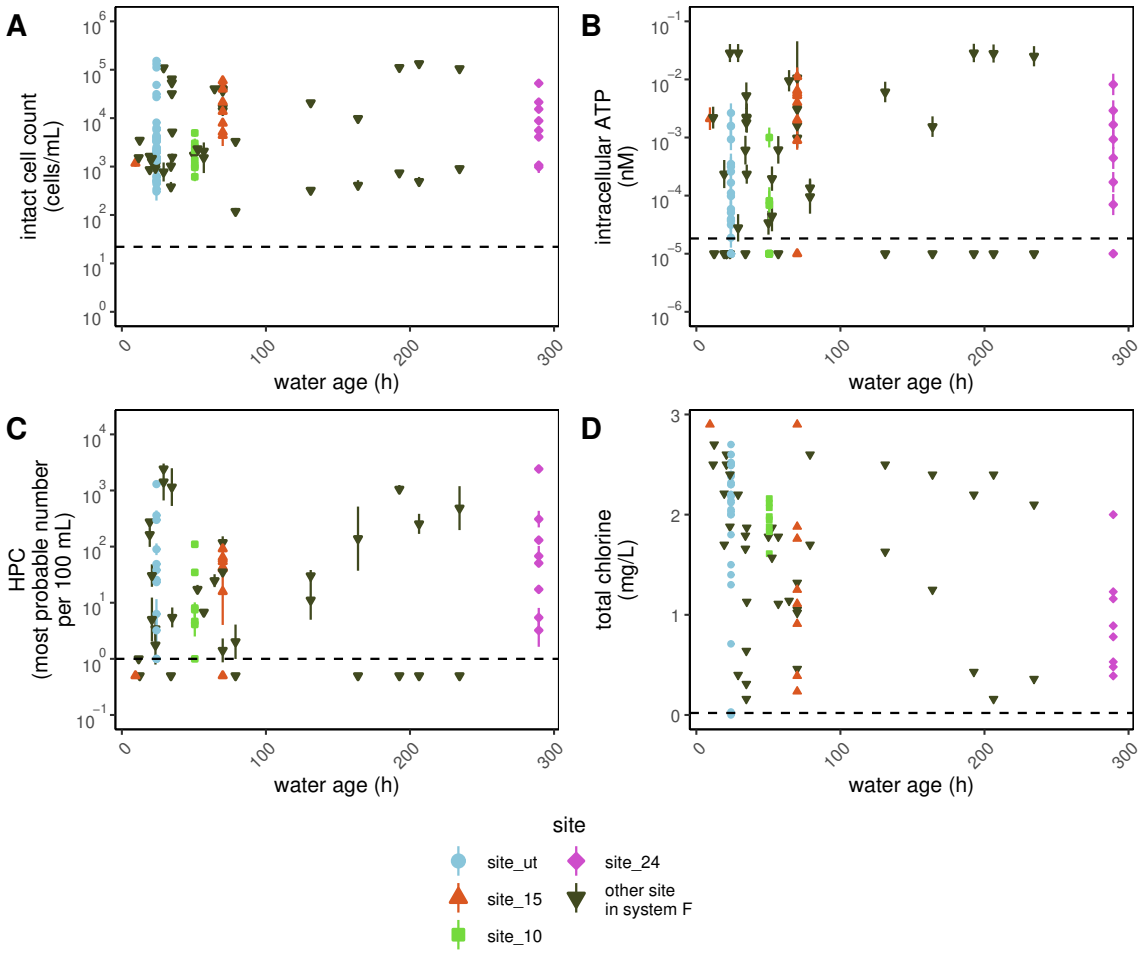

Figure 2.4: intact cell counts (A), intracellular ATP (B), HPC (C), and total chlorine concentration (D) by water age (hours) in distribution system F. Shapes denote locations in distribution system F that were sampled at least six times between August 2017 and April 2018. Horizontal dashed lines denote quantification limits for each assay. Points are the geometric mean of the technical replicates and error bars represent the variation associated with technical replicates as quantified by the geometric standard deviation for technical replicates.

Table 2.3: Percent of samples above quantification limit, below quantification limit, and quantifiable in all drinking water distribution systems sampled for this study for each microbial water quality assessment method. "n" is the number of samples per assay.

assay	n	percent quantifiable	percent below quantification limit	percent above quantification limit
intact cell counts	166	97.6	2.4	0
total cell counts	166	100	0	0
intracellular ATP	115	69.6	30.4	0
total ATP	115	100	0	0
HPC	102	81.4	14.7	3.9

Table 2.4: Ranges in coefficient of variation determined by geometric mean (%; min, median, and max) and average coefficient of variation (%) for replicates taken in all drinking water distribution systems sampled for this study for each microbial water quality assessment method. "n" is the number of samples per assay.

assay	n	min coefficient of variation	median coefficient of variation	max coefficient of variation	average coefficient of variation
intact cell counts	162	0.0266	9.78	148	16.9
total cell counts	166	0.318	6.15	255	17.0
intracellular ATP	80	42.9	48.6	328	56.0
total ATP	115	0.389	4.81	66.0	9.30
HPC	73	0	27.1	293	49.4

the arithmetic mean of all sample coefficients of variation (Table 2.4). Notably, variability was lower for total ATP (9.30%; Table 2.4), total cell counts (17.0%; Table 2.4), and intact cell counts (16.9%; Table 2.4), compared to intracellular ATP (56.0%; Table 2.4) and HPC (49.4%; Table 2.4).

2.4 Discussion

Five measures of microbial abundance were compared by surveying drinking water systems that apply residual disinfectants in California and Texas. In one chloraminated system, a generalized linear mixed model was used to estimate the effect of commonly measured

water quality parameters on intact cell counts. In the following sections, the purpose and interpretation of typical microbial water quality factors are discussed and the future role of enhanced measures of microbial water quality is considered for three applications: routine monitoring, diagnostics, and research.

Considerations for routine monitoring of drinking water systems

A key finding from this study is that disinfectant concentration in drinking water distribution systems provided an indirect measure of microbial abundance, which has useful implications for routine monitoring of distribution systems. Disinfectant residual had the largest inverse correlation coefficient regardless of residual type (Figures 2.2A and 2.2B). Furthermore, total chlorine had the greatest inverse effect on intact cell counts in a chloraminated drinking water distribution system (distribution system F). Gillespie et al. (2014) and Nescerecka et al. (2014) also surveyed disinfected distribution systems, but did not report trends between intact cell counts and disinfectant residual. Gillespie et al. (2014) sampled in chlorinated systems with free chlorine <0.8 mg/L as Cl_2 and recommend maintaining free chlorine above 0.5 mg/L as Cl_2 to keep the fraction of potentially viable cells below 0.2. In contrast, a similar trend was not observed with the fraction of viable cells (Figure A.2), but intact cell count decreased to <100 cells/mL at free chlorine concentrations above 1.5 mg/L as Cl_2. Intact cell counts were assessed at a wider range of disinfectant concentrations and a clear trend was observed between disinfectant residual and intact cell counts.

A proof of concept was presented that development of mixed models could help relate routinely monitored physicochemical data to intact cell counts in drinking water distribution systems. Drinking water providers in the United States commonly monitor pH, temperature, free chlorine, and total chorine, and these data were incorporated into a model to estimate intact cell counts using data from a chloraminated distribution system. The most optimal model (Equation 2) suggests that total chlorine had the largest effect on intact cell counts and that this effect depended on temperature. Zhang et al. (2002) also found that disinfectant concentration had an inverse effect on log-transformed HPC and visually observed higher values of log transformed HPC in the summer than in the winter, but statistical results were inconsistent, likely due to variability in HPC results. Using intact cell counts, instead of just the small fraction of total coliform bacteria or HPC, holds promise to model a commonly observed phenomenon: in summer, a higher residual disinfectant is necessary to maintain microbial water quality [235]. This study focused on routinely measured parameters in drinking water distribution systems in the southwestern United States, but more research is needed to expand the dataset and modeling approach. This approach could include a dataset that accounts for seasonal variability and source water quality changes as well as includes additional biological (e.g., assimilable organic carbon) and physicochemical parameters (e.g., total organic carbon concentration). However, including more parameters would require a larger sample size than was collected in this study (n=80). In addition, modeling completed using data from multiple distribution systems will introduce a nested dependency structure in which both samples from the same system will be correlated as well as samples from the

same site within a distribution system over time. With a more complete dataset, it might be possible to generate a model for which consistent deviations from model predictions at specific sites may be indicative of water quality problems, such as pipe corrosion or nitrification.

Intact cell counts and intracellular ATP assays as diagnostic tools

To better understand observed or expected changes in water quality, such the impact of nitrification, upgrading treatment processes, or incorporating a new treated water source (e.g., potable reuse), diagnostic monitoring can be necessary. However, the culturing methods commonly employed in routine monitoring, such as for total coliforms and HPC, often produce unquantifiable or unrepresentative results. For example, in a survey of U.S. drinking water providers, 57% of respondents reported never detecting total coliforms while the other 43% reported having fewer than 12 positive samples per year (n= 256 respondents; [216]). Similarly, the results of this study support previous claims that HPC vastly underestimates drinking water microbial abundance as compared with intact cell counts [148]. HPC only quantifies bacteria that can utilize organic nutrients for growth [146, 214] and they have been shown to comprise <1% of bacteria in some drinking water samples [207, 236]. Prest et al. (2016) reported a very high fraction of treated drinking water samples with HPC results below 5 CFU/mL while total cell counts ranged from $9.0x10^4$ to $4.5x10^5$ cells/mL.

For diagnostic purposes, use of intact cell counts would allow drinking water providers to detect changes in microbial water quality that are not observable using traditional microbial monitoring methods like HPC or total coliform quantification [214, 237, 238, 206, 148, 39]. In this study, 97.6% of samples had quantifiable intact cell counts. Only four samples were below the intact cell count quantification limit, which occurred at the highest residual concentration observed in chlorinated drinking water distribution systems (1.5 - 2.0 mg/L as Cl_2; Figure 2.1). Intact cell counts spanned four orders of magnitude in chloraminated systems (from <22 cell/mL to $1.09x10^5$ cells/mL) and more than two orders of magnitude in the chlorinated systems (<22 cells/mL to $2.12x10^3$ cells/mL). As might be expected, these cell counts were lower than those reported in other studies with lower maximum residual disinfectant values or in systems without disinfectant residuals. For chlorinated distribution systems, the maximum cell counts from this study are about 1000 times less than those reported in Gillespie et al. (2014). In addition, the geometric mean of intact cell counts of all distribution system samples in this study ($3x10^3$ cells/mL) was about 100 times lower than that of total cell counts reported for a system that does not apply a residual disinfectant ($1x10^5$ cells/ mL) [239].

Intracellular ATP may also be useful for diagnostic purposes because the values measured in this study correlated strongly with intact cell counts and ATP assays are less expensive. Drinking water providers monitoring microbial abundance for diagnostic purposes will need to choose measures of microbial abundance that maximize information gained and minimize expense. For this reason, it is important to consider how much each technique overlaps with other measures of microbial abundance and with chemical or physical water quality parameters. Intact cell counts and intracellular ATP results were strongly correlated (Figures

2.2A and 2.2B), and other studies have found similar correlations between ATP and intact cell counts among both chloraminated and chlorinated systems [70, 58, 236, 148]. The results in this study support the likelihood that most microbial abundance information will be obtained if either intact cell counts or intracellular ATP is measured. However, intact cell count was still more quantifiable and consistent compared to intracellular ATP. Intracellular ATP was quantifiable in only 69.6% of samples (Table 2.3) and technical replicates varied considerably (average coefficient of variation = 56.0%; Table 2.4). Thus, intracellular ATP may only be preferable when expense is a primary concern.

Assessment of biostability and risk in disinfected drinking water systems

While there is no evidence that the safety of drinking water is compromised simply due to variations in microbial abundance, microbial growth in distribution systems is generally considered to be a risk [206, 240, 241]. Choosing universal guidelines to maintain microbial water quality is not straightforward because microbial abundance is not directly linked to specific risks to infrastructure or public health. For example, setting a numerical operational limit for cell counts (e.g., 100 cells/mL) is not logical because microbial abundance varies considerably by water source and even within the same distribution system [59]. In lieu of numerical operational limits, researchers have proposed maintaining biologically stable water, in which microbial abundance and composition does not significantly change throughout a distribution system [242, 239]. However, biologically stable drinking water is difficult to maintain in disinfected drinking water distribution systems [59, 58] because disinfectant residual concentration has been shown to degrade in drinking water distribution systems as it reacts with pipe walls and organic matter (Figure A.4) [232]. In this study, disinfectant residual varied over a large range within chloraminated and chlorinated distribution systems, and there was a strong inverse correlation between the residual concentration and the microbial abundance.

Instead of maintaining biologically stable water, setting more subjective operational limits might be necessary in disinfected drinking water systems. Subjective operational limits have been set for HPC in the United Kingdom, France, the Netherlands, and Belgium where the upper limit is “no abnormal change” in HPC [148]. While it is difficult to define “normal” in drinking water systems, normal can be operationally defined by measuring microbial water quality under a range of conditions encountered in the system to establish a baseline and to discern contamination events from natural fluctuations [138, 140] that have been well documented in drinking water distribution system [243]. To establish a baseline microbial abundance in drinking water systems, water providers could monitor intact cell counts or intracellular ATP data throughout the range of chemical and physical water quality conditions encountered in their systems under routine operations. The generalized linear mixed model presented in this paper represents one way to establish such a baseline and the methodology could be applied in other systems.

To more thoroughly assess health risk in drinking water systems, more research is needed to pair absolute microbial abundance measures with assessments of microbial community composition and the concentration of specific pathogens of concern. Significant research is underway to characterize microbial communities in drinking water using high-throughput sequencing technologies (e.g., 16S rRNA gene amplicon and metagenomic sequencing). Some researchers have paired microbial abundance data with sequencing data using quantitative polymerase chain reaction (qPCR) methods to provide a deeper characterization of microbial water quality [244, 48, 245]. Combining qPCR with viability dyes brings a similar benefit as cell counts and ATP assays in that cell membrane damage can be used as a viability metric [171]. However, these methods have limitations discussed previously [246], including limited resolution (twofold changes in gene copies; [247]), bias introduced from assay design ([247, 248], and bias introduced with PCR [249]. Others have paired flow cytometry with sequencing data to provide a similar characterization of microbial water quality without bias introduced from PCR [247, 84, 38]. Ultimately, these studies may provide a sophisticated understanding of the complex interactions and factors that govern microbial ecology in drinking water systems. However, not all microbial ecology studies report absolute microbial abundance data. Pairing measures of microbial abundance with sequencing results has the potential to characterize microbial water quality in greater resolution than using any single method. This approach can provide more insight into risk in drinking water distribution systems including potential exposure to opportunistic pathogens and other microbially induced issues, such as pipe corrosion [17, 18], nitrification [21, 22], and aesthetic deterioration of finished water [250].

For meta-omics research, the microbial abundance measures in this study that will be most useful to include are intact and total cell counts. The flow cytometry results in this study indicate that a varied fraction of cells in the sites that were sampled were viable (Figure A.2). Intact and total cell counts are quantified by a fluorescent dye that intercalates with DNA [251] and are a more direct measure of microbial abundance compared to ATP assays. Though cell count data were correlated with ATP data, ATP results were varied and often unquantifiable in these systems. While total cell count is more reflective of the sequenced microbial community, intact cell count is more reflective of the risk imposed by the microbial community. Thus, both total and intact cell counts could be useful to pair with meta-omics data and provide a more informative assessment of microbial water quality in drinking water systems.

2.5 Conclusions

Applying measures of microbial abundance in piped drinking water systems can be useful for routine monitoring, diagnostics, and research. The results in this study support that disinfectant residual is an indirect measure of microbial abundance, and the necessity of pairing it with direct measures is questionable for routine monitoring. However, for diagnostic purposes, additional monitoring data in systems with large ranges in microbial and

physicochemical water quality conditions could help drinking water providers diagnose issues early and move beyond the goal of ensuring total coliforms are not detectable [243, 252]. For research, pairing meta-omics data with measures of microbial abundance can help researchers better characterize microbial water quality. The results in this study support that HPC assays are uninformative in these systems because these results are variable and often unquantifiable. Microorganisms are present throughout drinking water systems, and by limiting analyses to HPC, the true microbial water quality cannot be observed. Instead, either intracellular ATP or intact cell counts could be useful for diagnostic purposes and both intact and total cell counts could pair with meta-omics data. The main findings are summarized as follows:

- Intact cells were measured in all six piped drinking water distribution systems, including chloraminated sites with total chlorine > 2.5 mg/L as Cl_2
- Only 2.4% of sampling sites, with the highest free chlorine concentrations (i.e., 1.5-2 mg/L as Cl_2), had intact cell counts below quantification limits
- Residual disinfectant concentration was significantly and strongly correlated with intracellular ATP and intact cell counts in distribution systems
- Negative correlations between residual disinfectant concentration and intracellular ATP were stronger in chlorinated systems than in chloraminated systems
- The parameter that had the greatest impact on intact cell counts in a chloraminated drinking water distribution system was total chlorine concentration, which interacted with temperature
- Of the five measures of microbial abundance, only total cell counts and total ATP were quantifiable in all samples, but these assays do not assess viability of cells
- Total ATP had the least variability among technical replicates followed by intact cell counts and total cell counts

Chapter 3

Microbial impacts of transitioning a drinking water distribution system to a treated water augmentation system

3.1 Introduction

Water-stressed cities need diverse drinking water sources to become more resilient and prepare for future water demand. For many cities, direct potable reuse (DPR) could provide a relatively cost-effective and reliable source of drinking water compared to other alternative sources of water (e.g., seawater desalination [253]). In DPR systems, wastewater is treated to meet or even exceed the drinking water quality standards in the United States that are set for drinking water facilities that treat surface or groundwater (conventional treatment) [6, 91, 92, 93]. Even though wastewater contains more nutrients, pathogens, and other contaminants compared to ground or surface water, finished advanced-treated wastewater often contains fewer contaminants compared to finished conventional drinking water [78, 79]. Conventional treatment does not include the key components of advanced treatment that substantially improve water quality (e.g., reverse osmosis and advanced oxidation processes). Advanced-treated wastewater can be blended with either conventional surface water prior to treatment (raw water augmentation) or with finished conventional drinking water (treated water augmentation) [80]. Directly introducing advanced-treated wastewater into distribution systems circumvents treatment at a conventional drinking water facility, reduces the cost associated with treatment and, in some cases, reduces the cost associated with pumping advanced-treated wastewater to a drinking water treatment facility.

Microbial water quality in drinking water distribution systems will be impacted by the changes in water quality associated with transitioning a fully conventional system to a treated water augmentation system. However, expectations are limited for system-scale microbial issues that could arise during such transitions, partially because only three full-scale systems exist in the world [82]. In addition to a lack of full-scale systems to study, prior micro-

bial research simulating the introduction of advanced-treated wastewater to drinking water distribution systems is limited in scope (i.e., the transition from conventional treatment to advanced treatment has not been studied) [6, 89, 84, 85]. However, studies of conventional drinking water systems that have transitioned source waters or upgraded treatment could be applicable. For example, decreases in the concentration of nutrients feeding drinking water distribution systems could lead to chemical or microbial destabilization [254], which could expose consumers to microbial contaminants (e.g., sloughed opportunistic pathogens) [255]. Researchers have simulated the upgrade of conventional treatment to include membrane filtration and found that organic carbon and biomass decreased in bulk water and biofilm in simulated distribution systems [256, 257, 75], but full-scale upgrades in conventional treatment have been associated with biofilm sloughing [254, 71, 72]. Because of the limited experience in transitioning conventional drinking water systems to DPR systems, regulatory bodies in California have recommended applying enhanced microbial monitoring in drinking water distribution systems before and after transitioning to DPR [6].

The objective of this work was to characterize the impact on microbial community composition from transitioning a piped distribution system fed with surface water to a treated water augmentation system. Specifically, the objectives were to (1) evaluate the study design by comparing pipe loop feedwaters to their respective origins (i.e., full-scale drinking water distribution system or demonstration-scale RO permeate); characterize the impact on (2) bulk water and (3) biofilm microbial community composition of transitioning a conventional drinking water distribution system to a treated water augmentation system; (4) assess the potential for opportunistic pathogens to have higher absolute abundance in pipe loop rigs compared to feedwaters and respective origins. This study demonstrates the application of enhanced microbial water quality assessment before, during, and after transition to treated water augmentation in simulated distribution systems. Recommendations for future simulation studies are discussed.

3.2 Methods

In this study, five pipe loop rigs recirculated conventionally-treated drinking water that was either unaltered (conventional) or blended with advanced-treated wastewater (advanced blend; Figure 3.1). The advanced blends consisted of 90% conditioned reverse osmosis permeate from a demonstration-scale advanced wastewater treatment facility that was conditioned, stored, and then chemically disinfected in pipe loops reservoirs. All rigs underwent a one-week inoculation period with concentrated biomass from the full-scale conventional drinking water distribution system. Two transition loops were fed with only conventional feedwater for $\sim$ 10 weeks and then were fed with the advanced blend for $\sim$ 11 weeks. The transition loops were compared to a conventional control loop and two advanced blend loops that maintained the same feedwater over the study period. Grab samples for flow cytometry (total cell counts) were paired with concentrated bulk water and biofilm samples for 16S rRNA gene amplicon sequencing. The methods described in this dissertation have also been

described in Miller (2019).

Pipe loop rig design, start up, and operation

To simulate a transition to treated water augmentation, water from a full-scale conventional drinking water distribution system and from a demonstration-scale advanced treatment facility were used to feed pipe loop rigs that were located onsite at the conventional drinking water treatment facility. Five pipe loop rigs were designed to simulate drinking water distribution and were constructed identically using the materials that were most common in the full-scale conventional drinking water distribution system: PVC, copper, galvanized iron, leaded brass, and cement-lined ductile iron piping. 12 removable segments of 1-foot PVC pipe were included in each rig for biofilm collection. The pipe loops were designed to recirculate 100-L batches of water with residence times roughly equal for both the piping and reservoir sections of each rig (1.8 and 1.5 minutes respectively) to simulate drinking water distribution system conditions. During start up, pipe loop rigs were disinfected by recirculating 100-L of 100 mg/L as CL_2 of free chlorine, rinsed with four full batches of conventional drinking water, and then inoculated with concentrated biomass from the conventional drinking water distribution system (described in more detail in the bulk water collection section). The concentrated biomass was divided evenly across the five pipe loops and mixed with a fresh 100-L batch of conventional water. The pipe loops recirculated the inoculum for seven days, after which, Phase 1 of operation began (Figure 3.1).

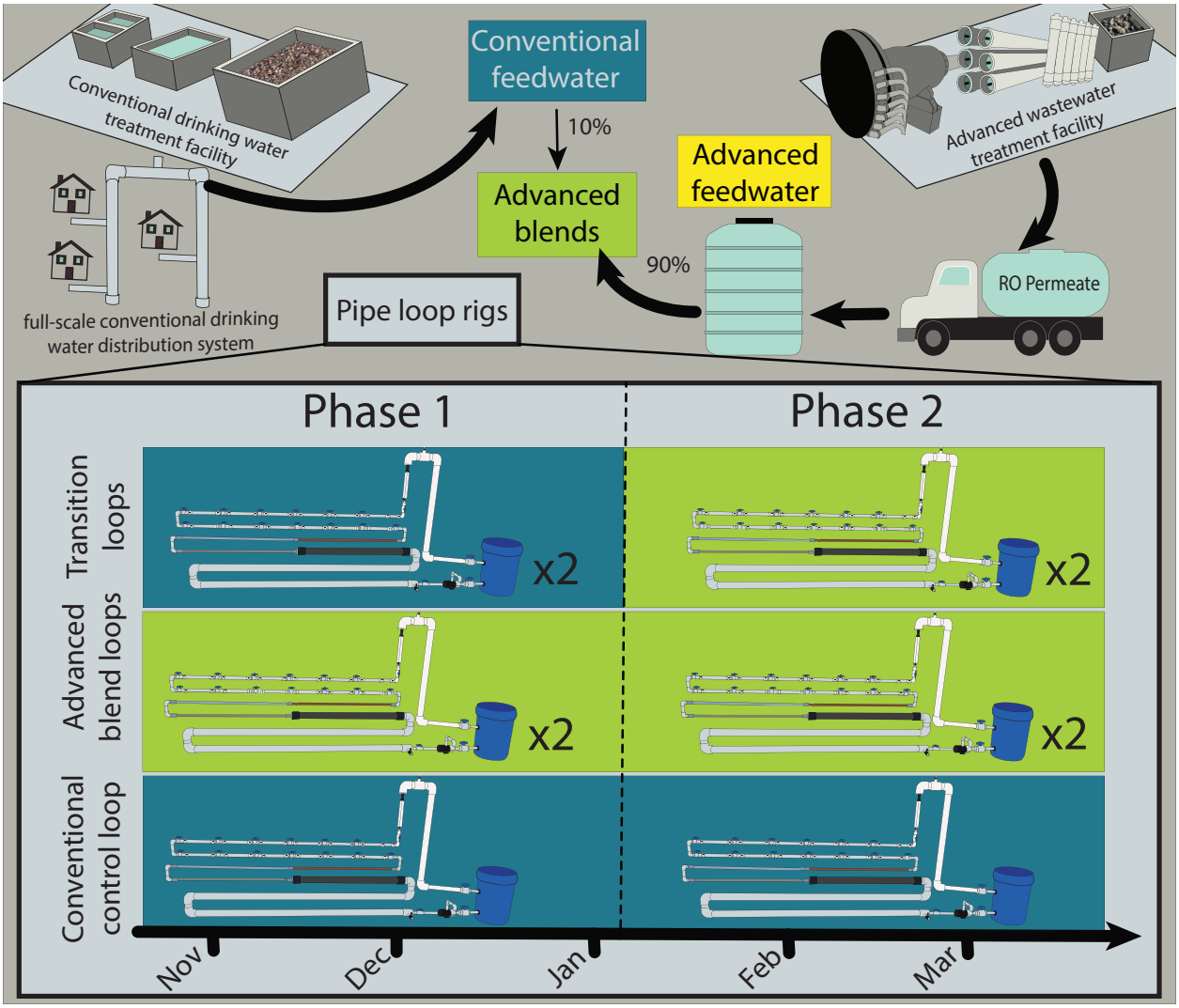

Figure 3.1: Pipe loop rigs were onsite at the conventional drinking water treatment facility (top left). Conventional feedwater originated from a tap in the full-scale conventional drinking water distribution system. RO permeate originated from the advanced wastewater treatment facility (top right) and was transported to the pipe loop site conditioned and stored until use. Advanced blends consisted of 10% conventional feedwater and 90% advanced feedwater. The bottom portion of the figure shows the feedwater composition in the pipe loops during Phases 1 (10/23/17-1/5/18) and 2 (1/5/18-3/26/18; with timeline represented by the arrow at the bottom).

Depending on the phase of the study, the pipe loops were fed with conventional water or advanced blend water (Figure 3.1). The chloraminated conventional drinking water was obtained onsite from the conventional drinking water distribution system (conventional feedwa-

ter). To compare the water quality in pipe loops to that in the full-scale distribution system, three additional sites in the distribution system were sampled six times throughout the study period (distribution system). The advanced feedwater originated from a demonstration-scale advanced wastewater treatment facility, at which tertiary-treated wastewater underwent ozonation, biological activated carbon filtration, microfiltration, reverse osmosis, and advanced oxidation. Reverse osmosis permeate (RO permeate) was transported from the demonstration-scale advanced treatment facility, conditioned with calcium hydroxide and carbon dioxide gas to achieve an alkalinity of 75-100 mg/L as CaCO3 and a pH of 8, and stored until use in a tank onsite at the conventional drinking water treatment facility (advanced feedwater; Figure 3.1). During batching, the pipe loops were drained entirely of water and refilled with 100 L of either 100% conventional feedwater or 10% conventional feedwater and 90% advanced feedwater (advanced blend). Pipe loops fed with the advanced blend also had a primary disinfection step completed in the reservoir with free chlorine followed by the addition of ammonia to produce a chloramine residual that is decribed in more detail in Miller (2019). The average water age in the pipe loops was 3.5 days, and the pipe loops recirculated over either a three-day or four-day batch period, with the exception of two short-term attempts to increase microbial activity in Phase 1: 1. Over four batch periods in November 2017, pipe loops recirculated over a seven-day batch period, and 2. over several batch periods in early December 2017, conventional feedwater was stored in a tank to allow for disinfectant decay over 3.5 days (instead of feeding directly to pipe loops).

Bulk water and biofilm concentration

Bulk water samples were collected from the full-scale drinking water distribution system sites, demonstration-scale RO permeate, feedwater to the pipe loops, and pipe loops (Figure 3.1). Before sample collection, taps were flushed at maximum flow rate for different time periods and volumes dependent on the sample: at least five minutes (distribution system, RO permeate, and conventional feedwater), at least two minutes (advanced feedwater hose), and about 1 L (pipe loop sampling ports). For all bulk water sampling locations, grab samples were collected in 500-mL autoclave-sterilized glass bottles with sodium thiosulfate in excess to quench chloramine residual, transported on ice, and stored at 4°C until flow cytometry analysis. Bulk water biomass was concentrated using dead-end ultrafiltration (DEUF) as per Smith et al. (2009) with different volumes concentrated depending on the biomass and volume available by sample type: pipe loop bulk water (60-100 L), pipe loop feedwaters (100-300 L), drinking water distribution system (350-900 L), and RO permeate (700-4,000 L).

The DEUF process involved three main steps: 1. Blocking: Ultrafilters (REXEED 25S, Henry Schein; Melville, NY) were "blocked" overnight before sampling with 5% w/v sterile-filtered bovine calf serum (catalog # 12133C; Fisher Scientific) as per Hill et al. (2005), and 1 L of sample was used to rinse the ultrafilter via crossflow filtration before the start of sample filtration. 2. Filtration: At sampling sites, the DEUF pump and ultrafilter setup were the as per Smith et al. (2009), and following filtration, all ultrafilter ports were

capped with autoclave-sterilized caps, and the ultrafilters were transported on ice for further processing. 3. Backflushing: In lab, the filtration setup was adjusted for backflushing as per Smith et al. (2009), and 500 mL of backflush solution (0.5% w/v Tween 80, 0.01% w/v sodium polyphosphate, and 0.001% w/v Y-30 antifoam emulsion) was pumped through the ultrafilter and collected in an autoclaved-sterilized 1-L glass bottle that was used for downstream secondary concentration using polyethylene glycol (PEG) flocculation.

Biofilm samples were collected from 12 PVC segments (length = 1 ft., diameter = 1 in.). During a biofilm sampling event, valves on either side of a segment were closed and the segment exterior was sterilized with 70% ethanol. The segment was removed, filled with 700 mL of 0.22-μm filtered bulk water from the respective pipe loop that was quenched with excess thiosulfate, capped, and transported on ice for further processing. A clean replacement PVC segment was produced by soaking a segment in 0.5% free chlorine solution for at least 30 minutes and thoroughly rinsing with conventional water. Removed PVC segments were sonicated (Branson 3510-DTH) in the laboratory in three steps. 1. The pipe segment was sonicated with one side submerged for 3 minutes with 100 mL of the filtered pipe loop bulk water inside the segment, and then the sonicated water was poured into a separate autoclaved-sterilized glass bottle. 2. The pipe segment was filled with an additional 100 mL of filtered pipe loop bulk water, rotated in the sonicator, and sonicated for an additional 3 minutes. This second set of sonicated water was combined with the first set of sonicated water. 3. The pipe segment was scraped with a sterile cell scraper (catalog # RPI-162423CS; Research Products International), filled with an additional 20 mL of filtered pipe loop bulk water, and shaken vigorously by hand for 15 seconds. The water was poured into an autoclave-sterilized glass bottle, the cell scraper was placed inside, and the bottle was sonicated for 30 seconds. This water was then combined with the first and second sets of sonicated water. In total, about 220 mL of water was recovered from the sonication procedure, and this recovered biomass was processed via PEG flocculation (the same procedure as bulk water samples).

PEG flocculation was used to concentrate sonicated water from biofilm samples and ultrafilter backflush from bulk water samples following a protocol from Mark Borchardt at the United States Department of Agriculture (USDA; Marshfield, WI). Briefly, backflush samples or sonicated biofilm samples were mixed with 1.15% w/v NaCl, 8% w/v polyethylene glycol 8000, and 1% w/v beef extract (catalog # DF0115173; Fisher Scientific). The solution was then kept at 4°C as it was stirred for 1 hour, incubated overnight, and centrifuged at 4,200 RPM for 45 minutes in a swing-bucket centrifuge. Supernatant was removed by decanting, and resulting pellets were resuspended in 1 to 4 mL of autoclave-sterilized tris-EDTA buffer and stored at -80°C for further processing through DNA extraction.

Pipe loop inoculum biomass and field blanks were also concentrated using DEUF and/or PEG flocculation. For the pipe loop inoculum samples, three premise plumbing taps in the conventional drinking water distribution system were filtered for 23 hours (6,070 L of tap water filtered in total). The filters were backflushed into autoclave-sterilized glass containers and stored at 4°C until inoculation of pipe loops ($\sim$10 days). Field blanks for DEUF sampling were prepared by blocking an ultrafilter, rinsing blocking solution with deionized water via

crossflow filtration, exposing the blank to conditions in the field without actually filtering, and then processing in parallel with bulk water samples. One field blank for pipe biofilm sampling was concentrated by filtering (0.22 μm) 225 mL of water from a pipe loop rig into a sterile bottle, keeping the bottle open during field sampling and laboratory sonication, and finally processing the water through PEG flocculation in parallel with biofilm samples.

Cell counts by fluorescent staining and flow cytometry

Total and intact cell counts were determined for bulk water grab samples as in Kennedy et al. (2020). Briefly, cell concentrations were measured using flow cytometry with SYBR Green I (S9430; Sigma-Aldrich, St. Louis, MO) and propidium iodide (30 mM P1304MP; Life Technologies, Carlsbad, CA) to distinguish cells with intact membranes. From each bulk water grab sample, a 1000-μL or 1500-μL aliquot of each triplicate was processed and the geometric mean and geometric standard deviation were calculated. Measurements were performed on two separate flow cytometers, an Accuri C6 flow cytometer (Accuri; BD Biosciences, San Jose, CA) and a BD FACSCanto cell analyzer (Canto; BD Biosciences, San Jose, CA). The Accuri was used to sample until February 6th, 2018, when it was sent in for repair, and the Canto was used for the remaining study period. The Accuri was equipped with a 50 mW laser emitting a fixed wavelength of 488 nm, and measurements were performed at the "fast" flow rate of 66 µL minute^{-1} on sample volumes of 50 μL. Microbial cell signals were distinguished and enumerated from background and instrument noise on density plots of green (FL1; 533 $\pm$ 30 nm) and red (FL3; >670 nm) fluorescence using FlowJo gating software (v10.5.3). Gate positions were modified slightly from a template publicly available for the BD Accuri C6 [147] to adapt for FlowJo software. The Canto was equipped with a 20 mW laser emitting a fixed wavelength of 488 nm, and measurements were performed at a flow rate of 1 µL s^{-1} for 50 seconds. Microbial cell signals were distinguished and enumerated from background and instrument noise on density plots of green (FTIC; 530 $\pm$ 30 nm) and red (PerCP; 695 $\pm$ 40 nm) fluorescence using FlowJo gating software. Gate positions were modified slightly compared to BD Accuri C6 gating based on calibration beads (Spherotech, Catalog # NFPPS-52-4K, Lake Forest, IL). For the Accuri, the lower quantification limits were determined for intact cell count (22 cells per mL) and total cell count (12 cells per mL) by Miller et al. using the same instrument used in this study [85]. For negative controls, 0.22 μm filtered, Millipore Milli-Q water was used.

DNA extraction, library preparation, and sequencing

DNA extraction from concentrated biomass samples was completed using a PowerSoil Pro extraction kit (Qiagen), with slight modifications. Briefly, sample pellets were thawed and vortexed for 10 seconds. For advanced feedwater, 200 μL of homogenized sample was added directly to each PowerSoil Pro Powerbead tube. For all other samples, sample homogenates were centrifuged at 34,000xg for 1 minute. The supernatant was aliquoted onto a centrifugal filtration unit (Amicon ultra-15 centrifugal filter unit; Millipore, Cork, Ireland) and the

pellet was stored on ice. The filtration unit was centrifuged at 7,500xg for 30 minutes and the concentrate was combined with the pellet and homogenized. 200 μL of the concentrated sample was added to the Powerbead Tube. The sample was incubated at 37°C for 30 minutes with an enzymatic digestion solution (50 μL of 0.001% lysozyme (Sigma-Aldrich, Damstadt, Germany), 50 μL of 0.00001% achromopeptidase (Sigma-Aldrich, Damstadt, Germany), and 8 μL of 0.01% carrier RNA in buffer AVL (Qiagen)). Solution CD1 was added to the sample (500 μL), and then the PowerSoil Pro kit was followed as specified by the manufacturer until the step immediately before elution, when a room-temperature incubation step was added (five-minutes). The sample was eluted and stored at -80°C until further processing.

Library preparation for amplicon sequencing followed the Schloss Lab MiSeq wet-lab protocol[1] for amplification of the V4 region of the 16S rRNA gene and Kantor et al. (2019), with slight modifications. Briefly, the V4 region was amplified using uniquely barcoded 515F and 806R primers with Phusion HotStart II polymerase (ThermoFisher Scientific), HF buffer (ThermoFisher Scientific), and 10 to 25 ng (up to 2 μL total) of genomic DNA. Triplicate 25 μL reactions were combined. For reactions that failed to amplify, 3% dimethyl sulfoxide and 0.2% bovine serum albumin were added (25 μL total reactions). At the Vincent J. Coates Genomics Sequencing Laboratory at UC Berkeley, the dual-barcoded libraries were pooled and then sequenced on an Illumina HiSeq 2500, yielding 150 bp paired-end reads.

Amplicon sequence data processing

Amplicon sequence data were processed as per Kantor et al. (2019) with slight modifications. Reads were demultiplexed, mapped to PhiX, and processed using DADA2 (v1.12.1) [261] to generate amplicon sequence variants (ASVs). Briefly, FastQC[2] was used to assess quality and to determine cutoffs for the following five quality control measures: 1. Truncation of all reads after 251 nucleotides (nts); 2. Trimming of all reads to remove 5 nts from the 5' end; 3. Truncation of a subset of reads where quality score dropped to 10 or below; 4. Removal of reads with expected errors greater than 1; and 5. Removal of reads with lengths less than 200 nts. The remaining reads were denoised, chimeras were removed from the dataset using removeBimeraDenovo, and taxonomy of sequences was assigned using the Ribosomal Database Project Naïve Bayesian classifier [262] trained using data from the SILVA database (v132) [263]. The resulting ASVs were analyzed using Phyloseq (v1.30.0) [264] in R (v3.6.2) [217].

Contamination in samples was assessed using DeSeq2 (v1.24.0) as per Kantor et al. (2019). In brief, samples were compared to extraction and field blanks and ASVs shared between samples and any negative control were determined. All of these ASVs were removed, except any ASV significantly enriched in samples over negative controls. Afterward, only samples with more than 300 reads were kept for further analysis.

[1] `https://github.com/SchlossLab/MiSeq_WetLab_SOP/blob/master/MiSeq_WetLab_SOP.md`

[2] `https://www.bioinformatics.babraham.ac.uk/projects/fastqc/`

The relative abundance of each ASV in each sample was determined and then Bray-Curtis dissimilarities were calculated. Non-metric multidimensional scaling (NMDS) of Bray-Curtis dissimilarities was completed for all bulk water samples as well as only pipe loop bulk water samples (i.e., not including samples from the full-scale distribution system, the demonstration-scale RO permeate, or the feedwater to the pipe loops). Clustering by sample date and feedwater composition was assessed in pipe loop bulk water samples using PERMANOVA (Vegan v2.5.6). Estimated absolute abundances were calculated for each sample by multiplying the relative abundance fraction with the total cell count measured.

3.3 Results and Discussion

Five pipe loop rigs were used to simulate the process of transitioning a conventional drinking water distribution system to a treated water augmentation system (Figure 3.1). The pipe loops were onsite at a conventional drinking water treatment facility, and conventional feedwater originated from a sampling site in the full-scale drinking water distribution system. The advanced feedwater originated as RO permeate from a demonstration-scale advanced wastewater treatment facility and then was conditioned and stored onsite until use. For Phase 1, the first 74 days of the study, pipe loops were fed with either 100% conventional feedwater (3 loops) or a blend of 10% conventional feedwater and 90% advanced feedwater (2 loops; advanced blend). In Phase 2, the last 80 days of the study, two of the conventional loops transitioned to the advanced blend and feedwater to all other loops remained the same as Phase 1.

Transport, conditioning, and storage altered the microbial community composition in the advanced feedwater to the pipe loop rigs

To evaluate the study design, the microbial community composition was compared in pipe loop feedwaters and the respective origins they were designed to represent (i.e., full-scale drinking water distribution system and demonstration-scale RO permeate). Ideally, the feedwater and origin samples would have similar microbial community composition. However, the microbial community composition in the advanced feedwater shifted compared to the RO permeate as evidenced by very few high abundance amplicon sequence variants (ASVs) were shared between the RO permeate and the advanced feedwater (Figure 3.2). While 43 ASVs were shared between the conventional feedwater and full-scale drinking water distribution system samples, only 10 ASVs were shared between advanced feedwater and RO permeate (Figure 3.3). Additionally, Bray-Curtis dissimilarities were compared using NMDS, and RO permeate samples clustered together tightly and separately from advanced feedwater, whereas the conventional feedwater overlapped with the full-scale drinking water distribution system but neither clustered tightly relative to the RO permeate and the advanced feedwater samples (Figure 3.4).

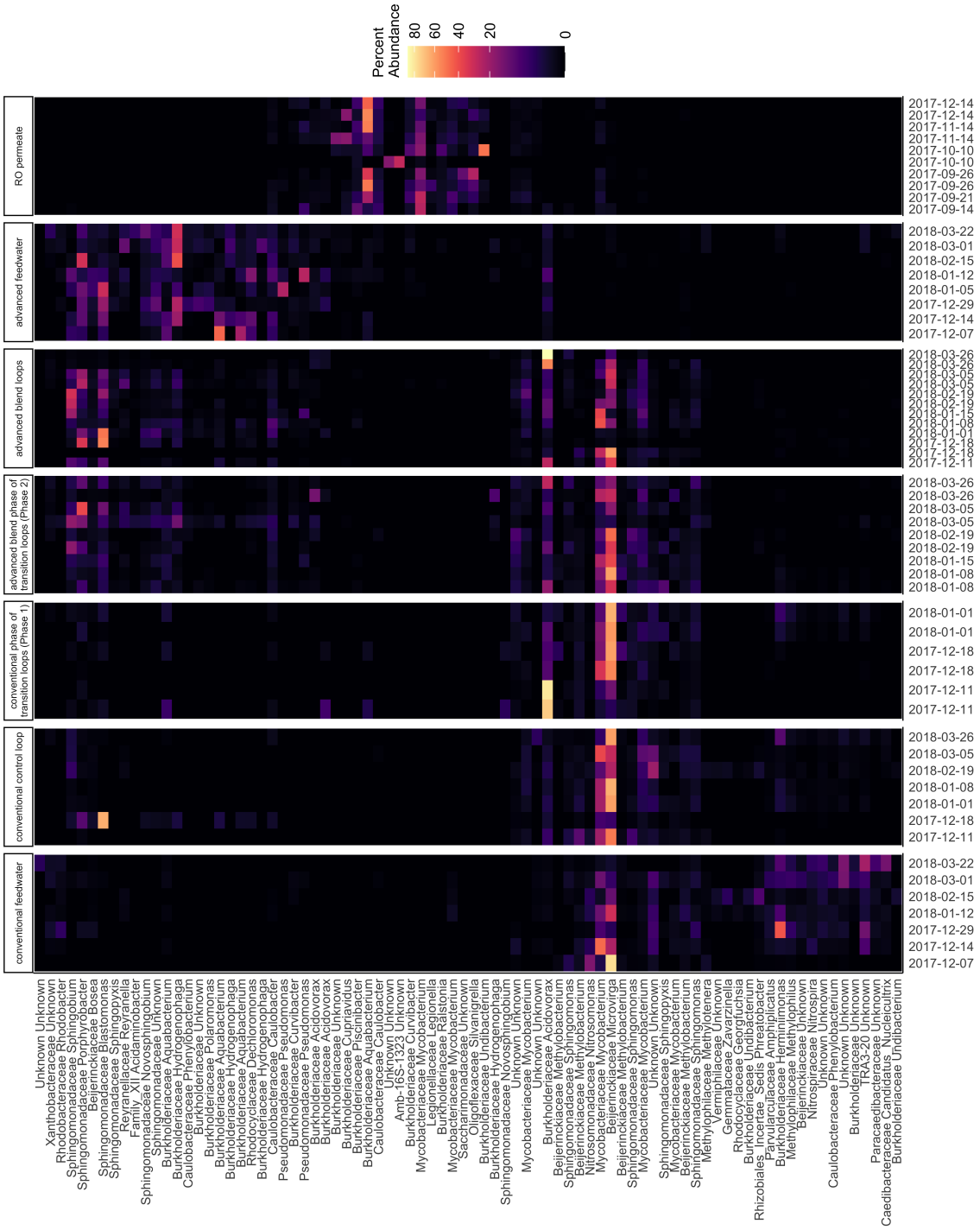

Figure 3.2: Heat map of relative abundances of ASVs (rows) by sample type (column facet) across sampling dates (columns). ASVs with a minimum of 3% abundance in at least one sample were included in the analysis.

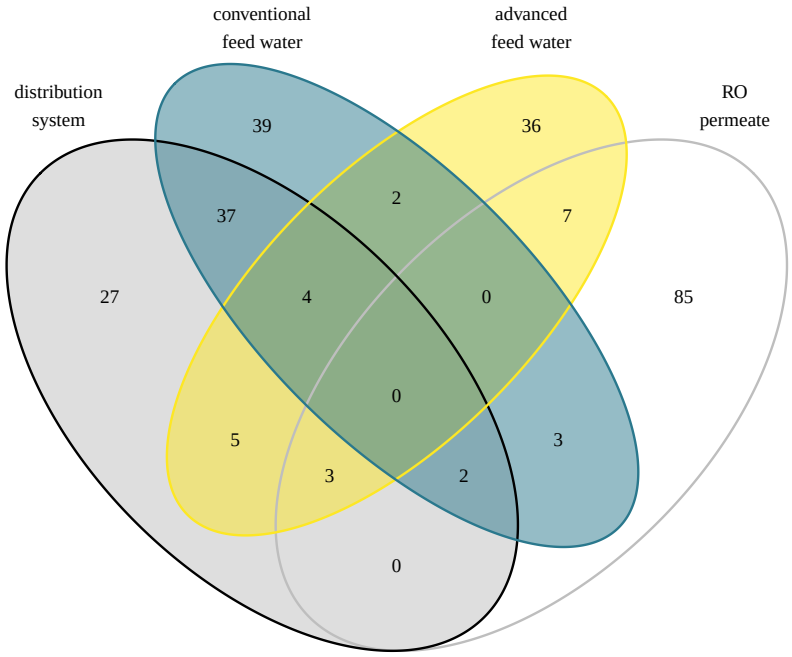

Figure 3.3: Comparison of recurring ASVs shared in pipe loop feedwaters compared to full-scale conventional drinking water distribution system and demonstration-scale RO permeate. Counts include ASVs with at least 100 reads in at least one sample from each location.

In this study, transportation, conditioning, and storage was only required for the demonstration-scale RO permeate because the pipe loop rigs were onsite at the conventional drinking water treatment facility. As a result of these experimental constraints, the conventional feedwater shared more high abundance ASVs with the full-scale drinking water distribution system samples compared to the amount of ASVs shared between the advanced feedwater and RO permeate. The only differences between the conventional feedwater and distribution system samples are sampling port (hose compared to tap) and water age (∼24 hours compared to between 9.43 and 289 hours). In contrast, the differences between RO permeate and advanced feedwater include transportation from the demonstration-scale facility to the pipe loops, conditioning to adjust the pH and alkalinity, and storage until use. Furthermore, large volumes of RO permeate (∼90 L of advanced feedwater) were required for each batching process for the advanced blend loops. Other studies assessing the impact of DPR on distribution system microbial communities only filtered about 1 L of water [84, 89] and simulated distribution systems were either located onsite with the advanced-treated wstewater [85, 84] or the impacts of storage on feedwater were not discussed [89]. Despite the changes

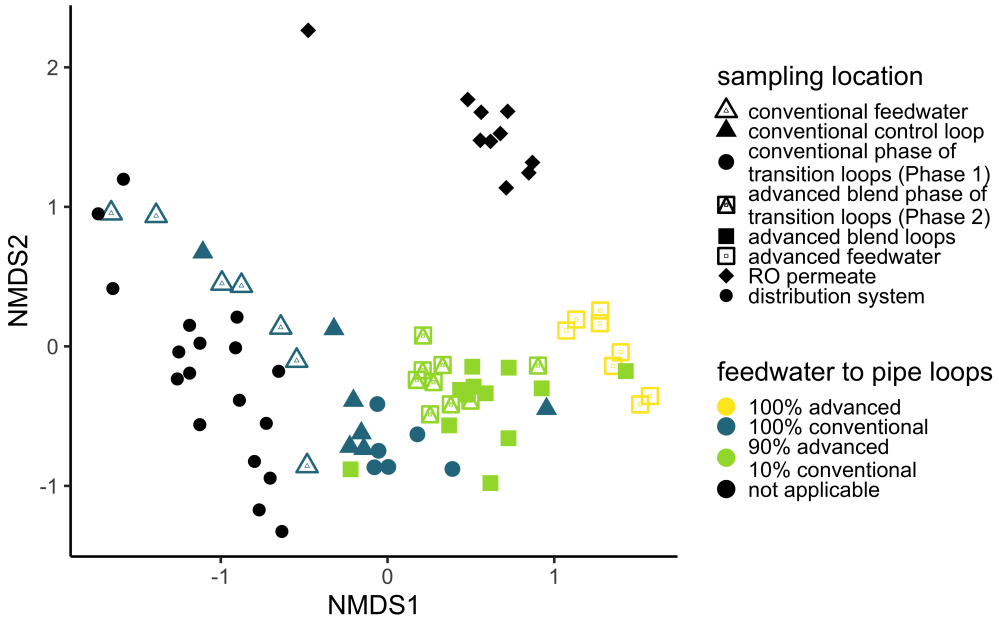

Figure 3.4: Non-metric multidimensional scaling of Bray-Curtis dissimilarity for all bulk water samples (i.e., pipe loop feedwaters, feedwater origins, and pipe loop samples) (stress= 0.17).

to the advanced feedwater microbial community composition in this study, these impacts are a conservative example of what could happen if advanced-treated wastewater is stored and conveyed without a disinfectant residual. Furthermore, even with the changes in microbial community composition in the transported, conditioned, and stored RO permeate, the advanced feedwater had a different microbial community composition than the conventional feedwater, which allowed for testing the impact of a transition in drinking water quality.

The pipe loop bulk water microbial community profile shifted depending on the feedwater composition

The feedwater was transitioned from 100% conventional to blends of 10% conventional and 90% advanced feedwater midway through the experiments in two pipe loop rigs (transition loops). To characterize the impact of transitioning to advanced blends on the microbial community composition of the transition loops, a comparison was made to the pipe loops that maintained the same feedwater composition throughout the sampling period. As expected, the advanced blend phase of the transition loops shared more unique and high abundance ASVs with the continuously operated advanced blend loops compared to the conventional phase of the transition loops (Figure 3.2). Specifically, the advanced blend loops shared three ASVs with Phase 1 transition loops (conventional) and eight ASVs with Phase 2 transition

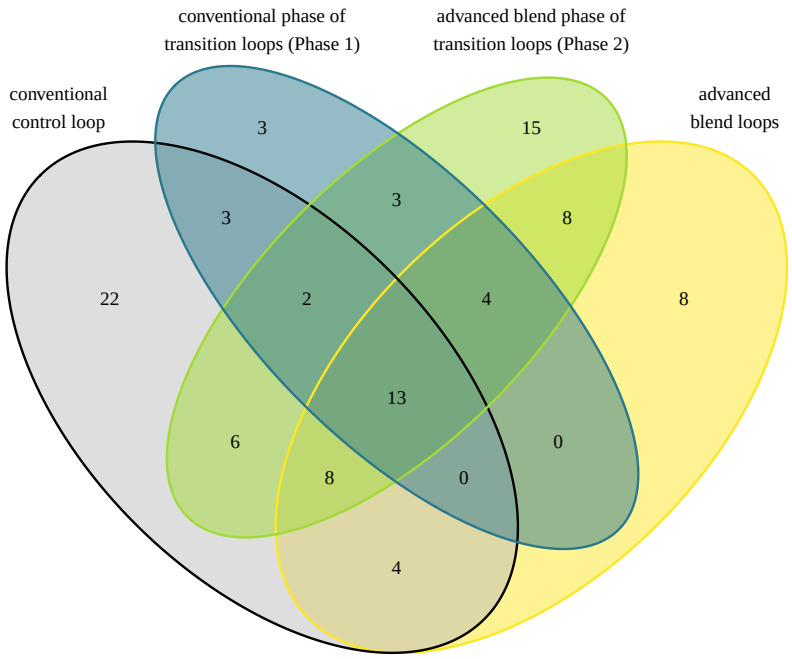

Figure 3.5: Comparison of recurring ASVs shared in transition pipe loop bulk water compared to pipe loops that maintained the same feedwater composition throughout the study period. Counts include ASVs with at least 100 reads in at least one sample from each location.

loops (advanced blends; Figure 3.5). In contrast, all pipe loops contained between 10% and 100% conventional water, and there were 13 shared ASVs across all pipe loop bulk water samples (Figure 3.5). Additionally, the transition loops had more distinct ASVs after transitioning to the advanced blend (15) than before (three) (Figure 3.5). Surprisingly, the conventional control loop, which was identical to the transition loops in Phase 1, had the most distinct ASVs (22) (Figure 3.5). One possible explanation is that the water quality of the conventional feedwater may have changed in Phase 2 of the study. Finally, Bray-Curtis dissimilarities in bulk water pipe loop samples were compared through NMDS (Figure 3.6), and samples clustered by feedwater composition (R^2= 0.26, p< 0.001) but not sample date (R^2= 0.03, p>0.05).

Introducing advanced feedwater to conventionally-fed pipe loops shifted the microbial community composition of the bulk water. A literature review did not reveal other work that assessed the microbial impacts of the transition from conventional to treated water augmentation in distribution systems. Other researchers have observed similar shifts in mi-

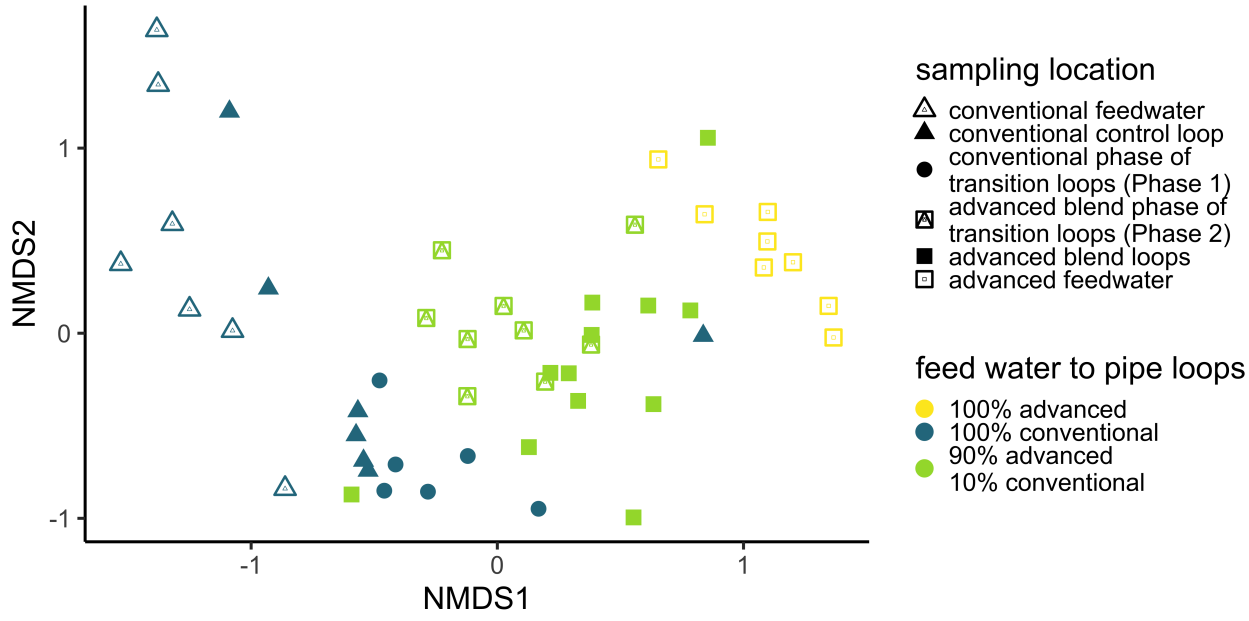

Figure 3.6: Non-metric multidimensional scaling of Bray-Curtis dissimilarity for pipe loop bulk water samples (stress= 0.16).

crobial community composition in conventional systems following the transition to a new feedwater or an upgrade in full-scale treatment [75, 71, 72]. However, the interpretation of the results of this study is limited by the confounding effects of transportation, storage, and conditioning of the RO permeate. Additionally, the advanced blend was not directly measurable prior to recirculation in the pipe loops because blending and disinfection occurred in batch and using the same volume of water filtered at the end of the batch period. Another inherent limitation of this study is that temporal changes in feedwater and other environmental conditions (e.g., ambient temperature fluctuations at the outdoor study site) could not be controlled for. Recommendations for future experimental design based on the limitations of this study are discussed in the conclusions of this chapter.

The bulk water and biofilm microbial community profiles of each pipe loop were similar throughout sampling and shifted depending on the feedwater composition

The microbial community profiles of pipe loop bulk water and biofilm samples were compared throughout the study period. The most abundant ASVs were similar within the same feedwater composition throughout the study in biofilm and bulk water (Figure 3.7). Similarly to the bulk water samples, the biofilm of the transition loops shared more high abundance

ASVs with pipe loops fed with the same composition of feedwater (Figure 3.7). However, the bulk water and biofilm microbial community composition in the transition loops shared more ASVs after the transition to advanced blends (41 or 84% of the ASVs in the biofilm of advanced blend transition loops) than in the conventional phase before the transition (21 or 53% of the ASVs in the biofilm of the conventional transition loops), with 20 of the ASVs shared across all conditions (40% and 50% of the ASVs in the biofilm of advanced blend and conventional phases of transition loops respectively; Figure 3.8).

The microbial community composition in the pipe loops shifted based on the feedwater composition, regardless of sample type (i.e., biofilm or bulk water). More ASVs were shared between bulk water and biofilm samples after transition to advanced blends, but microbial community profiles were similar in bulk water and biofilm samples of the same loop throughout the study, as others have observed [89]. Other researchers have observed shifts in microbial community composition in destabilized biofilm samples following upgrades in treatment that accompanyed biofilm sloughing in distribution systems [72, 71]. The findings in this study are limited because the experimental constraints affected the quality of the advanced feedwater. In this study, it might not have been possible to observe biofim destabilisation from introduction of low-nutrient water to distribution systems because the advanced feedwater after transportation was able to support the growth of more microorganisms than RO permeate [258], which suggests nutrients were introduced during transportation.

Estimated absolute abundances of genera containing opportunistic pathogens were low throughout the study

To assess the potential for opportunistic pathogens to have higher absolute abundance in pipe loop rigs compared to feedwaters and respective origins, estimated absolute abundances were calculated for all *Legionella*-, *Mycobacterium*-, and *Pseudomonas*- classified ASVs with at least 0.05% abundance in at least one sample (Figure 3.9). RO permeate was expected to have very few of these genera of concern. However, RO permeate had at least one ASV from each genera in at least 80% of samples (e.g., Legionella_ 144 and Pseudomonas_ 24). Six of the 18 *Mycobacterium*-classified ASVs were identified in at least 70% of RO permeate samples. Of the ASVs identified in RO permeate samples, two *Pseudomonas*-classified ASVs were observed in 100% of the advanced feedwater samples (24 and 55) and one was observed in >65% of the advanced blend loop samples (24). *Pseudomonas*-classified ASVs were otherwise identified in low percentages of samples (<45%). *Legionella*-classified ASVs were sparse in all sample types, including RO permeate (<33%), except one ASV in the conventional feedwater (67%; Legionella_ 245). In contrast, *Mycobacterium*-classified ASVs were found in all sample types with at least one ASV identified in 100% of samples, except for the advanced feedwater (<50% of samples).

Based on the assessment of opportunistic pathogen-containing genera, opportunistic pathogens of the genera *Mycobacterium* and *Pseudomonas* could be monitored more closely as qPCR targets. In this study, *Mycobacterium*-classified ASVs were identified in both

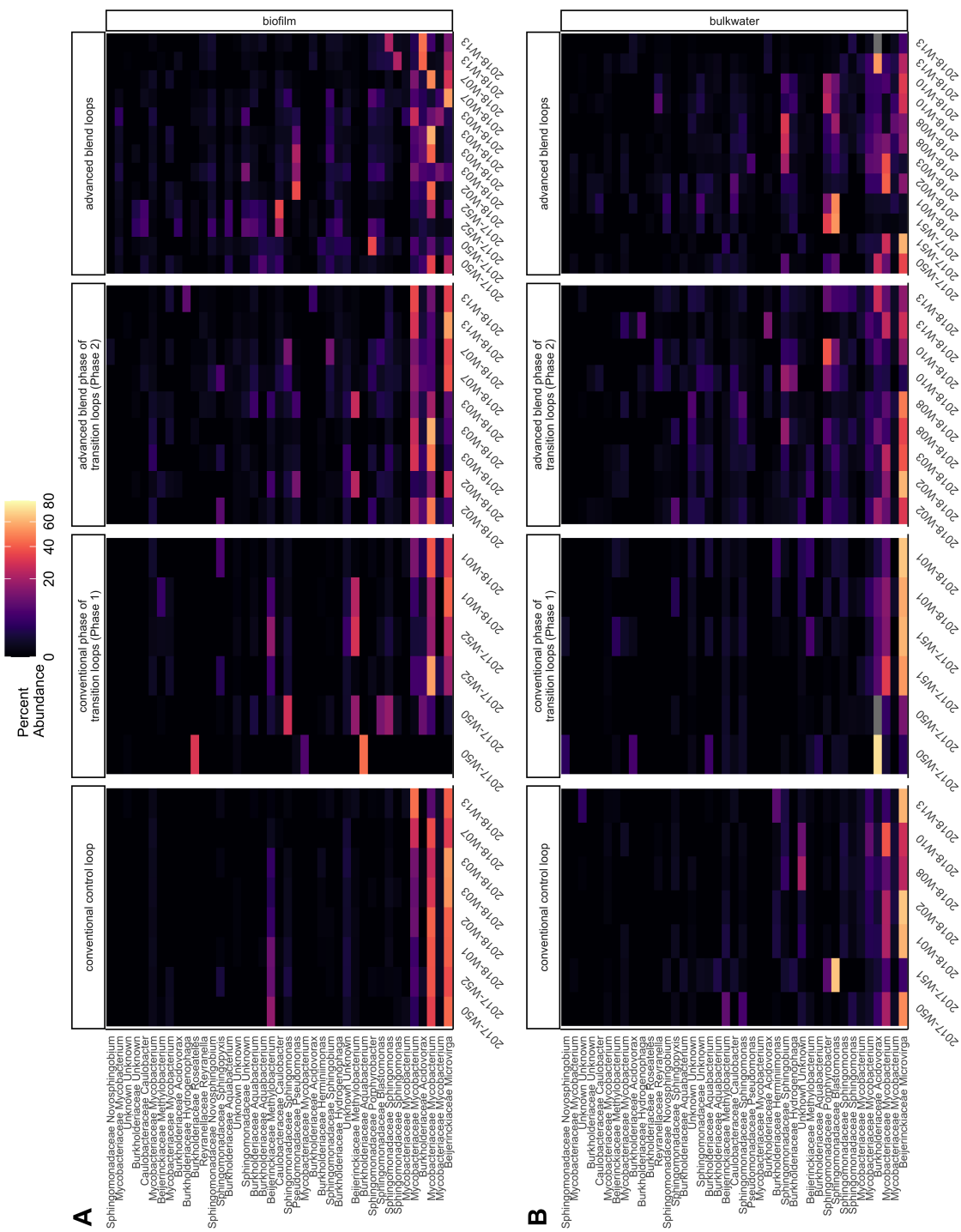

Figure 3.7: Heatmap of f biofilm (A) and bulk water (B) relative abundances of ASVs (rows) by sample type (column facet) across sampling dates (columns). ASVs with a minimum of 3% abundance in at least one sample were included.

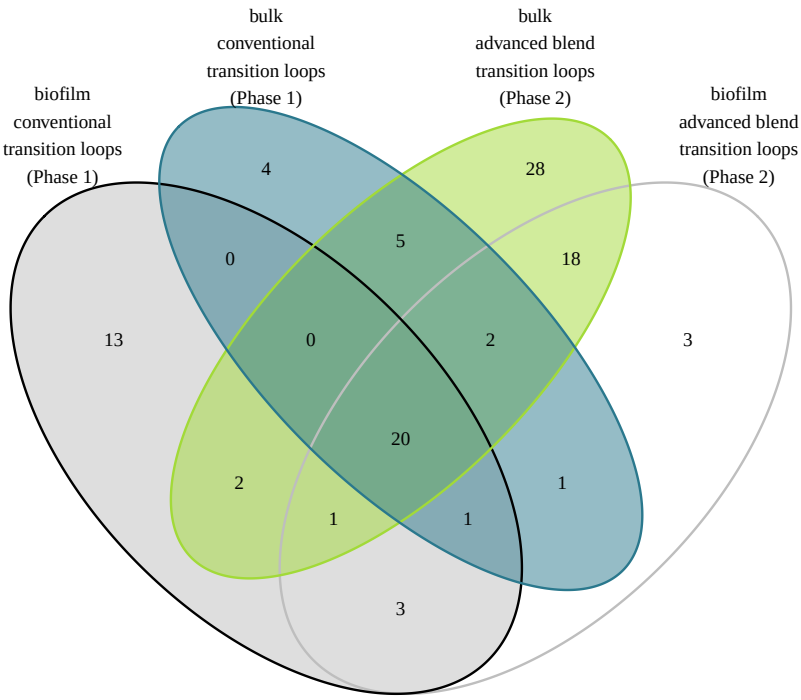

Figure 3.8: Comparison of recurring ASVs shared in transition pipe loops bulk water and biofilm samples. Counts include ASVs with at least 50 reads in at least one sample from each location.

full-scale drinking water distribution system samples and demonstration-scale RO permeate samples. Kantor et al. (2019) observed *Mycobacterium*-classified ASVs in simulated distribution systems fed with advanced-treated wastewater, and a similar maximum concentration to that of the advanced blend loops ($3.7\text{x}10^4$ compared to $4.2\text{x}10^4$, respectively). In this study, some *Mycobacterium*-classified ASVs were at higher abundance in the simulated distribution system compared to the RO permeate and drinking water distribution system samples. In contrast, Garner et al. (2019) found that *Mycobacterium spp.* gene copies decreased in pipe loops rigs relative to the advanced-treated feedwater. In addition, two *Pseudomonas*-classified ASVs increased in absolute abundance from the RO permeate to the advanced feedwater, and one remained at high abundance in the advanced blend pipe loops. These ASVs could have increased in abundance when exposed to the nutrients introduced during transportation of RO permeate [258], and warrant further study. In contrast, Garner et al. (2019) did not identify any *Pseudomonas aeruginosa* genes pipe loop rigs fed with advanced-treated wastewater or in the feedwater, and they found that all rigs fed with advanced-treated wastewater did not support the growth of any opportunistic pathogens

quantified. *Legionella*-classified ASVs were not found in as many samples as the other genera, possibly because of the chloramine residual applied in this study [265, 266, 51]. Results from 16S rRNA gene amplicon sequencing do not reveal if the ASVs identified are actual opportunistic pathogens or even if they were viable, but the methods shown here can be used to select targets to monitor more closely in the future with qPCR (such as *Mycobacterium Avium* complex and *Pseudomonas aruginosa*).

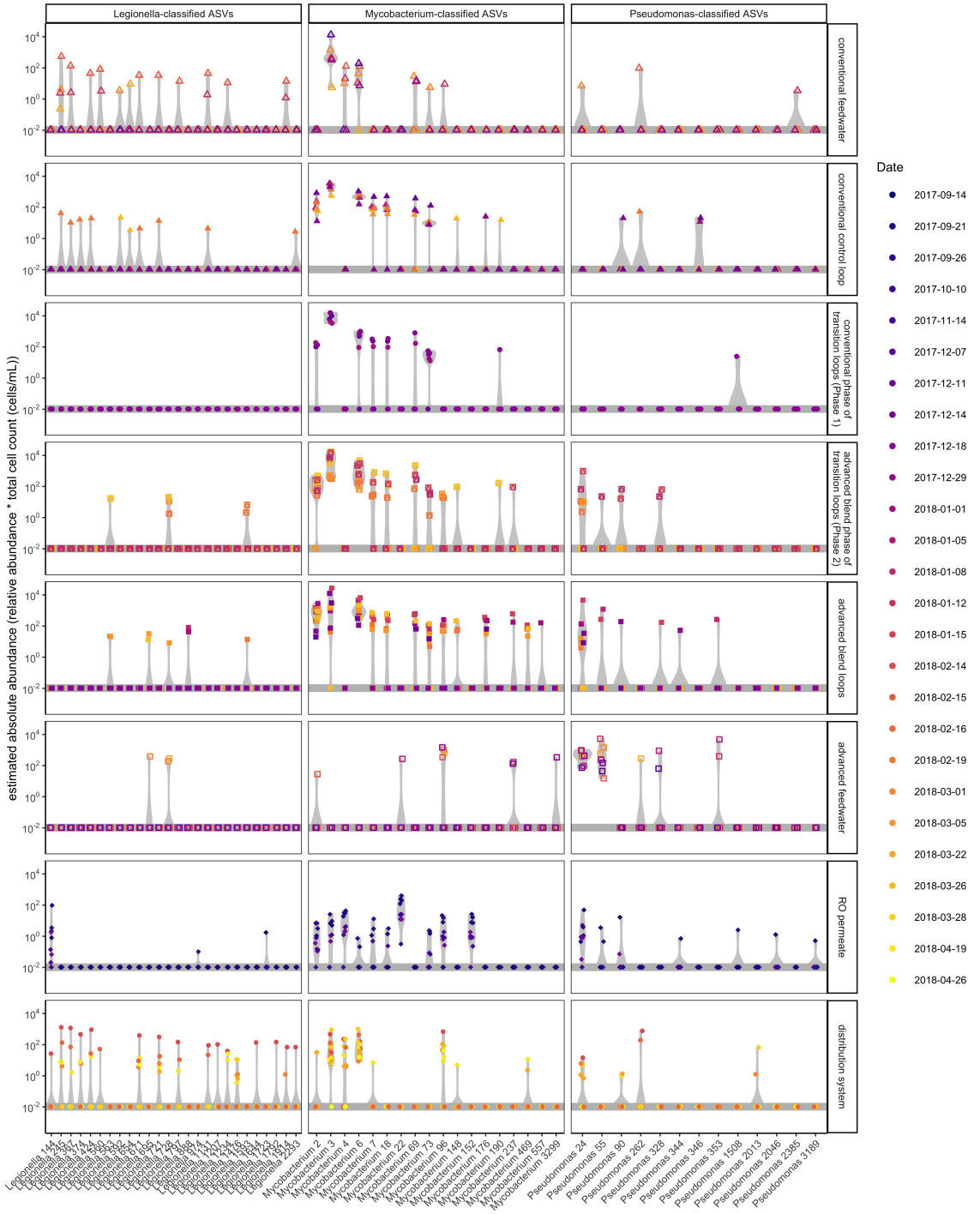

Figure 3.9: Estimated absolute abundances of potential opportunistic pathogens. ASVs (x-axis) are grouped by genera (column facets) and by sampling location (row facets). ASVs with 0% abundance are plotted on the grey horizontal line for visualization.

3.4 Conclusions

Though studies simulating the process of transitioning a fully conventional drinking water distribution system to a treated water augmentation system cannot fully capture the microbial issues that could arise during a full-scale transition, these studies can help prepare for a full-scale transition. For example, paired flow cytometry-based cell counts and 16S rRNA gene amplicon sequencing could be used in enhanced monitoring programs to identify microbial targets to monitor more closely using qPCR. However, key considerations need to be taken during design of simulation studies that include enhanced microbial assessment. This work is one of few studies investigating microbial community composition in distribution systems fed with advanced-treated wastewater. Based on the challenges encountered during this study, the following considerations are recommended for future studies:

- Despite the high water quality (e.g., low concentrations of organic carbon and nutrients) and low cell counts of advanced-treated wastewater, microorganisms will still be seeded and grow in RO permeate. Transporting advanced-treated wastewater for experiments should be avoided if possible or should mimic anticipated full-scale conditions. Rather, an ideal experimental setup would be located where the advanced-treated wastewater is produced. If that is not possible, as was the case in this study, only advanced-treated wastewater with a disinfectant residual should be transported and/or stored for microbial studies.

- DPR studies of microbial community composition in simulated distribution systems require controls and replication. DPR studies generally include samples from a large range in cell counts and nutrients, particularly if the advanced treatment facility is sampled (e.g., secondary treated wastewater to advanced oxidation). In this study, RO permeate was sampled and required large volumes of water to be filtered to collect enough biomass for high resolution of the microbial community composition (i.e., up to 4,000 L in this study). The negative controls that were collected during field sampling, extractions, and PCR helped with identification of contamination in these samples. Additionally, two comparisons were pivotal to contextualization of results (1) comparison of feedwaters to respective origins and (2) comparison of advanced-blend loops to the conventional control loop. Finally, several pipe loop rigs in this study had replicated experimental conditions. This decision was difficult to make considering the cost of operation and potential to add in additional conditions (e.g., other blend ratios). Yet, replication was important because even though pipe loop materials were all purchased from the same location, there were still inconsistencies between replicates for important chemical parameters, such as lead, as discussed in Miller (2019). While these did not notably alter the microbial community composition between transition loop replicates, it demonstrates the importance of having replicates to compare. Having at least two replicates for each condition (ideally three) is recommended for future studies.

- In general, collecting enough biomass to characterize changes in microbial community composition requires more water and more stringent sterile conditions compared to what is needed for chemical analyses, particularly if meta-omic techniques will be employed. Researchers studying both microbial and chemical impacts of treated water augmentation should consider trade-offs in experimental design.

- Pipe loop rigs can provide a higher volume of water for biomass collection compared to lab-scale annular reactors, but a trade-off has to be made with respect to choice of operation as continuous flow systems or batch systems. Continuous flow operation is advantageous from a labor perspective and does not require circulation of water, but it also requires residence times, pipe diameters, and shear forces that do not mimic full-scale distribution systems. In contrast, batch operation provides more flexibility in design to mimic full-scale distribution system residence times, pipe diameters, and shear forces, but circulation of water is required and batching large-volume systems likely requires more labor and time than flow through systems of the same volume.

Chapter 4

Assessment of SARS-CoV-2 wastewater testing as a public health surveillance strategy

The following chapter is adapted from Greenwald and Kennedy et al. (2021). Interpretation of temporal and spatial trends of SARS-CoV-2 RNA in San Francisco Bay Area wastewater, medRxiv : the preprint server for health sciences, with permission from Hannah D. Greenwald, Adrian Hinkle, Rose S. Kantor, and Kara L. Nelson.

4.1 Introduction

Increasing hospitalizations and limited diagnostic testing capacity early in the coronavirus disease 2019 (COVID-19) pandemic made it clear that multiple and robust methods to test circulation of severe acute respiratory syndrome coronavirus 2 (SARS-COV-2) are needed [37]. COVID-19 wastewater-based epidemiology (WBE) might serve this purpose because SARS-CoV-2 RNA has been detected in stool of infected individuals [32, 31, 33, 36, 35, 268] as well as in wastewater and sludge by researchers globally [130, 108, 134]. Together, WBE and clinical assessment of population-level COVID-19 occurrence might provide more reliable information about disease burden in communities than either method could provide alone. Clinical testing of individuals is resource-intensive and has well-known biases (e.g., selection bias based on symptom severity, symptom recognition, occupation, etc. [122, 121]), which have compounded negative impacts in communities with higher proportions of low-income residents and of Black, Indigenous, and People of Color, including in the San Francisco Bay Area [269, 270]. In contrast, WBE may provide a less biased assessment of COVID-19 occurrence [120, 121], but a better understanding is needed of the variability of SARS-CoV-2 in wastewater and how it relates to the occurrence of COVID-19 in the contributing population.

Smoothing procedures can assist in discerning temporal trends in SARS-CoV-2 occur-

rence. While seven-day moving averages have been widely used for assessing clinical data trends in real-time (e.g., the Johns Hopkins University of Medicine Testing Trends Tool[1]) wastewater sampling is often performed only 1-3 times per week. Therefore, smoothing techniques are needed that can be applied to data with lower sampling frequency that minimize loss of temporal resolution, such as locally weighted scatterplot smoothing (Lowess) [271, 272, 132, 106]. However, no standard value for the bandwidth parameter exists (analogous to the selection of a seven-day window for moving averages of clinical data) and the default parameter differs for two common languages used for data analysis (R spatialEco package:[2] 0.75 and Python statsmodels:[3] 0.67). Furthermore, the bandwidth selection process generally has not been specified in studies incorporating Lowess [271, 272, 132, 106].

Systematic approaches are also needed to estimate the minimum number of clinical COVID-19 cases for which SARS-CoV-2 RNA is reliably detected in wastewater (WBE case detection limit). The WBE case detection limit is dependent on the methods used to extract genetic material as well as the extent of local clinical testing and may require sewershed-specific assessment. However, a systematic approach to estimate this value across studies can aid interpretation of nondetects and elucidate the number of COVID-19 cases per capita above which COVID-19 WBE will be a reliable public health surveillance strategy. Wu et al. (2021) developed a systematic method for determination of a WBE case detection limit estimated using a dataset with 1,687 samples, which was large enough to include repeated wastewater measurements at low case numbers. With fewer data points, researchers have estimated this value observationally by reporting the number of cases they were able to detect or quantify [107, 105].

Finally, SARS-CoV-2 RNA signal in wastewater has been shown to provide lead time of population-level increases in occurrence compared to clinical testing data in some locations [105, 107, 118, 106, 114, 119, 115, 109], but there are discrepancies in the way wastewater data and clinical data are reported that complicate this assessment. Data collected by both clinical and wastewater testing laboratories can be associated by the sample collection date (e.g.,the date the nasal swab or wastewater composite sample was collected) or by the result date, which is highly influenced by the testing capabilities of the laboratory. Peccia et al. (2020) found that differences in clinical data date association alone could be the difference between no lead time and eight days lead time in the SARS-CoV-2 signal from wastewater compared to clinical testing data. However, the extent to which date discrepancies affect perceived wastewater lead times is still unclear and important to consider in assessments of early warning of outbreaks through wastewater testing.

The goal of this study was to develop and assess approaches for interpretation of SARS-CoV-2 signal in raw wastewater and compare with geocoded clinical testing data during the COVID-19 pandemic. The objectives of this research were to (i) evaluate a systematic method for trendline smoothing; (ii) apply this method to interpret spatial and temporal

[1] https://coronavirus.jhu.edu/testing/tracker/overview

[2] https://rdrr.io/cran/spatialEco/src/R/poly.regression.R

[3] https://www.statsmodels.org/dev/_modules/statsmodels/nonparametric/smoothers_lowess.html#lowess

trends in COVID-19 occurrence based on wastewater and clinical testing data (iii) develop a systematic method for estimating a WBE case detection limit; and (iv) determine whether wastewater trends lead clinical trends and could provide early warning of COVID-19 outbreaks. From April to September 2020, SARS-CoV-2 RNA in raw wastewater was measured weekly from five locations in the San Francisco Bay area. This dataset has variable trends in clinical testing data to assess correlation and smoothing and a wide range of COVID-19 per capita cases to enable assessment of WBE case detection limit.

4.2 Methods

Five locations in the San Francisco Bay area were sampled for this study (referred to throughout as locations A, S, N, K, and Q). Raw wastewater samples were collected weekly from April to September 2020, and biological replicates were processed for some locations as indicated in Table 4.1. SARS-CoV-2 and crAssphage were measured in wastewater samples via RT-qPCR in the laboratory. Associated physicochemical data were collected by wastewater utilities, and associated geocoded clinical COVID-19 data were collected by public health departments (Table 4.1). The methods described in this chapter are also described in Greenwald and Kennedy et al. (2021).

Wastewater composite sample collection

24-hour time-weighted composite samples of raw wastewater were collected using Teledyne ISCO autosamplers. Some samples were collected and processed in biological replicate (i.e., wastewater subsamples were aliquoted from the same composite sample but independently extracted). After collection, all samples were transported to the lab on ice, stored at either -20°C or -80°C, and then thawed at 4°C for 36-48 hours before hours before extractions. Wastewater data was not individually identifiable; therefore, no IRB was needed. More information on location-specific data collection and wastewater sampling, transport, storage, and biological replicates is provided in Table 4.1 and Appendix C.

One rainfall event occurred (May 12-19) during which sampling locations experienced 0.8 to 1.8 inches of precipitation (NOAA Climate Data Online database). Although none of the sampled locations was a combined sewer system, rainfall could still increase flow rates through infiltration and inflow. Daily wastewater flow rate values during this period varied <4%, which is negligible when compared to the near 100-fold increases observed during rainfall events in some sewer systems [274].

Clinical testing and population data

Geospatial vector data of the sewersheds (locations S, K, A, and N) were used to determine the COVID-19 clinical testing data that mapped to each wastewater catchment area (Table 4.1). For all locations, daily new case data correspond to the date that results were reported

Table 4.1: Descriptions of wastewater sampling locations including associated wastewater facility, clinical testing data sources, population, and flow rates. "d" represents the number of unique dates on which samples were collected. "n" represents the total number of wastewater samples collected, including biological replicates. For location Q, the population and clinical data is from people incarcerated only and does not include staff.

wastewater catchment area	wastewater treatment facility	COVID-19 clinical data source	population	mean flow rate (MGD)	mean per capita flow (L/person/ day)	d	n
Location K influent to the wastewater treatment facility	Central Contra Costa Sanitary District	Contra Costa County Public Health Department	483,600	33	261	13	39
Location S upstream of the wastewater treatment facility	East Bay Municipal Utility District	Alameda County Public Health Department	469,344	35	282	20	22
Location A upstream of the wastewater treatment facility	East Bay Municipal Utility District	Alameda County Public Health Department	82,818	6	274	11	17
Location N upstream of the wastewater treatment facility	East Bay Municipal Utility District	Contra Costa County and Alameda County Public Health Departments	139,037	10	272	18	18
Location Q wastewater collection point for San Quentin Prison	Central Marin Sanitation Agency	California Department of Corrections and Rehabilitation open data portal	Ranges from 3,587 (June) to 2,930 (September)	0.41	481	10	11

(result date) for each COVID-19 test. For location K, additional data were available that correspond to the sample collection date and the episode date, defined as the earliest of: (i) the date of first symptoms; (ii) the sample collection date; or (iii) the date the sample was received by the testing lab. Clinical testing data were provided by the corresponding county or open data portal (Table 4.1). Data were masked by public health departments to maintain confidentiality of the contributing population (below 11 new cases per day) and were provided as 7-day (A, S, K) or 14-day (N) moving averages. Masked values were substituted at 5.5 new cases per day for further analysis and plotting. For San Quentin Prison (location Q), unmasked COVID-19 clinical data were obtained from the California Department of Corrections and Rehabilitation open data portal,[4] and instances of zero cases were substituted at 0.5 cases for comparison to masked data in statistical data analysis (Figure 4.4). For clinical data obtained for this study, no IRB was needed because data were either provided masked or were publically available. More information about masking and population data is provided in Table 4.1 and Appendix C.

Wastewater sample processing via the 4S method

Samples were concentrated and extracted following the 4S method as detailed in a publicly available protocol[5] and in Whitney et al. (2021) with a minor modification: elution buffer was not pre-warmed; instead, it was added to the column, and the column was heated at 50°C for 10 minutes before centrifugation to collect the eluate. Each extraction batch contained a negative extraction control, and each sample or control was spiked with a surrogate virus control (Bovilis coronavirus; Merck Animal Health, BCoV) and a free RNA control (synthetic oligomer construct, SOC). Because it is not possible to independently quantify the surrogate spike without the influence of extraction efficiency [275], extraction controls were used to assess consistency of extractions rather than recovery. Outlier analysis (alpha=0.05) was conducted for BCoV and SOC Cq values using Grubbs test. No outliers were detected, and all samples tested were considered to have passed this quality control screen. Wastewater sample processing is further described in Appendix C.

RT-qPCR plate setup,controls, and data processing

Reverse transcription quantitative polymerase chain reaction (RT-qPCR) was performed on wastewater extract targeting five sequences: (i) SARS-CoV-2 CDC nucleocapsid gene (N1) assay duplexed with (ii) VetMAX^{TM} Xeno^{TM} Internal Positive Control (Xeno) assay; (iii) crAssphage CPQ_056 (crAssphage) assay [276]; (iv) bovine coronavirus transmembrane protein gene (BCoV) assay [277]; and (v) Synthetic Oligomer Construct T33-21 free-RNA (SOC) assay [278]. Reaction conditions (Table C.1), thermocycling conditions (Table C.2), and primers, amplicon sequences, and probes (Table C.3) are included in Appendix C. Reactions consisted of 20 μL total volume, including 5 μL of RNA extract, TaqMan Fast

[4] https://data.ca.gov/dataset/cdcr-population-covid-19-tracking

[5] https://www.protocols.io/view/v-4-direct-wastewater-rna-capture-and-purification-bpdfmi3n

Virus 1-Step Master Mix (ThermoFisher Scientific), primers, probes, and nuclease-free water. Reactions were completed on a QuantStudio 3 Real-Time qPCR system (ThermoFisher Scientific), where Cq values were determined through automatic thresholding on QuantStudio 3 Design and Analysis Software (v1.5.1). Every plate included samples, no template controls (NTCs), and standards, each quantified in technical triplicate (qPCR replicates). Individual standard curves were used as a quality control measure (efficiencies ranging from 83.2% to 97.8% and R^2 ranging from 0.974 to 0.999 for the N1 assay) and were later combined into master standard curves (Table C.5) to calculate quantities as in Ahmed et al. (2020). Further details on RT-qPCR materials are provided in Appendix C.

Raw Cq values that did not amplify or that amplified below the limit of detection were substituted with the Cq value corresponding to half the limit of detection (for N1) or half the lowest point of the master standard curve (for all other assays; TableC.5), and then outliers were assessed using a two-sided Grubbs test (alpha=0.05). The N1 qPCR limit of detection (LoD) was calculated by analyzing all RNA standard curves from the study as well as four additional extended triplicate standard curves. The N1 LoD was set at 5 gene copies per reaction, at which point 67% of technical replicates were positive (Table C.8).

Assessing PCR inhibition via serial dilution and an internal amplification control

There may be no standard methodology for assessing PCR inhibition in raw wastewater samples. Hence, two previously utilized approaches were combined. One approach included a non-competitive internal amplification control [280, 281, 282, 170] and the other involved serial dilution [283]. The internal amplification control can easily be included in every sample, but cannot detect assay-specific inhibition [170]. Serial dilution consumes more resources and risks diluting the target signal below the detection limit, but it more accurately tests the target itself and allows selection of a dilution value that best reduces the impacts of inhibition. Thus, the VetMAX^{TM} Xeno^{TM} Internal Positive Control (ThermoFisher Scientific) was used as a screening tool to select samples for further testing with serial dilution.

For all samples, Xeno RNA was spiked into the reaction mix (Table C.1), and NTCs were used as an inhibition-free baseline to compare each sample on that plate. Ten samples showed >2 Cq deviation from the baseline and were selected for further inhibition testing [280]. Subsequently, a dilution series (1x, 2x, 5x, 10x) was performed on the ten samples with a high enough Cq deviation, and the duplexed N1 and Xeno assay was repeated. A dilution was chosen by comparing SARS-CoV-2 N1 signal in each dilution to theoretical expectations (based on theoretical doubling per PCR cycle). If diluting the sample led to a 1 Cq difference between actual and expected change in Cq, then the sample at the base dilution was deemed inhibited [283]. Following the serial dilution test, only three samples required dilution (Tables C.7 and C.7), and subsequent qPCR results in this study are reported using this chosen dilution. Results from the internal amplification control were inconsistent with inhibition assessed via serial dilution, and the use of Xeno is not recommended for testing

N1 inhibition in future studies.

Normalization of SARS-CoV-2 N1 concentrations to adjust for fecal content

Researchers have measured wastewater SARS-CoV-2 concentrations as well as proportions of SARS-CoV-2 to endogenous biomarkers for fecal content (e.g., crAssphage [284, 285]) to help account for variability in wastewater signal. Dilution of target signal in wastewater because of precipitation is a contributor to target signal fluctuations [129] that is ideally reduced using normalization biomarkers. However, in this study, minimal rainfall and low flow rate variation for the locations that provided flow data (<4%), support that signal dilution from precipitation was not an issue for this dataset, and mean per capita flow rates were similar across sewersheds (Table 4.1). Thus, unnormalized N1 concentrations should not be influenced by precipitation, but there are additional sources of variablility that normalization biomarkers may address (e.g., signal degradation with residence time in sewersheds). Hence, unnormalized N1 is compared to crAssphage-normalized N1 throughout this chapter. More information about normalization of SARS-CoV-2 N1 concentrations to adjust for fecal content, including comparisons with additional biomarkers (e.g., pepper mild mottle virus), for this dataset can be found in Greenwald and Kennedy et al. (2021).

Data analysis

All data analysis was performed in Python (v3.6.9) using key modules Pandas (v1.1.5), NumPy (v1.19.5), SciPy (v1.4.1), and Plotnine (v0.6.0).

The WBE case detection limit was estimated as follows. The paired wastewater and case data for all sewersheds were combined and sorted from highest to lowest case counts. For each case count, all technical replicates in the wastewater data at and above that point were tallied to determine the cumulative percentage of replicates that amplified in RT-qPCR. Equation 4.1 was used to fit a logistic function [286] to the dataset (SciPy v1.4.1), where y is the fraction of amplified technical replicates, x is the $\log_{10}$(moving average of new cases per person per day), k sets the growth rate of y, and γ sets the inflection point. Zero new cases per capita cannot be represented in a logistic growth model, but in this study, case values of zero were only available for location Q, and these values were substituted as 0.5 cases before the analysis. The COVID-19 per capita case rate that corresponded to 95% cumulative amplification of technical replicates was reported as the estimated WBE case detection limit, and the analysis was repeated with samples where daily per capita cases were provided as masked values.

$$y = \frac{1}{1 + e^{-k*(x-\gamma)}} \tag{4.1}$$

Correlations between wastewater and case data were calculated as Kendall's tau-b coefficients (SciPy v1.4.1), a method adapted for left-censored data [287] (i.e., datasets with

data below a lower limit of detection) because 22% of the data are below the N1 LoD. For wastewater data, any smoothed trendline displayed in a figure was determined using a fitted local regression (Lowess; statsmodels v0.10.2) with bandwidth parameter (α, the fraction of the dataset used for smoothing), set as in Jacoby (2000) (Figures C.1, C.2, C.3, C.4, and 4.1). Lowess trends of SARS-CoV-2 N1 signal were also visualized as heatmaps to aid in discerning peaks (Figures C.6 and C.7). Full dataset and associated code are available through GitHub[6]).

4.3 Results

From April to September 2020, the raw wastewater from five locations in the San Francisco Bay area was sampled weekly, which generated 72 samples (107 with biological replicates). Each sample was tested for SARS-CoV-2 N1 and crAssphage and paired with associated geocoded clinical testing data. Unnormalized and crAssphage-normalized N1 signal are compared throughout this chapter to assess the impact of normalizing for fecal content on analyses. This dataset was used to interpret SARS-CoV-2 signal in raw wastewater and compare with geocoded clinical testing data during the COVID-19 pandemic.

The Lowess bandwidth parameter affected wastewater data trend interpretation

Variation in wastewater SARS-CoV-2 N1 signal from sources other than fluctuation in true COVID-19 incidence can obscure temporal trends (i.e., obscure increases or decreases in SARS-CoV-2 N1 at a location), and scatterplot smoothing techniques can be used to distinguish temporal trends from noise. Smoothing techniques can be used to visually distinguish temporal trends from noise. Similar to the choice of the number of days included for each average calculation for moving averages (window), Lowess requires selection of the fraction of the whole time series that is used for each local regression calculation (bandwidth). Thus, a method was employed to set the bandwidth parameter systematically based on residuals [288] independently for each location. The bandwidth was increased stepwise, beginning with inclusion of one point in each local regression calculation and ending with inclusion of all points (α =1). For each bandwidth value, the residuals were calculated and plotted by date, and a Lowess trendline with α =1 was fit to these residual plots to monitor residual trends as the bandwidth varied. Finally, the maximum bandwidth value was selected for which the residuals visually maintained horizontal Lowess trendlines (Figures 4.1, C.1, C.2, C.3, and C.4).

As an example, for unnormalized and crAssphage-normalized SARS-CoV-2 N1, bandwidth parameters of 0.39 and 0.33 were respectively chosen for location N (Figure 4.1 A). This process was repeated for all locations, and and bandwidths in the range of 0.25-0.6

[6] `https://zenodo.org/record/4730990#.YIxkrqlKgUo`

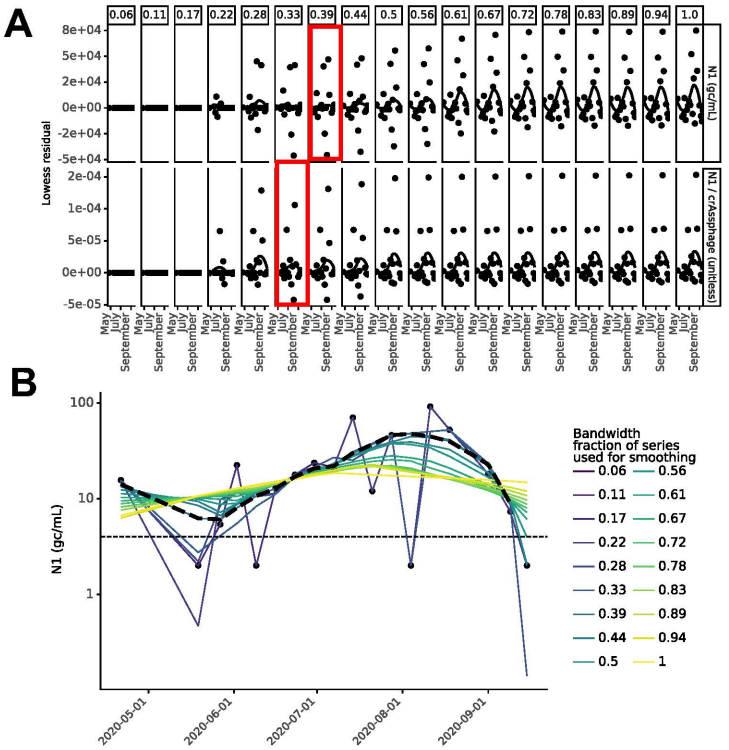

Figure 4.1: (A) Residual plots for Lowess bandwidth parameter (α; column labels) determination for location N where the bandwidth parameter increases from inclusion of 1 data point (far left) to inclusion of all data points (far right) in each local regression for unnormalized N1 (top) and crAssphage-normalized N1 (bottom). The value of α that minimized the residual was selected (red boxes). (B) Visualization of how bandwidth parameter affected the Lowess trendline for location N. Black dashed line indicates the resulting Lowess trendline when α=0.39. Similar figures for all locations can be found in Appendix C.

were selected based on the optimization procedure (Figures 4.1, C.1, C.2, C.3, and C.4). To assess the impact of bandwidth on SARS-CoV-2 N1 signal interpretation, Lowess was performed for all locations sampled and for all possible bandwidths (Figures 4.1 B, C.1, C.2, C.3, and C.4). The bandwidth parameter influenced the overall temporal trends of wastewater data for some locations (N and A; Figures C.4 and 4.1). For example, at location A, a bandwidth of 1 resulted in a gradual increase in SARS-CoV-2 N1 signal during sampling, while a bandwidth of 0.73 resulted in a peak around July. However, for location K, all bandwidths resulted in trends that would have similar interpretations (Figure 4.2). These results illustrate that choice of bandwidth could have implications for interpreting WBE data and informing COVID-19 response strategies, and systematic methods should be used to select the appropriate bandwidth.

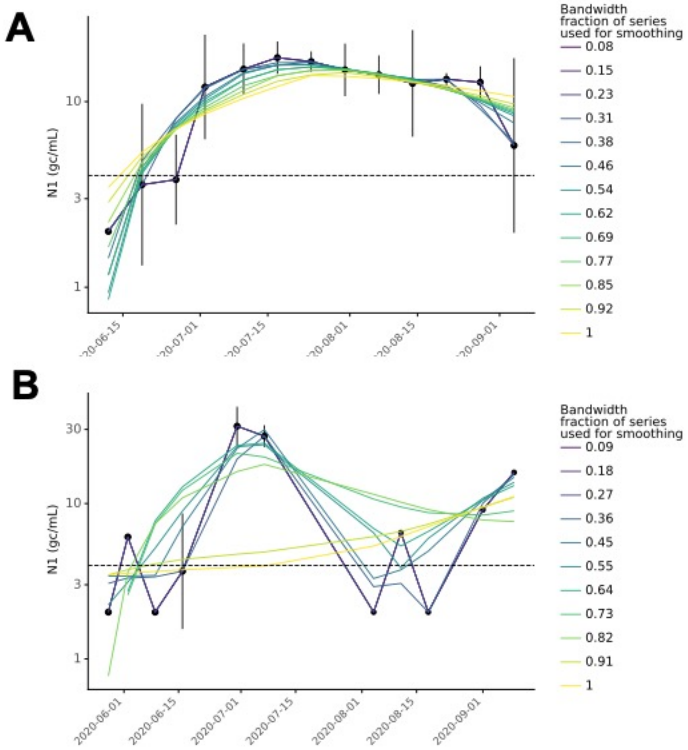

Figure 4.2: Visualizations of SARS-CoV-2 N1 Lowess trendlines to demonstrate the impact of adjusting the bandwidth parameter to include increasing amounts of data in each local regression calculation: from one data point (purple lines) to all data (yellow lines; α=1). Locations K (A) and A (B) are shown as examples of minimal and dramatic changes caused by changing bandwidth parameters, but similar figures for all locations can be found in Appendix C.

Interpretation of spatio-temporal trends

Relative spatio-temporal trends in clinical and wastewater testing results were compared across sampling sites (Figures 4.3, C.6, and C.7). In general, clinical and wastewater data at all locations paralleled one another, with San Quentin prison (Q) showing the highest COVID-19 burden across locations. Due to a COVID-19 outbreak, location Q had a maximum that was 53 times (SARS-CoV-2 N1 4.89x10^3 gc/mL), 17 times (crAssphage-normalized SARS-CoV-2 N1 2.9x10^{-3}), and 203 times ($\sim$ 85 new cases per 1000 people on 6/29) higher than the highest value at the sewershed scale. There were a few discrepancies between clinical and wastewater trends (heatmap visualizations in Figures C.6 and C.7 highlight discrepancies in peaks). For example, at location N, there may have been clinical undertesting, based on the peak in wastewater data in August (Figures 4.3 and C.6) and higher SARS-

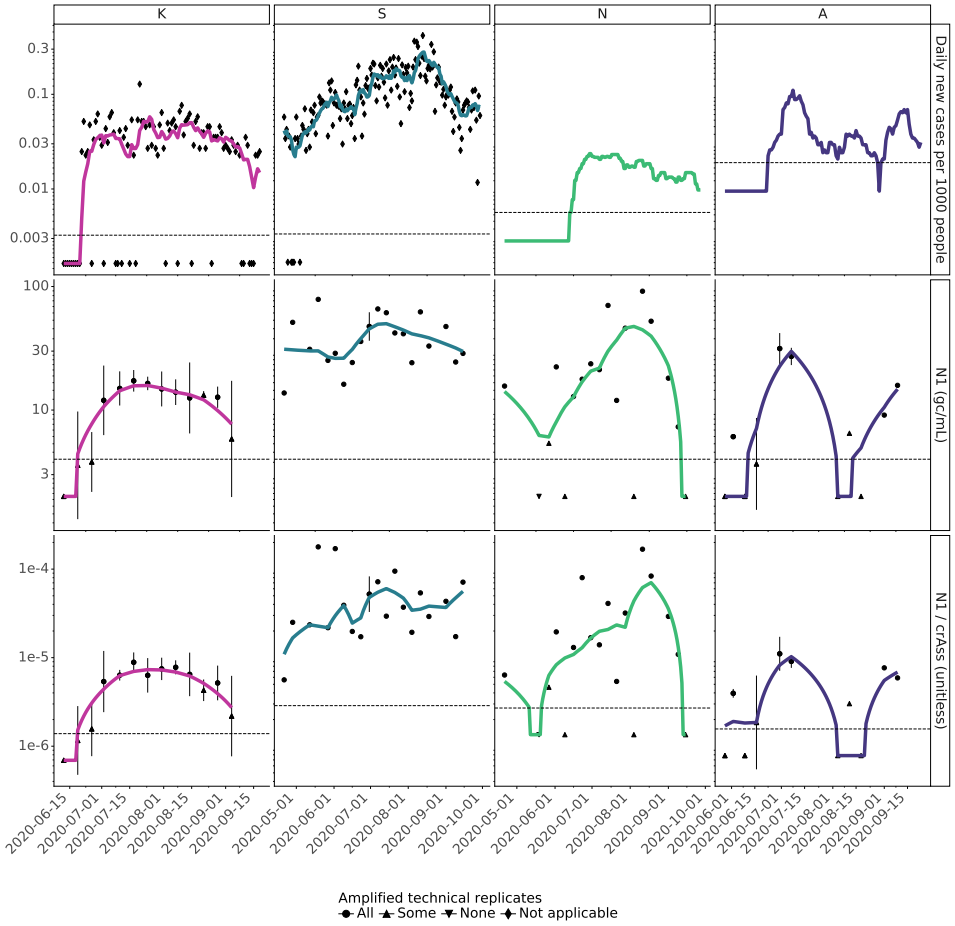

Figure 4.3: For sewershed-scale locations: (top) Daily per capita COVID-19 cases, where symbols are plotted at the daily new cases per 1000 people per day, the trendline represents the seven-day moving average of these data, and the horizontal dashed line indicates 1 case in 1000 people for each location. (middle) SARS-CoV-2 N1 signal in wastewater, where symbols indicate the amount of technical replicates that amplified during qPCR, horizontal dashed line indicates the limit of quantification, and solid lines represent the most optimal Lowess trendline. (bottom) SARS-CoV-2 N1 signal normalized to crAssphage signal in wastewater, where symbols indicate the amount of technical replicates that amplified during qPCR, horizontal dashed line indicates the limit of detection for N1 over the 75% quantile for crAssphage for each location, and solid lines represent the most optimal Lowess trendlines.

CoV-2 signal in wastewater at location N (relative to other locations) than represented by the clinical data (Figures 4.3 and C.7).

At location Q, clinical data included an estimate of active cases, which allowed for an observational comparison of wastewater data to estimates of incidence and prevalence. Un-normalized and crAssphage-normalized SARS-CoV-2 N1 signal in wastewater were visually compared to new cases per day per 1000 people (incidence) and the estimated active cases

per 1000 people (prevalence; Figure 4.4). The peaks for incidence and prevalence were close (8 days apart), but the spans were different (45 and 80 days, respectively; Table 4.2). The Lowess trendline for unnormalized SARS-CoV-2 N1 signal had a similar span to the COVID-19 incidence (41 days compared to 45 days), and the crAssphage-normalized signal had a shorter span compared to that of the incidence (27 days compared to 45 days). Based on these observations, the trend in SARS-CoV-2 N1 signal in wastewater aligned more with COVID-19 incidence compared to prevalence at location Q, as others have observed [115, 289, 290]. However, these findings are limited because the wastewater signal may have peaked before the start of the study period, only four points were positive in the time series, and the time series only included a decreasing trend. The conclusions might differ for an increasing trend depending on the shedding profile in relation to disease progression, but the clinical results about fecal shedding duration that would support this finding are less clear, with estimates of fewer than seven days [136] and up to over 30 days in some cases [34].

Table 4.2: At location Q, comparison of date when SARS-CoV-2 N1 signal was at the maximum or earliest minimum value for seven-day moving averages of daily per capita new cases and daily per capita active cases compared to that of the most optimal Lowess trendlines for SARS-CoV-2 N1 unnormalized and normalized in wastewater.

type	date of maximum value	date of earliest minimum value	days from maximum value to earliest minimum value
SARS-CoV-2 N1	7/1/20	8/11/20	41
New COVID-19 cases	6/29/20	8/13/20	45
SARS-CoV-2 N1/crAssphage	7/1/20	7/28/20	27
Active COVID-19 cases	7/7/20	9/25/20	80

The WBE case detection limit was estimated to be 2.4 COVID-19 cases per 100,000 people

Quantifying the minimum per capita new COVID-19 cases in a sewershed at which there is reliable detection of SARS-CoV-2 N1 in wastewater (WBE case detection limit) is important for gauging the utility of COVID-19 WBE when the true incidence is low. This WBE case detection limit depends on the detection limit of the wastewater measurement (i.e., the methods used to store, concentrate, extract, and measure SARS-CoV-2 RNA in wastewater) and the accuracy of the clinical testing data available. To estimate the WBE case detection limit in a way that is replicable across studies, the cumulative percentage of amplified technical replicates of the wastewater data for inversely-ranked daily per capita COVID-19 cases was fit to a logistic growth model (without samples associated with masked case values; see Methods). When COVID-19 case rates equaled or exceeded 2.4 daily cases

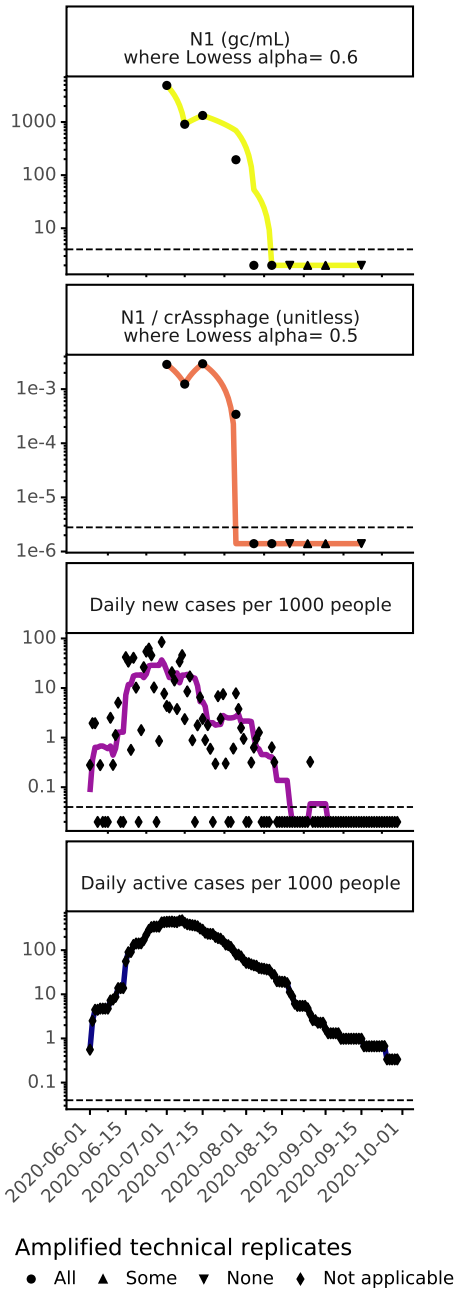

Figure 4.4: Comparison of wastewater and clinical data at location Q from June to September 2020, where symbols indicate the amount of technical replicates that amplified during qPCR for all plots. The top two plots show unnormalized and crAssphage-normalized SARS-CoV-2 N1 signal in wastewater, where the horizontal dashed line indicates the limit of detection and trendline is the most optimal Lowess trendline. The bottom two plots show the estimated incidence and prevalence, where the horizontal dashed line indicates 1 case in 1000 people.

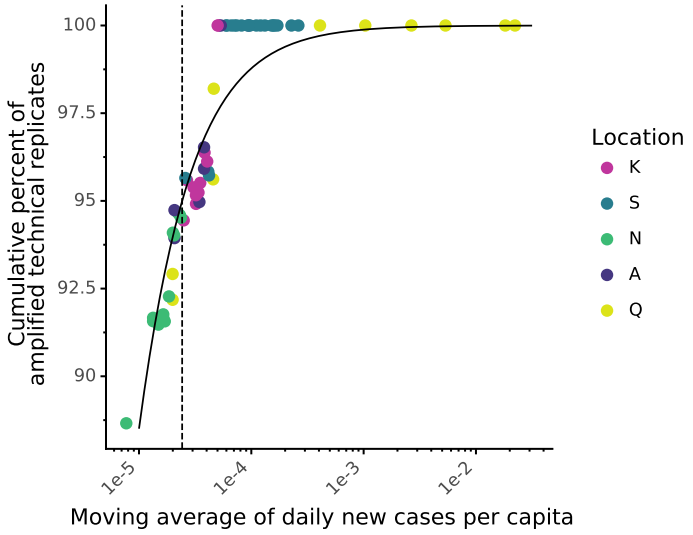

Figure 4.5: Estimated minimum number of COVID-19 cases needed for reliable detection of SARS-CoV-2 RNA in wastewater. The cumulative percentage of amplified wastewater technical replicates was calculated by ranking the moving averages of daily per capita cases (x-axis) from highest to lowest and calculating the fraction of qPCR replicates that amplified cumulatively (y-axis) for each value of x. The dashed line represents the daily new cases per capita value above which 95% of wastewater technical replicates amplified (2.4 cases in 100,000 people).

per 100,000 people, 95% of wastewater technical replicates amplified via RT-qPCR for N1 (Figure 4.5). Other researchers have used non-cumulative methods to estimate the WBE case detection limit by calculating the percent of amplified wastewater replicates for each case value [273]. This method requires repeated wastewater measurements associated with each possible clinical case value or range of case values (i.e., bins). Otherwise, the percent of amplified technical replicates is limited, as was the case in this study where only one biological replicate was often associated with each case number (Figure C.8 A). Ideally, all data would be unmasked when applying this method. To verify that the masked clinical data did not affect the estimated WBE case detection limit, the process was repeated with masked values, and the estimate was similar (2.2 cases in 100,000 people; Figure C.8 B). These limits are within the theoretical range possible [137] and similar in magnitude to Hata et al. (2021) (10 in 100,000 people) and Wu et al. (2021) (13 in 100,000).

Impact of the date associated with clinical testing data on lead time in wastewater surveillance at location K

The time for laboratories to process samples and return results (testing turnaround time) affects the potential for wastewater surveillance to provide lead time over clinical surveillance. In general, clinical testing data correspond to either the date the sample was collected or the date the results were returned. The ideal date to use for informing public health decisions would be the result date, to include differences between clinical and wastewater testing turnaround time in the analysis. Alternatively, sample collection dates should be compared to understand the timing of the underlying biological mechanisms that result in a positive wastewater signal (onset and duration of fecal shedding) and positive clinical test (onset and duration of nasopharyngeal shedding). Onset and duration of symptoms may influence the timing of the clinical test (sample collection date), depending on whether testing is routine or only available to symptomatic individuals. Hence, the ideal date to use for comparison of wastewater and clinical testing data differs depending on the goals of the comparison. The clinical testing data for location K included sample collection date, result date, and episode date (the earliest date associated with the case), allowing assessment of the correlation between case data and wastewater data with and without clinical testing turnaround time. Episode date was frequently the same as the sample collection date, unless a patient reported symptoms prior to test date (Figure C.5). In contrast, wastewater testing data for location K only correspond to the sample collection date because all samples were processed retroactively in this study. For example, in the COVID WEB laboratory,[7] the result date is generally 1-3 days after the sample collection date but varies depending on shipping time. The impact of date associated with clinical testing data was investigated for location K.

To test the influence of the date associated with clinical testing, correlation analysis was completed for location K (Figure 4.6). The wastewater testing data (sample collection date) correlated with the clinical testing data without offset for episode date ($tau_{unnormalized}$=0.56, $tau_{crAssphage}$ = 0.54, $p < 0.01$) and sample collection date ($tau_{unnormalized}$=0.59, $tau_{crAssphage}$ = 0.62, $p < 0.01$) without a lead or lag. When the result date was used for clinical testing data, the strongest correlation with wastewater data was associated with a two-week lead time (unnormalized N1 concentration) or one-week lead time (N1 normalized to crAssphage; Figure 4.6). When values below the N1 qPCR LoD were removed, wastewater data were no longer significantly correlated with episode date-associated clinical data, but the strongest correlations for the other date associations remained significant. This analysis is limited because of the small dataset, but the methodology presented here can be used to assess the lead time provided by wastewater surveillance with larger data sets and with wastewater data processed contemporaneously with decision-making.

[7] `https://www.covid-web.org`

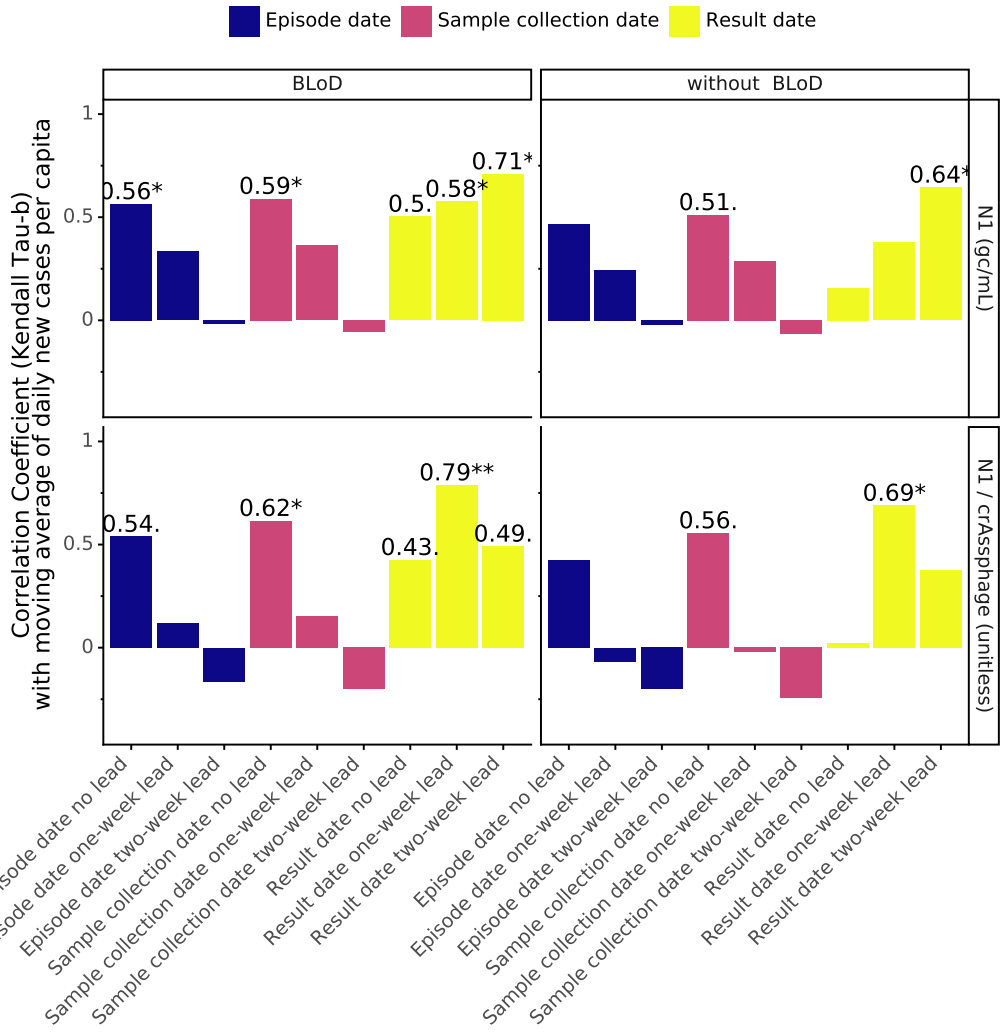

Figure 4.6: Kendall's Tau-b at location K for comparisons between wastewater SARS-CoV-2 N1 signal (associated with the sample collection date) and COVID-19 new cases (date association varies as indicated by color: episode date, sample collection date, and result date) both with and without samples below the N1 limit of detection (BLoD) included (column facets). Wastewater SARS-CoV-2 data (row facets; unnormalized N1 (gc/mL) and crAssphage-normalized N1 (unitless)) were compared to the seven-day moving average of average of geocoded COVID-19 new cases. The analysis was completed with wastewater date aligned with clinical date (no lead) as well as with one- and two-week lead times (wastewater leads clinical testing data by one or two weeks). Significance is indicated as <0.05 . , <0.01 *, and <0.001**.

4.4 Discussion

Potential use scenarios of SARS-CoV-2 wastewater testing data

At the sewershed scale, the benefit of WBE to public health extends beyond early warning. Discrepancies between wastewater testing data and clinical testing data trends from early in the time series at location N (April-July 2020; 4.3) could be used to infer clinical undertesting, which is supported by lower testing capacity in this time frame (Figure C.9). Although pairing COVID-19 clinical testing data with wastewater SARS-CoV-2 data can generate new insights for public health decision-making, it can be challenging in practice. Pairing wastewater SARS-CoV-2 data with geocoded COVID-19 clinical testing data required collaboration between academics, wastewater treatment facility representatives, and public health officials. These collaborations may be particularly difficult at sewershed-scale, where multiple public health department jurisdictions overlap (e.g., location N). Partnerships for data sharing between agencies are critical to support ongoing wastewater-based epidemiology for SARS-CoV-2 and other pathogens.

At the facility scale, monitoring raw wastewater for SARS-CoV-2 might be particularly useful for early detection of COVID-19 outbreaks. San Quentin Prison (location Q) had a COVID-19 outbreak during the study period after a transfer from the California Institution for Men [291], where, at its peak, 47% of the population had active cases. The maximum SARS-CoV-2 N1 concentration (4.89×10^3 gc/mL) was higher than any sewershed sampled in this study and among the highest values found in a literature review for N1 in raw wastewater [132, 105, 186, 115, 118, 273], despite regular clinical testing (Figure C.9). Prison conditions cause incarcerated people to be particularly susceptible to respiratory disease outbreaks, and maintaining safety in prisons requires deliberate planning and coordination by correctional institutions (e.g., coordination with local public health systems to develop pandemic response plans, coordination of transfers between institutions, etc.) [292]. Furthermore, the health of incarcerated people is linked to the health of the community, and incorporating correctional institutions into community safety plans will help ensure better protection against COVID-19 for everyone [292]. Once protective measures are implemented, WBE may be useful to monitor prisons and other high-risk facilities (e.g., skilled nursing facilities, homeless shelters, etc.), especially where clinical testing is not available or routine.

A critical question for public health decision-making is how much early warning WBE can provide ahead of clinical testing, which could allow more timely public health responses to slow COVID-19 outbreaks. However, lead time is difficult to measure. Biologically, the time between onset of fecal shedding and nasal shedding is unclear [136, 34]. Practically, lead time depends on testing turnaround time and frequency of sampling for both wastewater and clinical testing. For example, clinical testing capabilities can increase the lead time of wastewater data if patients are only tested after symptom onset and can decrease the lead time if asymptomatic and symptomatic individuals are regularly screened with rapid turnaround time. Ideal assessments of wastewater data lead time due to biological mechanisms would not include turnaround time, whereas assessments of the performance of clinical

and wastewater laboratories for public health action and practical limitations would include turnaround time. Although other studies observed lead time for wastewater data over clinical data starting on the order of days [109, 106], the weekly sampling in our study could explain why no lead time was determined when the sample collection date was used for both wastewater and clinical testing data (Figure 4.6). However, the impact of clinical testing strategy (i.e., only screening symptomatic individuals) could also be affecting this result. Wastewater and clinical result dates could not be compared in this retroactive study, but when clinical data were associated with the result date and wastewater data were associated with sample collection date, lead time of 1-2 weeks was observed (Figure 4.6). Other researchers have observed lead time in wastewater data of up to three weeks [105], and our results reflect a similar range in possible lead times (0-2 weeks) depending on which date is associated with the clinical data.

Systematic approaches for WBE data interpretation

In general, public health decisions are based on temporal trends in disease burden, not individual data points, but trends in wastewater and clinical data can be difficult to visually distinguish, especially when available resources constrain sampling frequencies. When Lowess was applied to wastewater data, the value of one parameter could influence the trend visualization such that the same dataset could lead to different public health responses (Figure 4.2). Based on our analysis, the bandwidth parameter for Lowess should be determined for each sewershed sampled. Lowess with a systematically chosen bandwidth could be used to smooth trendlines and minimize the loss of temporal resolution. The method presented here could be applied in retrospective analysis or in real-time analysis completed as part of wastewater public health surveillance programs. For real-time applications, the bandwidth parameter could be selected using a subset of data, and the residuals plot could be frequently checked to ensure no new residual patterns emerge over time that could obscure the smoothed trend.

In addition to data smoothing, an approach was developed for identifying a WBE case detection limit that can be applied systematically to studies using PCR-based methods. This analysis was applied to SARS-CoV-2 N1 signal in wastewater ato find that the daily new clinical cases at which wastewater surveillance could reliably detect clinically diagnosed COVID-19 cases in the contributing population was estimated at 2.4 cases per 100,000 people. There are multiple limitations to this analysis because wastewater detection depends on factors other than incidence, such as sampling methods (e.g., frequency of sampling aliquots), which can influence the probability of capturing shed viral particles from an infected individual. Additionally, the estimate may vary based on site-specific clinical testing availability, wastewater sampling methods (e.g., composite sampling, freezing before processing) and laboratory processing (e.g., 4S extraction method, RT-qPCR). The estimation method for a WBE case detection limit presented here could benefit both COVID-19 WBE and WBE for other diseases by providing a systematic method to compare the case detection limits across studies.

Chapter 5

Conclusions

5.1 Summary

As water systems become more integrated through management approaches, such as one water, and treatment processes, such as direct potable reuse, microbial monitoring strategies in these systems could benefit from inclusion of monitoring targets relevant across integrated systems. Current drinking water microbial monitoring strategies rely on both fecal indicator bacteria that can only indicate whether fecal contamination could have occurred (e.g., total coliform bacteria) and physicochemical parameters that indirectly assess microbial water quality (e.g., chlorine concentration in drinking water distribution systems with residual disinfectants). However, microbial monitoring strategies that only include these common parameters may not capture the microbial impacts from changes in water quality at local (i.e., site-to-site within a distribution system) or system (i.e., distribution system-wide) scale. For example, current drinking water microbial monitoring strategies would likely not capture microbial impacts in drinking water distribution systems during transition to direct potable reuse (DPR). Furthermore, in wastewater there are additional monitoring targets that could be monitored to inform treatment efficacy of DPR systems (e.g., enteric pathogens in raw wastewater). Microbial monitoring strategies that incorporate enhanced methods of microbial assessment could produce data that are mutually beneficial for drinking water providers, wastewater treatment service providers, and public health departments (Figure 1.1).

The overall goal of this work was to apply enhanced methods of microbial assessment in piped drinking water systems and to identify integrated microbial monitoring strategies that benefit public health. Enhanced methods of microbial assessment include methods to assess microbial abundance (e.g., intact cell counts, total cell counts, intracellular ATP, and total ATP), microbial community composition (e.g., 16S rRNA gene amplicon sequencing), and specific microbial targets (e.g., quantitative polymerase chain reaction; qPCR). In Chapter 2, five measures of microbial abundance were applied in six chlorinated and chloraminated drinking water distribution systems. Microbial impacts from site-scale changes in

physicochemical parameters were determined by comparing enhanced methods of microbial assessment (i.e., total and intact cell counts and total and intracellular ATP concentrations and heterotrophic plate counts). Chapter 3 expanded on the microbial abundance assessment in Chapter 2 to evaluate shifts in microbial community composition during augmentation of conventional drinking water with advanced-treated wastewater. Five pipe loop rigs were used to simulate this event and also included control loops that did not transition or only contained conventional water for comparison. The pipe loop rigs were sampled over 21 weeks using 16S rRNA gene amplicon sequencing and flow cytometry. In Chapter 4, the value of wastewater was explored beyond that of a potential source of drinking water, and the circulation of severe acute respiratory syndrome coronavirus 2 (SARS-CoV-2) in San Francisco Bay Area communities during the coronavirus infectious disease 2019 (COVID-19) pandemic was investigated using wastewater surveillance. From April to September 2020, one facility and four sewersheds were sampled weekly, and SARS-CoV-2 was quantified using RT-qPCR for the N1 gene target and compared with geocoded clinical testing data. The findings and implications of these studies are discussed in this chapter.

5.2 Diagnostic and preventative microbial monitoring strategies in disinfected drinking water distribution systems

In drinking water distribution systems, enhanced methods of microbial assessment could increase the success of monitoring for diagnostic and preventative purposes. Microbial monitoring can be completed in regular intervals (e.g., weekly; routine monitoring), in response to an issue (e.g., nitrification; diagnostic monitoring), or in preparation for a system-scale change (e.g., switching source waters; preventative monitoring). Routine monitoring in conventional systems (i.e., those that treat surface or ground water) is generally required by legislation such as the Revised Total Coliform Rule in the United States [14] and the Nitrification Action Plan in Texas [293]. Diagnostic monitoring has been recommended in response to elevated lead and copper levels and before switching source waters in the United States [294] as well as in response to the indicators of nitirification that are deemed "red flag alarm triggers" of nitrification action in Texas [41]. In these cases, chemical indicators were recommended, but in some situations, microbial targets could provide more insight.

For routine monitoring, chlorine was found to be a useful surrogate for microbial abundance in normal operating conditions, but enhanced microbial assessment could improve diagnostic and preventative monitoring practices in conventional drinking water systems. In Chapter 2, intact cell counts, total cell counts, intracellular ATP, and total ATP were significantly and strongly correlated with disinfectant residual concentration in the conventional drinking water systems sampled (Figure 2.2). This finding suggests that changes in disinfectant concentration should capture increases in microbial abundance associated with disinfectant decay in normal operating conditions. However, disinfectant concentration may

not be enough to capture the full extent of an issue. For example, an interaction between temperature and disinfectant concentration was observed that resulted in proportionally higher intact cell counts at low levels of disinfectant compared to the same conditions at lower temperatures (Figure 2.3). Thus, measurement of intact cell counts could be useful to pair with chlorine measurements during summer conditions, when disinfectant decay can become problematic [235] and higher temperatures can increase monochloramine decay [295]. However, a baseline of cell counts or ATP expected in a drinking water distribution system under normal operating conditions before implementing these practices would need to be established prior to the issue for comparison. Additionally, paired 16S rRNA gene amplicon sequencing data with total cell counts could help ensure that an increase in microbial abundance is not linked with taxa of concern and identify any targets to monitor using qPCR. For example, in Chapter 3, 16S rRNA gene amplicon sequencing was applied and opportunistic pathogens were investigated in simulated drinking water distribution system with total cell counts. *Mycobacterium*- and *Pseudomonas*-classified amplicon sequence variants were at higher estimated absolute abundance in simulated distribution systems compared to full-scale distribution system and demonstration-scale RO permeate samples. Thus, these amplicon sequence variants were flagged to investigate more closely during the full-scale implementation of potable reuse using qPCR for *Mycobacterium avium* complex and *Pseudomonas aeruginosa* (Figure 3.9).

The research in Chapters 2 and 3 contributes to a growing body of literature assessing microbial water quality in drinking water systems, but more work is needed applying DNA sequencing methods in full-scale systems as part of diagnostic or preventative monitoring and applying viability measures for PCR-based methods in systems with residual disinfectants. While researchers have applied DNA sequencing methods at treatment plants in short-term [296, 297, 23, 298, 299, 67, 64, 300] or long-term [48, 301, 70] (e.g., 2 or more years of sampling) sampling campaigns, application of these methods as diagnostic or preventative tools is rare. Previous studies have used 16S rRNA gene amplicon sequencing to assess the microbial impact of temporarily converting chloraminated drinking water systems to chlorinated systems [302, 303] and of treatment upgrades [72, 304, 71]. Diagnostic studies may be rare because they require collaboration with drinking water providers to obtain samples and publish resulting data. Additionally, more work is needed assessing viability with 16S rRNA gene amplicon sequencing or qPCR in full-scale drinking water distribution systems [171]. Staining bacterial cells with propidium iodine is a reproducible method to assess viability for flow cytometry-based microbial abundance [147] that has some caveats (e.g., staining intact but nonviable cells [171]), but is important to apply in systems with residual disinfectants to accurately quantify microbial abundance [305]. However, propidium iodide has not been successfully paired with subsequent DNA sequencing, and methods that are compatable with DNA sequencing (e.g., propidium monoazide) are not straightforward to apply in environmental matrices, but hold promise for future application [171]. For example, impacts of disinfection conditions on 16S rRNA gene amplicon sequencing results have been observed using propidium monoazide that were unclear without the viability assay [178]. In the future, longitudinal studies of drinking water distribution systems could generate

more complete datasets that include flow cytometry, 16S rRNA gene amplicon sequencing, and even metagenomics sequencing data with paired viability assays and high sampling frequency. High resolution datasets could be used to develop machine learning models for which consistent deviations from model predictions at specific sites may be indicative of water quality problems, such as pipe corrosion or nitrification, as has been simulated previously [306].

5.3 Integrated microbial monitoring strategies for integrated urban water management systems

Water-stressed cities need access to reliable drinking water sources to meet future drinking water demands, and DPR is an option that integrates drinking water with wastewater treatment and management. The process of implementing DPR to increase the drinking water supply of a city will constitute a disturbance in the conventional drinking water system, and there will be a transition period when advanced-treated wastewater is introduced. Microbial monitoring strategies for drinking water systems expecting a system-scale perturbation in water quality, such as transition to DPR, could benefit from enhanced microbial assessment. For DPR in particular, enhanced monitoring has been recommended before and after the transition in full-scale systems [6].

For potential treated water augmentation systems, enhanced methods of microbial assessment (e.g., flow cytometry, 16S rRNA gene amplicon sequencing, and qPCR) could be used before and after the transition to identify shifts in microbial water quality that may have unintended consequences. In Chapter 2, intact cell counts were demonstrated to be quantifiable throughout the distribution system in 97.6% of samples as opposed to other microbial abundance measures that assess viability: heterotrophic plate counts (81.4%) and intracellular ATP (69.6%) (Table 2.3). Thus, intact cell counts could be a useful measurement in these systems that would likely provide fewer non-detects and therefore more information than alternatives (heterotrophic plate counts and ATP assays). This finding is supported by other researchers who have successfully applied flow cytometry-based methods in advanced wastewater treatment systems [142, 85, 84] as well as by the total cell counts that were measured successfully in the demonstration-scale reverse osmosis permeate from Chapter 3 (reverse osmosis permeate, Figure 3.9). Also in Chapter 3, 16S rRNA gene amplicon sequencing was used both to identify targets to monitor more closely using qPCR (Figure 3.9) and to identify shifts in microbial community composition following the transition to DPR compared to pipe loop rigs that maintained the same feedwater composition throughout the study period (Figure 3.4). This approach could be applied in simulation studies in preparation for a full-scale change, as well as during the full-scale implementation of DPR. However, this approach to assessing shifts in microbial community composition is conservative because it does not account for viability.

Pathogen monitoring of raw wastewater with qPCR could serve multiple purposes in

DPR systems. First, enteric pathogen monitoring can be used to ensure that pathogen reduction targets through treatment are sufficient. Wastewater has variable enteric virus concentrations that have been found to be higher (i.e., 10^7 to 10^9 viral particles per L) than the concentrations used to set the $\log_{10}$ reduction targets for potable reuse in California (i.e., 10^5 to 10^6 viral particles per L) [28]. Second, the contributing population can be monitored for potential pathogen outbreaks to ensure public health. Public health surveillance is recommended after implementation of DPR systems to verify that consumption of advanced-treated wastewater does not result in transmission of pathogens back to the community, which will require collaboration from public health departments and water treatment providers [6]. In Chapter 4, SARS-CoV-2 was monitored in raw wastewater and compared with geocoded clinical testing data. While SARS-CoV-2 is likely not a concern for DPR [101, 102], this work demonstrated the types of collaboration between public health departments and wastewater treatment facilities recommended for public health surveillance following implementation of DPR. Pairing clinical surveillance with wastewater surveillance could help overcome some biases associated with clinical testing (e.g., sampling bias, undertesting, etc.), especially for diseases from enteric pathogens which have less robust clinical testing compared to SARS-CoV-2 [112, 116, 113].

The research presented in Chapter 3 is one of very few studies on drinking water distribution system microbial impacts from DPR, and more work is needed applying integrated monitoring methods in simulated and full-scale DPR systems. Previous research on microbial impacts of DPR in distribution systems found shifts in microbial community composition relative to feedwater during simulated distribution that were attributed to water stagnation [84] or bacterial regrowth [89] in drinking water distribution systems. Similar or lower levels antibiotic resistance genes or opportunistic pathogens compared to conventional systems were also reported [89, 84]. However, these studies did not simulate a transition from conventional drinking water to direct potable reuse. This process needs to be studied more thoroughly, particularly at full-scale, because it imparts a system-scale change in drinking water quality that is currently uncommon: one report only identified three planned full-scale treated water augmentation systems in the world [82]. However, El Paso, Texas is on track to build the first treated water augmentation system in the United States [82], and as of March 2021, the California Water Board just released a draft of a proposed regulation framework for DPR that specifically addresses treated water augmentation [94]. Thus, this practice will likely become more common. Once more full-scale systems are online, demonstration of integrated monitoring techniques across multiple systems are needed that benefit both public health and treatment facilities. For example, in the future, online flow cytometers could be combined with pathogen monitoring through (viability) qPCR to assess treatment performance with flow cytometry, while also monitoring treatment efficacy and the burden of pathogens of concern on the contributing population.

5.4 COVID-19 wastewater-based epidemiology

The coronavirus infectious disease 2019 (COVID-19) pandemic prompted a need for alternatives to clinical testing. SARS-CoV-2 is shed in feces [32, 31, 33, 36, 130], and researchers globally have quantified SARS-CoV-2 RNA in wastewater and sludge [130, 108, 134]. Wastewater testing for SARS-CoV-2 could help overcome bias and stigma associated with clinical testing [120, 121]. While COVID-19 wastewater-based epidemiology is a recent development, the practice of monitoring the pathogen burden in a population using wastewater signal has been applied in global efforts to help eradicate poliovirus for over 40 years [97, 98, 99, 100]. Routine wastewater testing could be supplemented with testing for pathogens of high public health relevance to help with pandemic response and outbreak prevention. For example, public health departments, wastewater treatment providers, and wastewater testing laboratories have worked together during the COVID-19 pandemic to provide wastewater testing results for communities[1].

During the COVID-19 pandemic, both the methodological research for SARS-CoV-2 testing in wastewater and the application of wastewater-based epidemiology have been occurring simultaneously, and systematic methods that would allow results comparisons across studies are not consistently applied. In Chapter 4, two systematic approaches were presented that have potential for real-time SARS-CoV-2 wastewater monitoring applications and retrospective analysis. First, the minimum number of COVID-19 cases needed to detect SARS-CoV-2 RNA in wastewater was estimated using a method that can be repeated in other studies. The limit was estimated at 2.4 daily COVID-19 cases in 100,000 people (Figure 4.5), which is within the range of what is theoretically possible [137] and is the same order of magnitude as others have found [107, 273]. This result is promising and suggests wastewater testing could still be useful when COVID-19 occurrence is low. Additionally, interpretation of trends in wastewater or clinical testing data is important to determine if the overall burden is increasing or decreasing and to assess pandemic mitigation strategies [307]. Wastewater data are generally not collected with a sampling frequency that would allow for calculation of a seven-day moving average, which is the smoothing method commonly applied to clinical testing data for public dashboards such as the Johns Hopkins University of Medicine Testing Trends Tool[2]. Indeed, a sampling frequency of at least two times weekly has been suggested for wastewater testing [308], and sampling at weekly intervals is common. Instead, some researchers have used locally weighted scatterplot smoothing (Lowess) for wastewater testing data, but they do not specify reasoning for choice of bandwidth parameter (the fraction of series used in each local regression calculation) [132, 106, 271, 272]. However, in Chapter 4, choice of bandwidth parameter was found to affect the overall trend interpretation for some locations sampled (Figure 4.2). Thus, Lowess with a systematic bandwidth selection process (Figures 4.1, C.1,C.2, C.3, and C.4) was applied that can be used to smooth and interpret weekly SARS-CoV-2 signal in wastewater (optimal bandwidth parameters ranged

[1] https://www.covid-web.org

[2] https://coronavirus.jhu.edu/testing/tracker/overview

from 0.25 to 0.6). Finally, comparisons across five locations in the San Francisco Bay Area showed consistency between trends in SARS-CoV-2 signal in wastewater and trends in daily per capita COVID-19 case data, with a few minor discrepancies that could indicate clinical undertesting for some locations (e.g., location N; Figure 4.3). When trends were compared across locations, the facility-scale location sampled was experiencing an outbreak that was clear in the clinical and wastewater testing data. The SARS-CoV-2 signal in San Quentin Prison's wastewater was 88 times higher than the maximum measured at any of the locations sampled, emphasizing the disproportionate COVID-19 burden on this underserved population.

The research in Chapter 4 contributes to a fast-growing body of work demonstrating that SARS-CoV-2 wastewater testing is a promising public health surveillance strategy, but it is a relatively new application that requires more research and development. First, variation in wastewater SARS-CoV-2 signal that is not reflective of the true COVID-19 incidence needs to be better characterized. Feng et al. (2021) found that the difference between signal on consecutive days was the largest contributor to variability compared to the qPCR SARS-CoV-2 N1 assay and wastewater concentration method. Similar work applying different collection methods is needed to characterize the main contributors to variation in wastewater signal and to determine how much this variation obscures actual disease-burden in the contributing population, so that approaches can be developed to account for or reduce this variability. Second, lead time provided by wastewater testing data over clinical testing data could be because of an underlying biological mechanism that results in peak fecal shedding before symptom onset, because wastewater laboratory turnaround time is faster than clinical laboratory turnaround time (situation-dependent), or a combination of both. Analyses to assess lead time in wastewater testing data should account for which comparison is being made by using the proper date association for clinical and wastewater testing data (i.e., result date versus sample collection date). While the dataset in Chapter 4 is limited, the date used for clinical data affected the correlation with wastewater data (associated with sample collection date) by showing earlier perceived lead time in wastewater data if clinical result date was used (Figure 4.6), as others have also observed [109]. Ideally, clinical and wastewater data would be compared using the same date association that depends on the comparison being made (e.g., result date to compare turnaround times from clinical versus wastewater testing laboratories in communities). More work is needed comparing date associations using larger datasets and determining whether fecal shedding could contribute to lead time [136, 34]. Third, more work is needed to determine whether wastewater SARS-CoV-2 signal aligns more with incidence or prevalence. In Chapter 4, a small dataset was used to investigate whether wastewater data reflects incidence or prevalence at the facility scale location sampled (Figure 4.4), and only a few other researchers have addressed this question [115, 289]. More of this research is needed to determine if the SARS-CoV-2 signal in wastewater is reflective of new cases or active cases and to properly interpret trends in wastewater signal. Fifth, as with any public health surveillance campaign, ethical considerations for WBE should be carefully considered to ensure privacy and prevent stigmatization or misuse of surveillance data, as others have discussed in detail [126, 129, 309, 310]. Finally,

more work is needed applying wastewater testing for other pathogens, especially now that the field of wastewater-based epidemiology is in a rapid development phase. In the future, wastewater treatment facilities could be screened for common pathogens in the population shed in feces (e.g., Influenza A and likely SARS-CoV-2 even post-pandemic) to determine if outbreaks are occurring and eventually employ metagenomics to catch emerging pathogens and strains.

5.5 Collaborative work in environmental engineering: reflections

The projects I have worked on during my Ph.D. have resulted from collaborations with representatives from water and wastewater treatment facilities, consultants, public health officials, and other academics. Working with collaborators has been beneficial in that I was able to conduct applied research: I sampled and studied full-scale drinking water distribution systems (Chapter 2), completed a pilot project prior to an actual implementation of potable reuse (Chapter 3), as well as monitored SARS-CoV-2 locally during a pandemic and provided results to public health departments (Chapter 4). However, working with many collaborators also had challenges, and a few are listed below:

- Balancing collaborator interests
  - Publishing and sharing data when there are perceptions that the data could reflect poorly on the facility being tested
  - Meeting academic goals within the constraints of industry projects (e.g., budget, project timeline, and client considerations)
  - Accepting the experimental design tradeoffs of shared microbial and chemical water quality studies for direct potable reuse (Chapter 3)
- Authorship and credit (discussed in detail below)
  - Clarifying roles and credit of multiple authors without diminishing the roles of others and disincentivizing collaboration
  - Overcoming perceptions about co-first authorship

Collaboration allows for Ph.D. students to work on projects that would otherwise be too large for one person to complete. Large and complex problems are the precise type of problems environmental engineers are trying to understand and solve. An example of this is the COVID-19 pandemic, during which environmental engineering and science academics and water industry professionals realized that monitoring SARS-CoV-2 in wastewater was possible and had potential at a time when supply chain issues, testing biases, and other constraints made it difficult to accurately assess COVID-19 occurence via clinical testing

alone [37]. I paused my planned dissertation research to work on a large interdisciplinary team contributing to COVID-19 wastewater-based epidemiology[3], and a direct result of this pivot has been my first co-first-authored manuscript [267]. The decision to pursue this path was difficult at first because of the controversy surrounding Equal Co-authorship, but once I learned more about this practice I realized that standardizing and normalizing Equal Co-authorship could be beneficial.

Equal Co-authorship is the practice of sharing one of the authorship positions on an academic paper (e.g., co-first authors or co-corresponding authors), and this practice is controversial because of the lack of guidelines for establishing these roles and the potential for diffusion of responsibility and accountability [311, 312]. Yet, Equal Co-first authorship is becoming more common [313, 314, 315, 316, 311], likely because this practice provides flexibility for collaboration on large and complex problems. However, there are challenges that need to be addressed. For example, academic journal platforms and citation practices inconsistently address Equal Co-authorship and often advantage the author whose name is listed first [311, 313]. Also, publishing first- and last-author papers has importance for hiring and promoting academics [313, 311], but there are no guidelines for how Equal Co-first authorship should be used during these processes [311], and it is likely inconsistent across institutions and disciplines. To address some of these concerns, it has been recommended that journals have a clear statement indicating whether Equal Co-authors are allowed [311] and guidelines that clarify how the order of author names should be determined [312]. Additionally, CASRAI's CRediT- Contributor Roles Taxonomy[4] has been recommended to address concerns about whether Equal Co-authors had truly equal contributions [311]. If there can only be one first author, and first authorship is a metric considered important for hiring and promoting academics, dismissing this practice as flawed will discourage large-scale collaboration. Instead, by encouraging collaboration in the ways we approach and talk about researchers, the field of environmental engineering will be able to tackle much larger challenges than can be addressed with only one person leading.

[3] urlhttps://www.covid-web.org

[4] https://casrai.org/credit/

Bibliography

[1] Glen T. Daigger. "Evolving Urban Water and Residuals Management Paradigms: Water Reclamation and Reuse, Decentralization, and Resource Recovery". In: *Water Environment Research* 81.8 (2009). https://doi.org/10.2175/106143009X425898, pp. 809–823. DOI: 10.2175/106143009x425898.

[2] Glen T. Daigger et al. "Transforming Environmental Engineering and Science Education, Research, and Practice". In: *Environmental Engineering Science* 34.1 (2017), pp. 42–50. DOI: 10.1089/ees.2015.0353.

[3] Andreas N. Angelakis et al. "Water Reuse: From Ancient to Modern Times and the Future". In: *Frontiers in Environmental Science* 6 (2018), p. 26. DOI: 10.3389/fenvs.2018.00026.

[4] John J. Batten. "Realizing a More Sustainable Water Future From a "One Water" View". In: *Journal - American Water Works Association* 110.6 (2018), pp. 50–56. DOI: 10.1002/awwa.1098.

[5] *Guidelines for Drinking-water Quality*. Tech. rep. 978-92-4-154995-0. World Health Organization, 2017.

[6] Adam Olivieri et al. *Expert Panel Final Report: Evaluation of the Feasibility of Developing Uniform Water Recycling Criteria for Direct Potable Reuse*. Tech. rep. National Water Research Institute, 2016.

[7] *Potable Reuse Guidance for Producing Safe Drinking Water*. Tech. rep. World Health Organization, 2017.

[8] *Potable Reuse Compendium*. Tech. rep. United States Environmental Protection Agency and CDM Smith, 2017.

[9] George Tchobanoglous et al. *Framework for Direct Potable Reuse*. Tech. rep. WaterReuse, the American Water Works Association, the Water Environment Federation, and the National Water Research Institute, 2015.

[10] Phil M. Choi et al. "Wastewater-based epidemiology biomarkers: Past, present and future". In: *TrAC Trends in Analytical Chemistry* 105 (2018), pp. 453–469. DOI: 10.1016/j.trac.2018.06.004.

[11] Troy M. Scott et al. "Microbial Source Tracking: Current Methodology and Future Directions". In: *Applied and Environmental Microbiology* 68.12 (2002), pp. 5796–5803. DOI: 10.1128/aem.68.12.5796-5803.2002.

[12] Albert Bosch. *Human viruses in water: Perspectives in medical virology*. Elsevier, 2007.

[13] Xiaotong Wen et al. "Microbial Indicators and Their Use for Monitoring Drinking Water Quality—A Review". In: *Sustainability* 12.6 (2020), p. 2249. DOI: 10.3390/su12062249.

[14] United States Environmental Protection Agency. "National Primary Drinking Water Regulations: Revisions to the Total Coliform Rule; Final Rule, 40 CFR Parts 141 and 142, Federal Register 78:30". In: (2017).

[15] Olga Savichtcheva and Satoshi Okabe. "Alternative indicators of fecal pollution: Relations with pathogens and conventional indicators, current methodologies for direct pathogen monitoring and future application perspectives". In: *Water Research* 40.13 (2006), pp. 2463–2476. DOI: 10.1016/j.watres.2006.04.040.

[16] Jean-François Loret and Nadine Dumoutier. "Non-tuberculous mycobacteria in drinking water systems: A review of prevalence data and control means". In: *International Journal of Hygiene and Environmental Health* 222.4 (2019), pp. 628–634. DOI: 10.1016/j.ijheh.2019.01.002.

[17] Sai Hyun Lee, John T. O'Connor, and Shankha K Banerji. "Biologically mediated corrosion and its effects on water quality in distribution systems". In: *Journal (American Water Works Association)* 72.11 (1980), pp. 636–645.

[18] Iwona B. Beech and Jan Sunner. "Biocorrosion: towards understanding interactions between biofilms and metals". In: *Environmental biotechnology/Energy biotechnology* 15.3 (2004), pp. 181–186.

[19] Huifang Sun et al. "Formation and release behavior of iron corrosion products under the influence of bacterial communities in a simulated water distribution system". In: *Environmental Science: Processes & Impacts* 16.3 (2014), pp. 576–585. DOI: 10.1039/c3em00544e.

[20] Yan Zhang, Allian Griffin, and Marc Edwards. "Nitrification in Premise Plumbing: Role of Phosphate, pH and Pipe Corrosion". In: *Environmental Science & Technology* 42.12 (2008), pp. 4280–4284. DOI: 10.1021/es702483d.

[21] Paul W. J. J. van der Wielen, Stefan Voost, and Dick van der Kooij. "Ammonia-Oxidizing Bacteria and Archaea in Groundwater Treatment and Drinking Water Distribution Systems". In: *Appl. Environ. Microbiol.* 75.14 (2009), p. 4687.

[22] John M. Regan et al. "Diversity of nitrifying bacteria in full-scale chloraminated distribution systems". In: *Water Research* 37.1 (2003), pp. 197–205.

[23] Mercedes Cecilia Cruz et al. "Nitrifying niche differentiation in biofilms from full-scale chloraminated drinking water distribution system". In: *Water Research* 176 (2020), p. 115738. DOI: 10.1016/j.watres.2020.115738.

[24] Mark D. Sobsey. "Inactivation of Health-Related Microorganisms in Water by Disinfection Processes". In: *Water Science and Technology* 21.3 (1989), pp. 179–195. DOI: 10.2166/wst.1989.0098.

[25] Joyce M. Simpson, Jorge W. Santo Domingo, and Donald J. Reasoner. "Microbial Source Tracking: State of the Science". In: *Environmental Science & Technology* 36.24 (2002), pp. 5279–5288. DOI: 10.1021/es026000b.

[26] Valerie J. Harwood et al. "Validity of the Indicator Organism Paradigm for Pathogen Reduction in Reclaimed Water and Public Health Protection". In: *Applied and Environmental Microbiology* 71.6 (2005), pp. 3163–3170. DOI: 10.1128/aem.71.6.3163-3170.2005.

[27] Lars Jurzik et al. "Chemical and microbiological parameters as possible indicators for human enteric viruses in surface water". In: *International Journal of Hygiene and Environmental Health* 213.3 (2010), pp. 210–216. DOI: 10.1016/j.ijheh.2010.05.005.

[28] Charles P. Gerba, Walter Q. Betancourt, and Masaaki Kitajima. "How much reduction of virus is needed for recycled water: A continuous changing need for assessment?" In: *Water Research* 108 (2017), pp. 25–31. DOI: 10.1016/j.watres.2016.11.020.

[29] Brendon King et al. "Cryptosporidium Attenuation across the Wastewater Treatment Train: Recycled Water Fit for Purpose". In: *Applied and Environmental Microbiology* 83.5 (2017), e03068–16. DOI: 10.1128/aem.03068-16.

[30] A. M. Nasser et al. "Prevalence and fate of giardia cysts in wastewater treatment plants". In: *Journal of Applied Microbiology* 113.3 (2012), pp. 477–484. DOI: 10.1111/j.1365-2672.2012.05335.x.

[31] Fei Xiao et al. "Infectious SARS-CoV-2 in Feces of Patient with Severe COVID-19 - Volume 26, Number 8—August 2020 - Emerging Infectious Diseases journal - CDC". In: *Emerging Infectious Diseases* 26.8 (2020), pp. 1920–1922. DOI: 10.3201/eid2608.200681.

[32] Ling Li et al. "Analysis of viral load in different specimen types and serum antibody levels of COVID-19 patients". In: *Journal of Translational Medicine* 19.1 (2021), p. 30. DOI: 10.1186/s12967-020-02693-2.

[33] Sravanthi Parasa et al. "Prevalence of Gastrointestinal Symptoms and Fecal Viral Shedding in Patients With Coronavirus Disease 2019". In: *JAMA Network Open* 3.6 (2020), e2011335. DOI: 10.1001/jamanetworkopen.2020.11335.

[34] Kieran A. Walsh et al. "SARS-CoV-2 detection, viral load and infectivity over the course of an infection". In: *Journal of Infection* 81.3 (2020), pp. 357–371. DOI: 10.1016/j.jinf.2020.06.067.

[35] Yi Xu et al. "Characteristics of pediatric SARS-CoV-2 infection and potential evidence for persistent fecal viral shedding". In: *Nature Medicine* 26.4 (2020), pp. 502–505. DOI: 10.1038/s41591-020-0817-4.

[36] Yongjian Wu et al. "Prolonged presence of SARS-CoV-2 viral RNA in faecal samples". In: *The Lancet Gastroenterology & Hepatology* 5.5 (2020), pp. 434–435. DOI: 10.1016/s2468-1253(20)30083-2.

[37] Aaron Bivins et al. "Wastewater-Based Epidemiology: Global Collaborative to Maximize Contributions in the Fight Against COVID-19". In: *Environmental Science & Technology* 54.13 (2020), pp. 7754–7757. DOI: 10.1021/acs.est.0c02388.

[38] E.I. Prest et al. "Combining flow cytometry and 16S rRNA gene pyrosequencing: A promising approach for drinking water monitoring and characterization". In: *Water Research* 63 (2014), pp. 179–189. DOI: 10.1016/j.watres.2014.06.020.

[39] Ryan Cheswick et al. "Comparing flow cytometry with culture-based methods for microbial monitoring and as a diagnostic tool for assessing drinking water treatment processes". In: *Environment International* 130 (2019), p. 104893. DOI: 10.1016/j.envint.2019.06.003.

[40] Nadia Farhat, Lan Hee Kim, and Johannes S. Vrouwenvelder. "Online characterization of bacterial processes in drinking water systems". In: *npj Clean Water* 3.1 (2020), p. 16. DOI: 10.1038/s41545-020-0065-7.

[41] "Controlling Nitrification in Public Water Systems with Chloramines". In: (2015).

[42] Ziming Han et al. "Assessing the impact of source water on tap water bacterial communities in 46 drinking water supply systems in China". In: *Water Research* 172 (2020), p. 115469. DOI: 10.1016/j.watres.2020.115469.

[43] Ya Zhang, Seungdae Oh, and Wen-Tso Liu. "Impact of drinking water treatment and distribution on the microbiome continuum: an ecological disturbance's perspective". In: *Environmental Microbiology* 19.8 (2017). doi: 10.1111/1462-2920.13800, pp. 3163–3174. DOI: 10.1111/1462-2920.13800.

[44] Guus Roeselers et al. "Microbial biogeography of drinking water: patterns in phylogenetic diversity across space and time". In: *Environmental Microbiology* 17.7 (2015). doi: 10.1111/1462-2920.12739, pp. 2505–2514. DOI: 10.1111/1462-2920.12739.

[45] Ameet J. Pinto, Chuanwu Xi, and Lutgarde Raskin. "Bacterial Community Structure in the Drinking Water Microbiome Is Governed by Filtration Processes". In: *Environmental Science & Technology* 46.16 (2012). doi: 10.1021/es302042t, pp. 8851–8859. DOI: 10.1021/es302042t.

[46] Marie-Claude Besner et al. "Pressure Monitoring and Characterization of External Sources of Contamination at the Site of the Payment Drinking Water Epidemiological Studies". In: *Environ. Sci. Technol.* 44.1 (2010). doi: 10.1021/es901988y, pp. 269–277. DOI: 10.1021/es901988y.

[47] Marie-Claude Besner, Michèle Prévost, and Stig Regli. "Assessing the public health risk of microbial intrusion events in distribution systems: Conceptual model, available data, and challenges". In: *Water Research* 45.3 (2011), pp. 961–979. DOI: 10.1016/j.watres.2010.10.035.

[48] Natalie M Hull et al. "Longitudinal and Source-to-Tap New Orleans, LA, U.S.A. Drinking Water Microbiology". In: *Environ. Sci. Technol.* 51.8 (2017). doi: 10.1021/acs.est.6b06064, pp. 4220–4229. DOI: 10.1021/acs.est.6b06064.

[49] Hong Wang et al. "Effect of GAC pre-treatment and disinfectant on microbial community structure and opportunistic pathogen occurrence". In: *Water Research* 47.15 (2013), pp. 5760–5772. DOI: 10.1016/j.watres.2013.06.052.

[50] Xiao Ma et al. "Centralized Drinking Water Treatment Operations Shape Bacterial and Fungal Community Structure". In: *Environ. Sci. Technol.* 51.13 (2017). doi: 10.1021/acs.est.7b00768, pp. 7648–7657. DOI: 10.1021/acs.est.7b00768.

[51] Quyen M. Bautista-de los Santos et al. "Emerging investigators series: microbial communities in full-scale drinking water distribution systems – a meta-analysis". In: *Environ. Sci.: Water Res. Technol.* 2.4 (2016), pp. 631–644. DOI: 10.1039/c6ew00030d.

[52] Zihan Dai et al. "Disinfection exhibits systematic impacts on the drinking water microbiome". In: *Microbiome* 8.1 (2020), p. 42. DOI: 10.1186/s40168-020-00813-0.

[53] Paul W. J. J. van der Wielen and Dick van der Kooij. "Nontuberculous Mycobacteria, Fungi, and Opportunistic Pathogens in Unchlorinated Drinking Water in the Netherlands". In: *Applied and Environmental Microbiology* 79.3 (2013), pp. 825–834. DOI: 10.1128/aem.02748-12.

[54] Timothy G. Otten et al. "Elucidation of Taste- and Odor-Producing Bacteria and Toxigenic Cyanobacteria in a Midwestern Drinking Water Supply Reservoir by Shotgun Metagenomic Analysis". In: *Applied and Environmental Microbiology* 82.17 (2016), pp. 5410–5420. DOI: 10.1128/aem.01334-16.

[55] Andrew Westbrook and Francis A. Digiano. "Rate of chloramine decay at pipe surfaces". In: *Journal - American Water Works Association* 101.7 (2009), pp. 59–70. DOI: 10.1002/j.1551-8833.2009.tb09924.x.

[56] Charles N. Haas et al. "Chlorine Demand in disinfecting Water Mains". In: *Journal - American Water Works Association* 94.1 (2002), pp. 97–102. DOI: 10.1002/j.1551-8833.2002.tb09385.x.

[57] A.O. Al-Jasser. "Chlorine decay in drinking-water transmission and distribution systems: Pipe service age effect". In: *Water Research* 41.2 (2007), pp. 387–396. DOI: 10.1016/j.watres.2006.08.032.

[58] Alina Nescerecka et al. "Biological Instability in a Chlorinated Drinking Water Distribution Network". In: *PLoS ONE* 9.5 (2014), e96354. DOI: 10.1371/journal.pone.0096354.

[59] Alina Nescerecka, Talis Juhna, and Frederik Hammes. "Identifying the underlying causes of biological instability in a full-scale drinking water supply system". In: *Water Research* 135 (2018), pp. 11–21. DOI: 10.1016/j.watres.2018.02.006.

[60] Huiping Huang et al. "High-performance size exclusion chromatography with a multi-wavelength absorbance detector study on dissolved organic matter characterisation along a water distribution system". In: *Journal of Environmental Sciences* 44 (2016), pp. 235–243.

[61] Simon Gillespie et al. "Assessing microbiological water quality in drinking water distribution systems with disinfectant residual using flow cytometry". In: *Water Research* 65 (2014), pp. 224–234. DOI: 10.1016/j.watres.2014.07.029.

[62] Vanessa C. F. Dias et al. "Identification of Factors Affecting Bacterial Abundance and Community Structures in a Full-Scale Chlorinated Drinking Water Distribution System". In: *Water* 11.3 (2019), p. 627. DOI: 10.3390/w11030627.

[63] Stacia T. McCoy and Jeanne M. VanBriesen. "Temporal Variability of Bacterial Diversity in a Chlorinated Drinking Water Distribution System". In: *Journal of Environmental Engineering* 138.7 (2012), pp. 786–795. DOI: 10.1061/(asce)ee.1943-7870.0000539.

[64] Yoann Perrin et al. "Microbiome of drinking water: A full-scale spatio-temporal study to monitor water quality in the Paris distribution system". In: *Water Research* 149 (2019), pp. 375–385. DOI: 10.1016/j.watres.2018.11.013.

[65] Vicente Gomez-Alvarez et al. "Bacterial composition in a metropolitan drinking water distribution system utilizing different source waters". In: *Journal of Water and Health* 13.1 (2014), pp. 140–151. DOI: 10.2166/wh.2014.057.

[66] I. Douterelo et al. "Spatial and temporal analogies in microbial communities in natural drinking water biofilms". In: *Science of The Total Environment* 581 (2017), pp. 277–288. DOI: 10.1016/j.scitotenv.2016.12.118.

[67] Ameet J. Pinto et al. "Spatial-Temporal Survey and Occupancy-Abundance Modeling To Predict Bacterial Community Dynamics in the Drinking Water Microbiome". In: *mBio* 5.3 (2014), e01135–14. DOI: 10.1128/mbio.01135-14.

[68] Fangqiong Ling et al. "Core-satellite populations and seasonality of water meter biofilms in a metropolitan drinking water distribution system". In: *The ISME Journal* 10.3 (2016), pp. 582–595. DOI: 10.1038/ismej.2015.136.

[69] Joline El-Chakhtoura et al. "Dynamics of bacterial communities before and after distribution in a full-scale drinking water network". In: *Water Research* 74 (2015), pp. 180–190. DOI: 10.1016/j.watres.2015.02.015.

[70] E. I. Prest et al. "Long-Term Bacterial Dynamics in a Full-Scale Drinking Water Distribution System". In: *PLoS ONE* 11.10 (2016), e0164445. DOI: 10.1371/journal.pone.0164445.

[71] Lihua Chen et al. "Assessing the transition effects in a drinking water distribution system caused by changing supply water quality: an indirect approach by characterizing suspended solids". In: *Water Research* 168 (2020), p. 115159. DOI: 10.1016/j.watres.2019.115159.

[72] Sandy Chan et al. "Bacterial release from pipe biofilm in a full-scale drinking water distribution system". In: *npj Biofilms and Microbiomes* 5.1 (2019), p. 9. DOI: 10.1038/s41522-019-0082-9.

[73] Fan Yang et al. "Effect of sulfate on the transformation of corrosion scale composition and bacterial community in cast iron water distribution pipes". In: *Water Research* 59 (2014), pp. 46–57. DOI: 10.1016/j.watres.2014.04.003.

[74] Huifang Sun et al. "Effects of sulfate on heavy metal release from iron corrosion scales in drinking water distribution system". In: *Water Research* 114 (2017), pp. 69–77. DOI: 10.1016/j.watres.2017.02.021.

[75] Yue Hu et al. "Potential shift of bacterial community structure and corrosion-related bacteria in drinking water distribution pipeline driven by water source switching". In: *Frontiers of Environmental Science & Engineering* 15.2 (2020), p. 28. DOI: 10.1007/s11783-020-1320-3.

[76] Susan J. Masten, Simon H. Davies, and Shawn P. Mcelmurry. "Flint Water Crisis: What Happened and Why?" In: *Journal - American Water Works Association* 108.12 (2016), pp. 22–34. DOI: 10.5942/jawwa.2016.108.0195.

[77] David Otto Schwake et al. "Legionella DNA Markers in Tap Water Coincident with a Spike in Legionnaires' Disease in Flint, MI". In: *Environ. Sci. Technol. Lett.* 3.9 (2016). doi: 10.1021/acs.estlett.6b00192, pp. 311–315. DOI: 10.1021/acs.estlett.6b00192.

[78] Brian M. Pecson et al. "Reliability of pathogen control in direct potable reuse: Performance evaluation and QMRA of a full-scale 1 MGD advanced treatment train". In: *Water Research* 122 (2017), pp. 258–268. DOI: 10.1016/j.watres.2017.06.014.

[79] Jeffrey A. Soller et al. "Evaluation of microbiological risks associated with direct potable reuse". In: *Quantitative Microbial Risk Assessment of Reclaimed Water* 5 (2017), pp. 3–14.

[80] California Water Boards. "A PROPOSED FRAMEWORK FOR REGULATING DIRECT POTABLE REUSE IN CALIFORNIA". In: (2018).

[81] P. du Pisani and J. G. Menge. "Direct potable reclamation in Windhoek: a critical review of the design philosophy of new Goreangab drinking water reclamation plant". In: *Water Science & Technology: Water Supply* 13.2 (2013), pp. 214–226.

[82] *All options on the table: Lessons learned from the journeys of others*. Tech. rep. Water Services Association of Australia, 2019.

[83] Blake W. Stamps et al. "Characterization of the Microbiome at the World's Largest Potable Water Reuse Facility". In: *Frontiers in Microbiology* 9 (2018), pp. 2435–2435.

[84] Rose S. Kantor, Scott E. Miller, and Kara L. Nelson. "The Water Microbiome Through a Pilot Scale Advanced Treatment Facility for Direct Potable Reuse". In: *Frontiers in Microbiology* 10 (2019), p. 21. DOI: 10.3389/fmicb.2019.00993.

[85] Scott E. Miller, Roberto A. Rodriguez, and Kara L. Nelson. "Removal and growth of microorganisms across treatment and simulated distribution at a pilot-scale direct potable reuse facility". In: *Environ. Sci.: Water Res. Technol.* 107.11 (2020), p. 36. DOI: 10.1039/c9ew01087d.

[86] Takahiro Fujioka and Sandrine Boivin. "Assessing bacterial infiltration through reverse osmosis membrane". In: *Environmental Technology & Innovation* 19 (2020), p. 100818. DOI: 10.1016/j.eti.2020.100818.

[87] Moustapha Harb et al. "Background Antibiotic Resistance and Microbial Communities Dominate Effects of Advanced Purified Water Recharge to an Urban Aquifer". In: *Environmental Science & Technology Letters* 6.10 (2019), pp. 578–584. DOI: 10.1021/acs.estlett.9b00521.

[88] Blake W. Stamps and John R. Spear. "Identification of Metagenome-Assembled Genomes Containing Antimicrobial Resistance Genes, Isolated from an Advanced Water Treatment Facility". In: *Microbiology Resource Announcements* 9.14 (2020). DOI: 10.1128/mra.00003-20.

[89] Emily Garner et al. "Impact of blending for direct potable reuse on premise plumbing microbial ecology and regrowth of opportunistic pathogens and antibiotic resistant bacteria". In: *Water Research* 151 (2019), pp. 75–86. DOI: 10.1016/j.watres.2018.12.003.

[90] Sharon P. Nappier, Jeffrey A. Soller, and Sorina E. Eftim. "Potable Water Reuse: What Are the Microbiological Risks?" In: *Current Environmental Health Reports* 5.2 (2018), pp. 283–292. DOI: 10.1007/s40572-018-0195-y.

[91] California Code of Regulations. "Water Recycling Criteria, Title 22, Division 4, Chapter 3". In: *Sacramento, CA* (2015).

[92] California State Water Resources Control Board. *Regulations Related to Recycled Water, Title 22, Division 4, Chapter 3*. 2018.

[93] United States Environmental Protection Agency. *Long Term 2 Enhanced Surface Water Treatment Rule. 40 CFR Parts 9, 141, and 142.* 2006.

[94] *Addendum to A Framework for Direct Potable Reuse*. 2021. URL: https://www.waterboards.ca.gov/drinking%5C_water/certlic/drinkingwater/documents/direct%5C_potable%5C_reuse/dprframewkaddendum.pdf (visited on 03/29/2021).

[95] Charles P. Gerba et al. "Reducing uncertainty in estimating virus reduction by advanced water treatment processes". In: *Water Research* 133 (2018), pp. 282–288. DOI: 10.1016/j.watres.2018.01.044.

[96] Stig Regli et al. "Modeling the Risk From Giardia and Viruses in Drinking Water". In: *Journal - American Water Works Association* 83.11 (1991), pp. 76–84. DOI: 10.1002/j.1551-8833.1991.tb07252.x.

[97] Radboud J. Duintjer Tebbens et al. "Insights from a Systematic Search for Information on Designs, Costs, and Effectiveness of Poliovirus Environmental Surveillance Systems". In: *Food and Environmental Virology* 9.4 (2017), pp. 361–382. DOI: 10.1007/s12560-017-9314-4.

[98] Yakir Berchenko et al. "Estimation of polio infection prevalence from environmental surveillance data". In: *Science Translational Medicine* 9.383 (2017), eaaf6786. DOI: 10.1126/scitranslmed.aaf6786.

[99] T. Pöyry, M. Stenvik, and T. Hovi. "Viruses in sewage waters during and after a poliomyelitis outbreak and subsequent nationwide oral poliovirus vaccination campaign in Finland." In: *Appl. Environ. Microbiol.* 54.2 (1988), p. 371.

[100] Pedro Más Lago et al. "Poliovirus detection in wastewater and stools following an immunization campaign in Havana, Cuba". In: *International Journal of Epidemiology* 32.5 (2003), pp. 772–777. DOI: 10.1093/ije/dyg185.

[101] Brian Pecson et al. "Editorial Perspectives: will SARS-CoV-2 reset public health requirements in the water industry? Integrating lessons of the past and emerging research". In: *Environmental Science: Water Research & Technology* 6.7 (2020), pp. 1761–1764. DOI: 10.1039/d0ew90031a.

[102] Aaron Bivins et al. "Persistence of SARS-CoV-2 in Water and Wastewater". In: *Environmental Science & Technology Letters* 7.12 (2020), pp. 937–942. DOI: 10.1021/acs.estlett.0c00730.

[103] Irene Xagoraraki and Evan O'Brien. "Women in Water Quality, Investigations by Prominent Female Engineers". In: *Women in Engineering and Science* (2019), pp. 75–97. DOI: 10.1007/978-3-030-17819-2_5.

[104] Shinobu Kazama et al. "Environmental Surveillance of Norovirus Genogroups I and II for Sensitive Detection of Epidemic Variants". In: *Applied and Environmental Microbiology* 83.9 (2017), e03406–16. DOI: 10.1128/aem.03406-16.

[105] Gertjan Medema et al. "Presence of SARS-Coronavirus-2 RNA in Sewage and Correlation with Reported COVID-19 Prevalence in the Early Stage of the Epidemic in The Netherlands". In: *Environmental Science & Technology Letters* 7.7 (2020), pp. 511–516. DOI: 10.1021/acs.estlett.0c00357.

[106] Artem Nemudryi et al. "Temporal detection and phylogenetic assessment of SARS-CoV-2 in municipal wastewater". In: *Cell Reports Medicine* 1.6 (2020), p. 100098. DOI: 10.1016/j.xcrm.2020.100098.

[107] Akihiko Hata et al. "Detection of SARS-CoV-2 in wastewater in Japan during a COVID-19 outbreak". In: *Science of The Total Environment* 758 (2021), p. 143578. DOI: 10.1016/j.scitotenv.2020.143578.

[108] Mohamed Hamouda et al. "Wastewater surveillance for SARS-CoV-2: Lessons learnt from recent studies to define future applications". In: *Science of The Total Environment* 759 (2020), p. 143493. DOI: 10.1016/j.scitotenv.2020.143493.

[109] Jordan Peccia et al. "Measurement of SARS-CoV-2 RNA in wastewater tracks community infection dynamics". In: *Nature Biotechnology* 38.10 (2020), pp. 1164–1167. DOI: 10.1038/s41587-020-0684-z.

[110] Gerald Sedmak, David Bina, and Jeffrey MacDonald. "Assessment of an Enterovirus Sewage Surveillance System by Comparison of Clinical Isolates with Sewage Isolates from Milwaukee, Wisconsin, Collected August 1994 to December 2002". In: *Applied and Environmental Microbiology* 69.12 (2003), pp. 7181–7187. DOI: 10.1128/aem.69.12.7181-7187.2003.

[111] Maria Hellmér et al. "Detection of Pathogenic Viruses in Sewage Provided Early Warnings of Hepatitis A Virus and Norovirus Outbreaks". In: *Applied and Environmental Microbiology* 80.21 (2014), pp. 6771–6781. DOI: 10.1128/aem.01981-14.

[112] Giuseppina La Rosa et al. "Surveillance of hepatitis A virus in urban sewages and comparison with cases notified in the course of an outbreak, Italy 2013". In: *BMC Infectious Diseases* 14.1 (2014), p. 419. DOI: 10.1186/1471-2334-14-419.

[113] Walter Jakubowski et al. "Determining Giardiasis Prevalence by Examination of Sewage". In: *Water Science and Technology* 24.2 (1991), pp. 173–178. DOI: 10.2166/wst.1991.0052.

[114] Warish Ahmed et al. "SARS-CoV-2 RNA monitoring in wastewater as a potential early warning system for COVID-19 transmission in the community: A temporal case study". In: *Science of The Total Environment* 761 (2021), p. 144216. DOI: 10.1016/j.scitotenv.2020.144216.

[115] Daniel Gerrity et al. "Early-pandemic wastewater surveillance of SARS-CoV-2 in Southern Nevada: Methodology, occurrence, and incidence/prevalence considerations". In: *Water Research X* 10 (2021), p. 100086. DOI: 10.1016/j.wroa.2020.100086.

[116] Maxime Bisseux et al. "Monitoring human enteric viruses in wastewater and relevance to infections encountered in the clinical setting: a one-year experiment in central France, 2014 to 2015". In: *Eurosurveillance* 23.7 (2018), pp. 17–00237. DOI: 10.2807/1560-7917.es.2018.23.7.17-00237.

[117] Kang Mao et al. "The potential of wastewater-based epidemiology as surveillance and early warning of infectious disease outbreaks". In: *Current Opinion in Environmental Science & Health* 17 (2020), pp. 1–7. DOI: 10.1016/j.coesh.2020.04.006.

[118] Walter Randazzo et al. "SARS-CoV-2 RNA in wastewater anticipated COVID-19 occurrence in a low prevalence area". In: *Water Research* 181 (2020), p. 115942. DOI: 10.1016/j.watres.2020.115942.

[119] Walter Randazzo et al. "Metropolitan wastewater analysis for COVID-19 epidemiological surveillance". In: *International Journal of Hygiene and Environmental Health* 230 (2020), p. 113621. DOI: 10.1016/j.ijheh.2020.113621.

[120] Michio Murakami et al. "Letter to the Editor: Wastewater-Based Epidemiology Can Overcome Representativeness and Stigma Issues Related to COVID-19". In: *Environmental Science & Technology* 54.9 (2020), pp. 5311–5311. DOI: 10.1021/acs.est.0c02172.

[121] Natalie Sims and Barbara Kasprzyk-Hordern. "Future Perspectives of Wastewater-Based Epidemiology: Monitoring Infectious Disease Spread and Resistance to the Community Level". In: *Environment International* 139 (2020), p. 105689. DOI: 10.1016/j.envint.2020.105689.

[122] Gareth J. Griffith et al. "Collider bias undermines our understanding of COVID-19 disease risk and severity". In: *Nature Communications* 11.1 (2020), p. 5749. DOI: 10.1038/s41467-020-19478-2.

[123] S. M. Cacciò and R. M. Chalmers. "Human cryptosporidiosis in Europe". In: *Clinical Microbiology and Infection* 22.6 (2016), pp. 471–480. DOI: 10.1016/j.cmi.2016.04.021.

[124] Wayne Hall et al. "An analysis of ethical issues in using wastewater analysis to monitor illicit drug use". In: *Addiction* 107.10 (2012), pp. 1767–1773. DOI: 10.1111/j.1360-0443.2012.03887.x.

[125] Janelle R Thompson et al. "Making waves: Wastewater surveillance of SARS-CoV-2 for population-based health management". In: *Water Research* 184 (2020), p. 116181. DOI: 10.1016/j.watres.2020.116181.

[126] *Guidelines on Ethical Issues in Public Health Surveillance*. Tech. rep. World Health Organization, 2017.

[127] Olga E. Hart and Rolf U. Halden. "Simulated 2017 nationwide sampling at 13,940 major U.S. sewage treatment plants to assess seasonal population bias in wastewater-based epidemiology". In: *Science of The Total Environment* 727 (2020), p. 138406. DOI: 10.1016/j.scitotenv.2020.138406.

[128] Olga E. Hart and Rolf U. Halden. "Modeling wastewater temperature and attenuation of sewage-borne biomarkers globally". In: *Water Research* 172 (2020), p. 115473. DOI: 10.1016/j.watres.2020.115473.

[129] Alireza Zahedi et al. "Wastewater-based epidemiology—surveillance and early detection of waterborne pathogens with a focus on SARS-CoV-2, Cryptosporidium and Giardia". In: *Parasitology Research* (2021), pp. 1–22. DOI: 10.1007/s00436-020-07023-5.

[130] Masaaki Kitajima et al. "SARS-CoV-2 in wastewater: State of the knowledge and research needs". In: *Science of The Total Environment* 739 (2020), p. 139076. DOI: 10.1016/j.scitotenv.2020.139076.

[131] Christian G. Daughton. "Wastewater surveillance for population-wide Covid-19: The present and future". In: *Science of The Total Environment* 736 (2020), p. 139631. DOI: 10.1016/j.scitotenv.2020.139631.

[132] Raul Gonzalez et al. "COVID-19 surveillance in Southeastern Virginia using wastewater-based epidemiology". In: *Water Research* 186 (2020), p. 116296. DOI: 10.1016/j.watres.2020.116296.

[133] Fuqing Wu et al. "SARS-CoV-2 Titers in Wastewater Are Higher than Expected from Clinically Confirmed Cases". In: *mSystems* 5.4 (2020), e00614–20. DOI: 10.1128/msystems.00614-20.

[134] Manish Kumar et al. "First proof of the capability of wastewater surveillance for COVID-19 in India through detection of genetic material of SARS-CoV-2". In: *Science of The Total Environment* 746 (2020), p. 141326. DOI: 10.1016/j.scitotenv.2020.141326.

[135] Amarylle S. Doorn et al. "Systematic review with meta-analysis: SARS-CoV-2 stool testing and the potential for faecal-oral transmission". In: *Alimentary Pharmacology & Therapeutics* 52.8 (2020), pp. 1276–1288. DOI: 10.1111/apt.16036.

[136] Amy E. Benefield et al. "SARS-CoV-2 viral load peaks prior to symptom onset: a systematic review and individual-pooled analysis of coronavirus viral load from 66 studies". In: *medRxiv : the preprint server for health sciences* (). DOI: 10.1101/2020.09.28.20202028.

[137] Olga E. Hart and Rolf U. Halden. "Computational analysis of SARS-CoV-2/COVID-19 surveillance by wastewater-based epidemiology locally and globally: Feasibility, economy, opportunities and challenges". In: *Science of The Total Environment* 730 (2020), p. 138875. DOI: 10.1016/j.scitotenv.2020.138875.

[138] Michael D. Besmer et al. "Evaluating Monitoring Strategies to Detect Precipitation-Induced Microbial Contamination Events in Karstic Springs Used for Drinking Water". In: *Frontiers in Microbiology* 8 (2017), p. 81. DOI: 10.3389/fmicb.2017.02229.

[139] Michael D. Besmer et al. "Online flow cytometry reveals microbial dynamics influenced by concurrent natural and operational events in groundwater used for drinking water treatment". In: *Scientific Reports* 6 (2016), 38462 EP –. DOI: 10.1038/srep38462.

[140] Michael D. Besmer et al. "Laboratory-Scale Simulation and Real-Time Tracking of a Microbial Contamination Event and Subsequent Shock-Chlorination in Drinking Water". In: *Frontiers in Microbiology* 8 (2017), p. 366. DOI: 10.3389/fmicb.2017.01900.

[141] Ruben Props et al. "Detection of microbial disturbances in a drinking water microbial community through continuous acquisition and advanced analysis of flow cytometry data". In: *Water Research* 145 (2018), pp. 73–82. DOI: 10.1016/j.watres.2018.08.013.

[142] Nicole Rockey et al. "The utility of flow cytometry for potable reuse". In: *Current Opinion in Biotechnology* 57 (2019), pp. 42–49. DOI: 10.1016/j.copbio.2018.12.009.

[143] Franciszek Pistelok et al. "Using ATP tests for assessment of hygiene risks". In: *Ecological Chemistry and Engineering S* 23.2 (2016), pp. 259–270. DOI: 10.1515/eces-2016-0018.

[144] Frederik Hammes et al. "Measurement and interpretation of microbial adenosine tri-phosphate (ATP) in aquatic environments". In: *Water Research* 44.13 (2010), pp. 3915–3923. DOI: 10.1016/j.watres.2010.04.015.

[145] Patrícia Dolabela Costa et al. "ATP - bioluminescence as a technique to evaluate the microbiological quality of water in food industry". In: *Brazilian Archives of Biology and Technology* 47.3 (2004), pp. 399–405. DOI: 10.1590/s1516-89132004000300010.

[146] Martin J. Allen, Stephen C. Edberg, and Donald J. Reasoner. "Heterotrophic plate count bacteria—what is their significance in drinking water?" In: *International Journal of Food Microbiology* 92.3 (2004), pp. 265–274. DOI: 10.1016/j.ijfoodmicro.2003.08.017.

[147] E. Gatza, F. Hammes, and E. Prest. "Assessing water quality with the BD Accuri™ C6 flow cytometer". In: *White paper. BD Biosciences* (2013).

[148] S. Van Nevel et al. "Flow cytometric bacterial cell counts challenge conventional heterotrophic plate counts for routine microbiological drinking water monitoring". In: *Water Research* 113 (2017), pp. 191–206. DOI: 10.1016/j.watres.2017.01.065.

[149] Karin Lautenschlager et al. "A microbiology-based multi-parametric approach towards assessing biological stability in drinking water distribution networks". In: *Water Research* 47.9 (2013), pp. 3015–3025. DOI: 10.1016/j.watres.2013.03.002.

[150] Weiying Li et al. "Effect of disinfectant residual on the interaction between bacterial growth and assimilable organic carbon in a drinking water distribution system". In: *Chemosphere* 202 (2018), pp. 586–597.

[151] Tingting Liu et al. "Bacterial characterization of Beijing drinking water by flow cytometry and MiSeq sequencing of the 16S rRNA gene". In: *Ecology and Evolution* 6.4 (2016). doi: 10.1002/ece3.1955, pp. 923–934. DOI: 10.1002/ece3.1955.

[152] Mark W. LeChevallier. "Monitoring distribution systems for Legionella pneumophila using Legiolert". In: *AWWA Water Science* 1.1 (2019). DOI: 10.1002/aws2.1122.

[153] Kaveh Amini and Heinz-Bernhard Kraatz. "Recent advances and developments in monitoring biological agents in water samples". In: *Reviews in Environmental Science and Bio/Technology* 14.1 (2015), pp. 23–48. DOI: 10.1007/s11157-014-9351-5.

[154] M. M. Lleo et al. "Molecular vs culture methods for the detection of bacterial faecal indicators in groundwater for human use". In: *Letters in Applied Microbiology* 40.4 (2005), pp. 289–294. DOI: 10.1111/j.1472-765x.2005.01666.x.

[155] Lucia Bonadonna, Rossella Briancesco, and Giuseppina La Rosa. "Innovative analytical methods for monitoring microbiological and virological water quality". In: *Microchemical Journal* 150 (2019), p. 104160. DOI: 10.1016/j.microc.2019.104160.

[156] J. Vierheilig et al. "Potential applications of next generation DNA sequencing of 16S rRNA gene amplicons in microbial water quality monitoring". In: *Water Science and Technology* 72.11 (2015), pp. 1962–1972. DOI: 10.2166/wst.2015.407.

[157] K. A. Wetterstrand. *DNA Sequencing Costs: Data from the NHGRI Genome Sequencing Program (GSP)*. 2020. URL: https://www.genome.gov/about-genomics/fact-sheets/DNA-Sequencing-Costs-Data (visited on 02/28/2021).

[158] Daniel Straub et al. "Interpretations of Environmental Microbial Community Studies Are Biased by the Selected 16S rRNA (Gene) Amplicon Sequencing Pipeline". In: *Frontiers in Microbiology* 11 (2020), p. 550420. DOI: 10.3389/fmicb.2020.550420.

[159] Agata Wesolowska-Andersen et al. "Choice of bacterial DNA extraction method from fecal material influences community structure as evaluated by metagenomic analysis". In: *Microbiome* 2.1 (2014), p. 19. DOI: 10.1186/2049-2618-2-19.

[160] Martin F. Laursen, Marlene D. Dalgaard, and Martin I. Bahl. "Genomic GC-Content Affects the Accuracy of 16S rRNA Gene Sequencing Based Microbial Profiling due to PCR Bias". In: *Frontiers in Microbiology* 8 (2017), p. 1934. DOI: 10.3389/fmicb.2017.01934.

[161] Jakob Brandt and Mads Albertsen. "Investigation of Detection Limits and the Influence of DNA Extraction and Primer Choice on the Observed Microbial Communities in Drinking Water Samples Using 16S rRNA Gene Amplicon Sequencing". In: *Frontiers in Microbiology* 9 (2018), p. 2140. DOI: 10.3389/fmicb.2018.02140.

[162] Ann McCarthy et al. "RNA Preservation Agents and Nucleic Acid Extraction Method Bias Perceived Bacterial Community Composition". In: *PLOS ONE* 10.3 (2015), e0121659. DOI: 10.1371/journal.pone.0121659.

[163] L. F. Stinson, J. A. Keelan, and M. S. Payne. "Identification and removal of contaminating microbial DNA from PCR reagents: impact on low-biomass microbiome analyses". In: *Letters in Applied Microbiology* 68.1 (2019), pp. 2–8. DOI: 10.1111/lam.13091.

[164] Susannah J. Salter et al. "Reagent and laboratory contamination can critically impact sequence-based microbiome analyses". In: *BMC Biology* 12.1 (2014), p. 87. DOI: 10.1186/s12915-014-0087-z.

[165] Marcus C. de Goffau et al. "Recognizing the reagent microbiome". In: *Nature Microbiology* 3.8 (2018), pp. 851–853. DOI: 10.1038/s41564-018-0202-y.

[166] Simon Toze. "PCR and the detection of microbial pathogens in water and wastewater". In: *Water Research* 33.17 (1999), pp. 3545–3556. DOI: 10.1016/s0043-1354(99)00071-8.

[167] K. E. Gibson et al. "Measuring and mitigating inhibition during quantitative real time PCR analysis of viral nucleic acid extracts from large-volume environmental water samples". In: *Water Research* 46.13 (2012), pp. 4281–4291. DOI: 10.1016/j.watres.2012.04.030.

[168] Jennifer Gentry-Shields et al. "Determination of specific types and relative levels of QPCR inhibitors in environmental water samples using excitation–emission matrix spectroscopy and PARAFAC". In: *Water Research* 47.10 (2013), pp. 3467–3476. DOI: 10.1016/j.watres.2013.03.049.

[169] Akihiko Hata, Hiroyuki Katayama, and Hiroaki Furumai. "Organic Substances Interfere with Reverse Transcription-Quantitative PCR-Based Virus Detection in Water Samples". In: *Applied and Environmental Microbiology* 81.5 (2015), pp. 1585–1593. DOI: 10.1128/aem.03082-14.

[170] C. Schrader et al. "PCR inhibitors – occurrence, properties and removal". In: *Journal of Applied Microbiology* 113.5 (2012), pp. 1014–1026. DOI: 10.1111/j.1365-2672.2012.05384.x.

[171] Joanne B. Emerson et al. "Schrödinger's microbes: Tools for distinguishing the living from the dead in microbial ecosystems". In: *Microbiome* 5.1 (2017), p. 86. DOI: 10.1186/s40168-017-0285-3.

[172] Andreas Nocker et al. "Discrimination between live and dead cells in bacterial communities from environmental water samples analyzed by 454 pyrosequencing". In: *International Microbiology* 13.2 (2010), pp. 59–65.

[173] Mariana Fittipaldi, Andreas Nocker, and Francesc Codony. "Progress in understanding preferential detection of live cells using viability dyes in combination with DNA amplification". In: *Journal of Microbiological Methods* 91.2 (2012), pp. 276–289. DOI: 10.1016/j.mimet.2012.08.007.

[174] Andreas Nocker, Katherine E. Sossa, and Anne K. Camper. "Molecular monitoring of disinfection efficacy using propidium monoazide in combination with quantitative PCR". In: *Journal of Microbiological Methods* 70.2 (2007), pp. 252–260. DOI: 10.1016/j.mimet.2007.04.014.

[175] Kaare M. Nielsen et al. "Release and persistence of extracellular DNA in the environment". In: *Environmental Biosafety Research* 6.1-2 (2007), pp. 37–53. DOI: 10.1051/ebr:2007031.

[176] K. L. Josephson, C. P. Gerba, and I. L. Pepper. "Polymerase chain reaction detection of nonviable bacterial pathogens." In: *Applied and Environmental Microbiology* 59.10 (1993), pp. 3513–3515.

[177] Andreas Nocker et al. "When are bacteria dead? A step towards interpreting flow cytometry profiles after chlorine disinfection and membrane integrity staining". In: *Environmental Technology* (2016). doi: 10.1080/09593330.2016.1262463, pp. 1–29. DOI: 10.1080/09593330.2016.1262463.

[178] Tzu-Hsin Chiao et al. "Differential Resistance of Drinking Water Bacterial Populations to Monochloramine Disinfection." In: *Environmental Science & Technology* 48.7 (2014). doi: 10.1021/es4055725, pp. 4038–4047. DOI: 10.1021/es4055725.

[179] Hang Shi, Elodie V. Pasco, and Volodymyr V. Tarabara. "Membrane-based methods of virus concentration from water: a review of process parameters and their effects on virus recovery". In: *Environmental Science: Water Research & Technology* 3.5 (2017), pp. 778–792. DOI: 10.1039/c7ew00016b.

[180] Rashmi Sinha et al. "Assessment of variation in microbial community amplicon sequencing by the Microbiome Quality Control (MBQC) project consortium". In: *Nature Biotechnology* 35.11 (2017), pp. 1077–1086.

[181] Benjamin J. Tscharke et al. "Harnessing the Power of the Census: Characterizing Wastewater Treatment Plant Catchment Populations for Wastewater-Based Epidemiology". In: *Environmental Science & Technology* 53.17 (2019), pp. 10303–10311. DOI: 10.1021/acs.est.9b03447.

[182] Kyle Curtis et al. "Wastewater SARS-CoV-2 Concentration and Loading Variability from Grab and 24-Hour Composite Samples". In: *medRxiv : the preprint server for health sciences* (2020). DOI: 10.1101/2020.07.10.20150607.

[183] Harishankar Kopperi et al. "Methodological Approach for Wastewater Based Epidemiological Studies for SARS-CoV-2". In: *medRxiv : the preprint server for health sciences* (2021). DOI: 10.1101/2021.02.17.21251905.

[184] Nikiforos Alygizakis et al. "Analytical methodologies for the detection of SARS-CoV-2 in wastewater: Protocols and future perspectives". In: *TrAC Trends in Analytical Chemistry* 134 (2020), p. 116125. DOI: 10.1016/j.trac.2020.116125.

[185] Oscar N. Whitney et al. "Sewage, Salt, Silica, and SARS-CoV-2 (4S): An Economical Kit-Free Method for Direct Capture of SARS-CoV-2 RNA from Wastewater". In: *Environmental Science & Technology* (2021). DOI: 10.1021/acs.est.0c08129.

[186] S. Wurtzer et al. "Several forms of SARS-CoV-2 RNA can be detected in wastewaters: Implication for wastewater-based epidemiology and risk assessment". In: *Water Research* 198 (2021), p. 117183. DOI: https://doi.org/10.1016/j.watres.2021.117183.

[187] Andrea I. Silverman and Alexandria B. Boehm. "Systematic Review and Meta-Analysis of the Persistence and Disinfection of Human Coronaviruses and Their Viral Surrogates in Water and Wastewater". In: *Environmental Science & Technology Letters* 7.8 (2020), pp. 544–553. DOI: 10.1021/acs.estlett.0c00313.

[188] Y.-S.C. Shieh et al. "Methods to remove inhibitors in sewage and other fecal wastes for enterovirus detection by the polymerase chain reaction". In: *Journal of Virological Methods* 54.1 (1995), pp. 51–66. DOI: 10.1016/0166-0934(95)00025-p.

[189] Lauren C. Kennedy et al. "Effect of disinfectant residual, pH, and temperature on microbial abundance in disinfected drinking water distribution systems". In: *Environ. Sci.: Water Res. Technol.* (2020). DOI: 10.1039/d0ew00809e.

[190] Quyen M. Bautista-de los Santos, Karina A. Chavarria, and Kara L. Nelson. "Understanding the impacts of intermittent supply on the drinking water microbiome". In: *Environmental biotechnology/Energy biotechnology* 57 (2019), pp. 167–174.

[191] Isabel Douterelo et al. "Whole metagenome sequencing of chlorinated drinking water distribution systems". In: *Environ. Sci.: Water Res. Technol.* 4.12 (2018), pp. 2080–2091. DOI: 10.1039/c8ew00395e.

[192] Natalie M. Hull et al. "Drinking water microbiome project: is it time?" In: *Trends in Microbiology* 27.8 (2019). doi: 10.1016/j.tim.2019.03.011, pp. 670–677. DOI: 10.1016/j.tim.2019.03.011.

[193] Emily Kumpel and Kara L. Nelson. "Intermittent water supply: prevalence, practice, and microbial water quality". In: *Environ. Sci. Technol.* 50.2 (2015). doi: 10.1021/acs.est.5b03973, pp. 542–553. DOI: 10.1021/acs.est.5b03973.

[194] Caitlin R. Proctor and Frederik Hammes. "Drinking water microbiology—from measurement to management". In: *Environmental biotechnology/Energy biotechnology* 33 (2015), pp. 87–94.

[195] Ya Zhang and Wen-Tso Liu. "The application of molecular tools to study the drinking water microbiome – Current understanding and future needs". In: *Critical Reviews in Environmental Science and Technology* 49.13 (2019). doi: 10.1080/10643389.2019.1571351, pp. 1188–1235. DOI: 10.1080/10643389.2019.1571351.

[196] Feng Ju and Tong Zhang. "Experimental Design and Bioinformatics Analysis for the Application of Metagenomics in Environmental Sciences and Biotechnology". In: *Environmental Science & Technology* 49.21 (2015), pp. 12628–12640. DOI: 10.1021/acs.est.5b03719.

[197] Eila Torvinen et al. "Mycobacteria in Water and Loose Deposits of Drinking Water Distribution Systems in Finland". In: *Appl. Environ. Microbiol.* 70.4 (2004), p. 1973.

[198] Pierre Payment and Will Robertson. "The microbiology of piped distribution systems and public health". In: *Ainsworth R. Safe Piped Water: Managing Microbial Water Quality in Piped DistributionSystems. World Health Organization, London, IWA Publishing* (2004).

[199] Lee H. Odell et al. "Controlling nitrification in chloraminated systems". In: *Journal (American Water Works Association)* 88.7 (1996). doi: 10.1002/j.1551-8833.1996.tb06587.x, pp. 86–98. DOI: 10.1002/j.1551-8833.1996.tb06587.x.

[200] Andrzej Wilczak et al. "Occurrence of nitrification in chloraminated distribution systems". In: *Journal (American Water Works Association)* 88.7 (1996). doi: 10.1002/j.1551-8833.1996.tb06586.x, pp. 74–85. DOI: 10.1002/j.1551-8833.1996.tb06586.x.

[201] Fangqiong Ling et al. "Drinking water microbiome assembly induced by water stagnation". In: *The Isme Journal* 12.6 (2018), pp. 1520–1531.

[202] Karin Lautenschlager et al. "Overnight stagnation of drinking water in household taps induces microbial growth and changes in community composition". In: *Water Research* 44.17 (2010), pp. 4868–4877.

[203] Jamie Bartram et al. *Heterotrophic plate counts and drinking-water safety*. IWA publishing, 2003.

[204] Frederik Hammes et al. "Assessing biological stability of drinking water without disinfectant residuals in a full-scale water supply system". In: *Journal of Water Supply: Research and Technology—AQUA* 59.1 (2010), pp. 31–40. DOI: 10.2166/aqua.2010.052.

[205] Kejia Zhang et al. "A novel method: using an adenosine triphosphate (ATP) luminescence–based assay to rapidly assess the biological stability of drinking water". In: *Applied Microbiology & Biotechnology* 103.11 (2019), pp. 4269–4277.

[206] Frederik Hammes et al. "Flow-cytometric total bacterial cell counts as a descriptive microbiological parameter for drinking water treatment processes". In: *Water Research* 42.1 (2008), pp. 269–277.

[207] Dick van der Kooij et al. "Biofilm formation on surfaces of glass and Teflon exposed to treated water". In: *Water Research* 29.7 (1995), pp. 1655–1662.

[208] A. Thore et al. "Detection of bacteriuria by luciferase assay of adenosine triphosphate." In: *J. Clin. Microbiol.* 1.1 (1975), p. 1.

[209] Osmund Holm-Hansen. *Determination of microbial biomass in deep ocean profiles*. Tech. rep. 1970.

[210] D. M. Karl. "Cellular nucleotide measurements and applications in microbial ecology". In: *Microbiological reviews* 44.4 (1980), pp. 739–796.

[211] H. S. C. Eydal and K. Pedersen. "Use of an ATP assay to determine viable microbial biomass in Fennoscandian Shield groundwater from depths of 3–1000 m". In: *Journal of Microbiological Methods* 70.2 (2007), pp. 363–373.

[212] Paul W. J. J. van der Wielen et al. "A survey of indicator parameters to monitor regrowth in unchlorinated drinking water". In: *Environ. Sci.: Water Res. Technol.* 2.4 (2016), pp. 683–692. DOI: 10.1039/c6ew00007j.

[213] E. I. Prest et al. "Monitoring microbiological changes in drinking water systems using a fast and reproducible flow cytometric method". In: *Water Research* 47.19 (2013), pp. 7131–7142.

[214] K. Helmi et al. "Monitoring of three drinking water treatment plants using flow cytometry". In: *Water Science & Technology: Water Supply* 14.5 (2014), pp. 850–856.

[215] John C. Crittenden et al. *MWH's water treatment: principles and design*. John Wiley & Sons, 2012.

[216] Ashley Pifer et al. *2017 Water Utility Disinfection Survey Report*. Tech. rep. 2018.

[217] R Core Team. *R: A Language and Environment for Statistical Computing*. Tech. rep. 2019.

[218] Frank E Harrell Jr. *Hmisc: Harrell Miscellaneous*. Tech. rep. R package version 4.3-1. 2020.

[219] Barret Schloerke et al. *GGally: Extension to 'ggplot2'*. Tech. rep. R package version 1.4.0. 2018.

[220] Alain F. Zuur, Elena N. Ieno, and Chris S. Elphick. "A protocol for data exploration to avoid common statistical problems". In: *Methods in Ecology and Evolution* 1.1 (2009). doi: 10.1111/j.2041-210X.2009.00001.x, pp. 3–14. DOI: 10.1111/j.2041-210x.2009.00001.x.

[221] Alain F. Zuur et al. *A Beginner's Guide to GLM and GLMM with R: A Frequentist and Bayesian Perspective for Ecologists*. Highland Statistics Ltd., 2013.

[222] Alain F. Zuur and Elena N. Ieno. "A protocol for conducting and presenting results of regression-type analyses". In: *Methods in Ecology and Evolution* 7.6 (2016). doi: 10.1111/2041-210X.12577, pp. 636–645. DOI: 10.1111/2041-210x.12577.

[223] José A. Villaseñor and Elizabeth González-Estrada. "A variance ratio test of fit for Gamma distributions". In: *Statistics & Probability Letters* 96 (2015), pp. 281–286.

[224] Elizabeth González-Estrada and Jose A. Villasenor-Alva. *goft: Tests of Fit for some Probability Distributions*. Tech. rep. R package version 1.3.4. 2017.

[225] Douglas Bates et al. *lme4: Linear Mixed-Effects Models using 'Eigen' and S4*. Tech. rep. R package version 1.1-23. 2020.

[226] Kamil Bartoń. *MuMIn: Multi-Model Inference*. Tech. rep. R package version 1.43.15. 2019.

[227] Hadley Wickham et al. *ggplot2: Create Elegant Data Visualisations Using the Grammar of Graphics*. Tech. rep. R package version 3.3.0. 2020.

[228] Marek Hlavac. *stargazer: Well-Formatted Regression and Summary Statistics Tables*. Tech. rep. R package version 5.2.2. 2018.

[229] Winston Chang. *extrafont: Tools for using fonts*. Tech. rep. R package version 0.17. 2014.

[230] Baptiste Auguie. *gridExtra: Miscellaneous Functions for "Grid" Graphics*. Tech. rep. R package version 2.3. 2017.

[231] Simon Garnier. *viridis: Default Color Maps from 'matplotlib'*. Tech. rep. R package version 0.5.1. 2018.

[232] John J. Vasconcelos et al. "Kinetics of chlorine decay". In: *Journal (American Water Works Association)* 89.7 (1997). doi: 10.1002/j.1551-8833.1997.tb08259.x, pp. 54–65. DOI: 10.1002/j.1551-8833.1997.tb08259.x.

[233] George F. Reed, Freyja Lynn, and Bruce D. Meade. "Use of Coefficient of Variation in Assessing Variability of Quantitative Assays". In: *Clinical and Vaccine Immunology* 9.6 (2002), p. 1235.

[234] Weidong Zhang and Francis A DiGiano. "Comparison of bacterial regrowth in distribution systems using free chlorine and chloramine: a statistical study of causative factors". In: *Water Research* 36.6 (2002), pp. 1469–1482.

[235] M. W. LeChevallier. "Conditions favouring coliform and HPC bacterial growth in drinking". In: *Heterotrophic Plate Counts and Drinking-water Safety: The Significance of HPCs for Water Quality and Human Health* (2003), p. 177.

[236] E Siebel et al. "Correlations between total cell concentration, total adenosine triphosphate concentration and heterotrophic plate counts during microbial monitoring of drinking water". In: *DWES* 1.1 (2008), pp. 1–6.

[237] Michael Berney et al. "Assessment and interpretation of bacterial viability by using the LIVE/DEAD BacLight Kit in combination with flow cytometry". In: *Applied and Environmental Microbiology* 73.10 (2007), pp. 3283–3290.

[238] P. Foladori et al. "Surrogate parameters for the rapid microbial monitoring in a civil protection module used for drinking water production". In: *Chemical Engineering Journal* 265 (2015), pp. 67–74.

[239] Frederik Hammes et al. "Assessing biological stability of drinking water without disinfectant residuals in a full-scale water supply system". In: *Journal of Water Supply: Research & Technology-AQUA* 59.1 (2010), pp. 31–40. DOI: 10.2166/aqua.2010.052.

[240] D Van Der Kooij. "Biological stability: A multidimensional quality aspect of treated water". In: *Water, Air, and Soil Pollution* 123.1/4 (2000), pp. 25–34. DOI: 10.1023/a:1005288720291.

[241] Emmanuelle I. Prest et al. "Biological Stability of Drinking Water: Controlling Factors, Methods, and Challenges". In: *Frontiers in Microbiology* 7.41 (2016), p. 133. DOI: 10.3389/fmicb.2016.00045.

[242] Bruce E Rittmann and Vernon L Snoeyink. "Achieving biologically stable drinking water". In: *Journal (American Water Works Association)* 76.10 (1984), pp. 106–114.

[243] Hannah R. Safford and Heather N. Bischel. "Flow cytometry applications in water treatment, distribution, and reuse: A review". In: *Water Research* 151 (2019), pp. 110–133.

[244] Antonia Bruno et al. "Changes in the Drinking Water Microbiome: Effects of Water Treatments Along the Flow of Two Drinking Water Treatment Plants in a Urbanized Area, Milan (Italy)". In: *Frontiers in Microbiology* 9 (2018), p. 631. DOI: 10.3389/fmicb.2018.02557.

[245] Michael B Waak et al. "Comparison of the microbiomes of two drinking water distribution systems-with and without residual chloramine disinfection". In: *Microbiome* 7.1 (2019), pp. 87–87.

[246] Ruben Props et al. "Absolute quantification of microbial taxon abundances". In: *The Isme Journal* 11.2 (2017), pp. 584–587.

[247] Robert Brankatschk et al. "Simple Absolute Quantification Method Correcting for Quantitative PCR Efficiency Variations for Microbial Community Samples". In: *Applied and Environmental Microbiology* 78.12 (2012), pp. 4481–4489. DOI: 10.1128/aem.07878-11.

[248] Cindy J. Smith and A. Mark Osborn. "Advantages and limitations of quantitative PCR (Q-PCR)-based approaches in microbial ecology". In: *FEMS Microbiology Ecology* 67.1 (2009), pp. 6–20.

[249] Friedrich V. Wintzingerode, Ulf B. Göbel, and Erko Stackebrandt. "Determination of microbial diversity in environmental samples: pitfalls of PCR-based rRNA analysis". In: *FEMS Microbiology Reviews* 21.3 (1997), pp. 213–229.

[250] J. C. Block et al. "Biofilm accumulation in drinking water distribution systems". In: *Biofouling* 6.4 (1993). doi: 10.1080/08927019309386235, pp. 333–343. DOI: 10.1080/08927019309386235.

[251] Hubert Zipper et al. "Investigations on DNA intercalation and surface binding by SYBR Green I, its structure determination and methodological implications." In: *Nucleic Acids Research* 32.12 (2004), e103. DOI: 10.1093/nar/gnh101.

[252] R. Fabris et al. "Bacteriological water quality changes in parallel pilot distribution systems". In: *Water Science & Technology: Water Supply* 16.6 (2016), pp. 1710–1720.

[253] Colin Reith and Brian Birkenhead. "Membranes enabling the affordable and cost effective reuse of wastewater as an alternative water source". In: *Desalination* 117.1 (1998), pp. 203–209.

[254] Gang Liu et al. "Potential impacts of changing supply-water quality on drinking water distribution: A review". In: *Water Research* 116 (2017), pp. 135–148.

[255] Elias Bardouniotis, Howard Ceri, and Merle E. Olson. "Biofilm Formation and Biocide Susceptibility Testing of Mycobacterium fortuitum and Mycobacterium marinum". In: *Current Microbiology* 46.1 (2003), pp. 0028–0032.

[256] I. Sibille et al. "Microbial characteristics of a distribution system fed with nanofiltered drinking water". In: *Water Research* 31.9 (1997), pp. 2318–2326. DOI: 10.1016/s0043-1354(97)00070-5.

[257] Mark C. Meckes et al. "Impact on water distribution system biofilm densities from reverse osmosis membrane treatment of supply water". In: *Journal of Environmental Engineering and Science* 6.4 (2007), pp. 449–454. DOI: 10.1139/s06-062.

[258] Scott E. Miller. "The Microbiology of Direct Potable Reuse Systems". PhD thesis. 2019.

[259] Carmela M. Smith and Vincent R. Hill. "Dead-End Hollow-Fiber Ultrafiltration for Recovery of Diverse Microbes from Water". In: *Applied and Environmental Microbiology* 75.16 (2009), pp. 5284–5289.

[260] Vincent R. Hill et al. "Development of a Rapid Method for Simultaneous Recovery of Diverse Microbes in Drinking Water by Ultrafiltration with Sodium Polyphosphate and Surfactants". In: *Applied and Environmental Microbiology* 71.11 (2005), pp. 6878–6884. DOI: 10.1128/aem.71.11.6878-6884.2005.

[261] Benjamin J. Callahan et al. "DADA2: High-resolution sample inference from Illumina amplicon data". In: *Nature Methods* 13.7 (2016), pp. 581–583. DOI: 10.1038/nmeth.3869.

[262] Qiong Wang et al. "Naive Bayesian Classifier for Rapid Assignment of rRNA Sequences into the New Bacterial Taxonomy". In: *Applied and Environmental Microbiology* 73.16 (2007), pp. 5261–5267. DOI: 10.1128/aem.00062-07.

[263] Christian Quast et al. "The SILVA ribosomal RNA gene database project: improved data processing and web-based tools". In: *Nucleic Acids Research* 41.D1 (2013), pp. D590–D596. DOI: 10.1093/nar/gks1219.

[264] Paul J. McMurdie and Susan Holmes. "phyloseq: An R Package for Reproducible Interactive Analysis and Graphics of Microbiome Census Data". In: *PLoS ONE* 8.4 (2013), e61217. DOI: 10.1371/journal.pone.0061217.

[265] Maura J. Donohue et al. "Impact of Chlorine and Chloramine on the Detection and Quantification of Legionella pneumophila and Mycobacterium Species". In: *Applied and Environmental Microbiology* 85.24 (2019). DOI: 10.1128/aem.01942-19.

[266] Brendan Flannery et al. "Reducing Legionella Colonization of Water Systems with Monochloramine". In: *Emerging Infectious Diseases* 12.4 (2006), pp. 588–596. DOI: 10.3201/eid1204.051101.

[267] Hannah D. Greenwald and Lauren C. Kennedy et al. *Interpretation of temporal and spatial trends of SARS-CoV-2 RNA in San Francisco Bay Area wastewater.* 2021. DOI: 10.1101/2021.05.04.21256418.

[268] An Tang et al. "Detection of Novel Coronavirus by RT-PCR in Stool Specimen from Asymptomatic Child, China". In: *Emerging Infectious Diseases* 26.6 (2020), pp. 1337–1339. DOI: 10.3201/eid2606.200301.

[269] James Peng et al. "Estimation of secondary household attack rates for emergent SARS-CoV-2 variants detected by genomic surveillance at a community-based testing site in San Francisco". In: *medRxiv : the preprint server for health sciences* (2021), p. 2021.03.01.21252705. DOI: 10.1101/2021.03.01.21252705.

[270] Nana-Yaa Misa et al. "Racial/ethnic disparities in COVID-19 disease burden & mortality among emergency department patients in a safety net health system". In: *The American Journal of Emergency Medicine* (2020). DOI: 10.1016/j.ajem.2020.09.053.

[271] Juan A Vallejo et al. "Highly predictive regression model of active cases of COVID-19 in a population by screening wastewater viral load". In: *medRxiv : the preprint server for health sciences* (). DOI: 10.1101/2020.07.02.20144865.

[272] Cynthia Gibas et al. "Implementing Building-Level SARS-CoV-2 Wastewater Surveillance on a University Campus". In: *Science of the Total Environment* (2021). DOI: 10.1016/j.scitotenv.2021.146749.

[273] Fuqing Wu et al. "Wastewater Surveillance of SARS-CoV-2 across 40 U.S. states". In: *medRxiv : the preprint server for health sciences* (2021). DOI: 10.1101/2021.03.10.21253235.

[274] Bryant McDonnell, Richard W. Hayslett, and Nathanial J. Tetrick. "Dry Weather Channel Impacts on Wet Weather Combined Sewer Overflow Pollution Rates". In: *Journal of Water Management Modeling* (2015). DOI: 10.14796/jwmm.c384.

[275] Rose S. Kantor et al. "Challenges in Measuring the Recovery of SARS-CoV-2 from Wastewater". In: *Environmental Science & Technology* 55.6 (2021), pp. 3514–3519. DOI: 10.1021/acs.est.0c08210.

[276] Elyse Stachler et al. "Quantitative CrAssphage PCR Assays for Human Fecal Pollution Measurement". In: *Environmental science & technology* 51.16 (2017), pp. 9146–9154. DOI: 10.1021/acs.est.7b02703.

[277] Nicola Decaro et al. "Detection of bovine coronavirus using a TaqMan-based real-time RT-PCR assay". In: *Journal of Virological Methods* 151.2 (2008), pp. 167–171. DOI: 10.1016/j.jviromet.2008.05.016.

[278] Yang Hsia et al. "Design of a hyperstable 60-subunit protein icosahedron". In: *Nature* 535.7610 (2016), pp. 136–139. DOI: 10.1038/nature18010.

[279] Warish Ahmed et al. "Surveillance of SARS-CoV-2 RNA in wastewater: Methods optimization and quality control are crucial for generating reliable public health information". In: *Current Opinion in Environmental Science & Health* 17 (2020), pp. 82–93. DOI: 10.1016/j.coesh.2020.09.003.

[280] Christopher Staley et al. "Performance of Two Quantitative PCR Methods for Microbial Source Tracking of Human Sewage and Implications for Microbial Risk Assessment in Recreational Waters". In: *Applied and Environmental Microbiology* 78.20 (2012), pp. 7317–7326. DOI: 10.1128/aem.01430-12.

[281] Warish Ahmed et al. "Comparison of virus concentration methods for the RT-qPCR-based recovery of murine hepatitis virus, a surrogate for SARS-CoV-2 from untreated wastewater". In: *Science of The Total Environment* 739 (2020), p. 139960. DOI: 10.1016/j.scitotenv.2020.139960.

[282] Tania Nolan et al. "SPUD: A quantitative PCR assay for the detection of inhibitors in nucleic acid preparations". In: *Analytical Biochemistry* 351.2 (2006), pp. 308–310. DOI: 10.1016/j.ab.2006.01.051.

[283] Katherine E. Graham et al. "SARS-CoV-2 RNA in Wastewater Settled Solids Is Associated with COVID-19 Cases in a Large Urban Sewershed". In: *Environ. Sci. Technol.* 55.1 (2021). doi: 10.1021/acs.est.0c06191, pp. 488–498. DOI: 10.1021/acs.est.0c06191.

[284] Warish Ahmed et al. "Intraday variability of indicator and pathogenic viruses in 1-h and 24-h composite wastewater samples: implications for wastewater-based epidemiology". In: *Environmental Research* (2020), p. 110531. DOI: 10.1016/j.envres.2020.110531.

[285] Maxwell L. Wilder et al. "Co-quantification of crAssphage increases confidence in wastewater-based epidemiology for SARS-CoV-2 in low prevalence areas". In: *Water Research X* 11 (2021), p. 100100. DOI: https://doi.org/10.1016/j.wroa.2021.100100.

[286] Nikolay Kyurkchiev and Svetoslav Markov. "On the Hausdorff distance between the Heaviside step function and Verhulst logistic function". In: *Journal of Mathematical Chemistry* 54.1 (2016), pp. 109–119. DOI: 10.1007/s10910-015-0552-0.

[287] M. D. Wood, N.A. Beresford, and D. Copplestone. "Limit of detection values in data analysis: Do they matter?" In: *Radioprotection* 46.6 (2011), S85–S90. DOI: 10.1051/radiopro/20116728s.

[288] William G. Jacoby. "Loess:: a nonparametric, graphical tool for depicting relationships between variables". In: *Electoral Studies* 19.4 (2000), pp. 577–613. DOI: 10.1016/s0261-3794(99)00028-1.

[289] Patrick M. D'Aoust et al. "Quantitative analysis of SARS-CoV-2 RNA from wastewater solids in communities with low COVID-19 incidence and prevalence". In: *Water Research* 188 (2021), p. 116560. DOI: 10.1016/j.watres.2020.116560.

[290] Xavier Fernandez-Cassi et al. "Wastewater monitoring outperforms case numbers as a tool to track COVID-19 incidence dynamics when test positivity rates are high". In: *medRxiv : the preprint server for health sciences* (2021), p. 2021.03.25.21254344. DOI: 10.1101/2021.03.25.21254344.

[291] Megan Cassidy and Jason Fagone. "200 Chino inmates transferred to San Quentin, Corcoran. Why weren't they tested first?" In: *San Francisco Chronicle* (2020).

[292] Andre G. Montoya-Barthelemy et al. "COVID-19 and the Correctional Environment: The American Prison as a Focal Point for Public Health". In: *American Journal of Preventive Medicine* 58.6 (2020), pp. 888–891. DOI: 10.1016/j.amepre.2020.04.001.

[293] Texas Commission on Environmental Quality. *Title 30, Texas Administrative Code (30 TAC), Subsection 290.46(z).*

[294] *Optimal Corrosion Control Treatment Evaluation Technical Recommendations for Primacy Agencies and Public Water Systems.* Tech. rep. EPA 816-B-16-003. Office of Water (4606M), 2016.

[295] Peter J. Vikesland, Kenan Ozekin, and Richard L. Valentine. "Monochloramine Decay in Model and Distribution System Waters". In: *Water Research* 35.7 (2001), pp. 1766–1776. DOI: 10.1016/s0043-1354(00)00406-1.

[296] Gang Liu et al. "Hotspots for selected metal elements and microbes accumulation and the corresponding water quality deterioration potential in an unchlorinated drinking water distribution system". In: *Water Research* 124 (2017), pp. 435–445. DOI: 10.1016/j.watres.2017.08.002.

[297] Charlotte D. Vavourakis et al. "Spatial and Temporal Dynamics in Attached and Suspended Bacterial Communities in Three Drinking Water Distribution Systems with Variable Biological Stability". In: *Environmental Science & Technology* 54.22 (2020), pp. 14535–14546. DOI: 10.1021/acs.est.0c04532.

[298] Masaaki Kitajima et al. "Microbial abundance and community composition in biofilms on in-pipe sensors in a drinking water distribution system". In: *Science of The Total Environment* 766 (2021), p. 142314. DOI: 10.1016/j.scitotenv.2020.142314.

[299] Gang Liu et al. "Assessing the origin of bacteria in tap water and distribution system in an unchlorinated drinking water system by SourceTracker using microbial community fingerprints". In: *Water Research* 138 (2018), pp. 86–96. DOI: 10.1016/j.watres.2018.03.043.

[300] Jennifer L. A. Shaw et al. "Using Amplicon Sequencing To Characterize and Monitor Bacterial Diversity in Drinking Water Distribution Systems". In: *Applied and Environmental Microbiology* 81.18 (2015), pp. 6463–6473. DOI: 10.1128/aem.01297-15.

[301] Sarah Potgieter et al. "Long-term spatial and temporal microbial community dynamics in a large-scale drinking water distribution system with multiple disinfectant regimes". In: *Water Research* 139 (2018), pp. 406–419. DOI: 10.1016/j.watres.2018.03.077.

[302] Katherine Alfredo. "The "Burn": water quality and microbiological impacts related to limited free chlorine disinfection periods in a chloramine system". In: *Water Research* (2021), p. 117044. DOI: 10.1016/j.watres.2021.117044.

[303] Hong Wang et al. "Microbial Community Response to Chlorine Conversion in a Chloraminated Drinking Water Distribution System". In: *Environmental Science & Technology* 48.18 (2014), pp. 10624–10633. DOI: 10.1021/es502646d.

[304] Kristjan Pullerits et al. "Impact of coagulation–ultrafiltration on long-term pipe biofilm dynamics in a full-scale chloraminated drinking water distribution system". In: *Environmental Science: Water Research & Technology* 6.11 (2020), pp. 3044–3056. DOI: 10.1039/d0ew00622j.

[305] Maaike K. Ramseier et al. "Kinetics of membrane damage to high (HNA) and low (LNA) nucleic acid bacterial clusters in drinking water by ozone, chlorine, chlorine dioxide, monochloramine, ferrate(VI), and permanganate". In: *Water Research* 45.3 (2010), pp. 1490–1500.

[306] Vicente Gomez-Alvarez and Randy P. Revetta. "Monitoring of Nitrification in Chloraminated Drinking Water Distribution Systems With Microbiome Bioindicators Using Supervised Machine Learning". In: *Frontiers in Microbiology* 11 (2020), p. 571009. DOI: 10.3389/fmicb.2020.571009.

[307] *Wastewater Surveillance of the COVID-19 Genetic Signal in Sewersheds: Recommendations from Global Experts*. 2020. URL: https://www.waterrf.org/sites/default/files/file/2020-06/COVID-19%5C_SummitHandout-v3b.pdf (visited on 03/29/2021).

[308] Shuchen Feng et al. "Evaluation of sampling frequency and normalization of SARS-CoV-2 wastewater concentrations for capturing COVID-19 burdens in the community". In: *medRxiv : the preprint server for health sciences* (2021). DOI: 10.1101/2021.02.17.21251867.

[309] Lance Gable, Natalie Ram, and Jeffrey L Ram. "Legal and Ethical Implications of Wastewater SARS-CoV-2 Monitoring for COVID-19 Surveillance". In: *Journal of Law and the Biosciences* 7.1 (2020), lsaa039–. DOI: 10.1093/jlb/lsaa039.

[310] Elizabeth E Joh. "COVID-19 Sewage Testing as a Police Surveillance Infrastructure". In: *SSRN Electronic Journal* (2020). DOI: 10.2139/ssrn.3742320.

[311] Mohammad Hosseini. "Equal Co-authorship Practices: Review and Recommendations". In: *Science and Engineering Ethics* 26.3 (2020), pp. 1133–1148. DOI: 10.1007/s11948-020-00183-8.

[312] Elise Smith. "A Theoretical Foundation for the Ethical Distribution of Authorship in Multidisciplinary Publications". In: *Kennedy Institute of Ethics Journal* 27.3 (2017), pp. 371–411. DOI: 10.1353/ken.2017.0032.

[313] Amy Lapidow and Paige Scudder. "Shared first authorship". In: *Journal of the Medical Library Association* 107.4 (2019), pp. 618–620. DOI: 10.5195/jmla.2019.700.

[314] Marisa L. Conte, Stacy L. Maat, and M. Bishr Omary. "Increased co-first authorships in biomedical and clinical publications: a call for recognition". In: *The FASEB Journal* 27.10 (2013), pp. 3902–3904. DOI: 10.1096/fj.13-235630.

[315] Ehimare Akhabue and Ebbing Lautenbach. ""Equal" Contributions and Credit: An Emerging Trend in the Characterization of Authorship". In: *Annals of Epidemiology* 20.11 (2010), pp. 868–871. DOI: 10.1016/j.annepidem.2010.08.004.

[316] Zhiwei Jia et al. "Equal contributions and credit: an emerging trend in the characterization of authorship in major spine journals during a 10-year period". In: *European Spine Journal* 25.3 (2016), pp. 913–917. DOI: 10.1007/s00586-015-4314-2.

Appendix A

Supporting information for Chapter 2

A.1 Flow cytometer comparison

Two flow cytometers were used for these sampling campaigns, an Accuri C6 flow cytometer (Accuri; BD Biosciences, San Jose, CA) and a BD FACSCanto cell analyzer (Canto; BD Biosciences, San Jose, CA). DWDS F is the only location for which the Canto was used because the Accuri broke down during field sampling (the supplemental data files include which cytometer was used to produce which data point: `https://zenodo.org/record/3993877#.X5n0Qy9h1TZ`). Once the Accuri was repaired and returned, a comparison experiment was completed. For both cytometers, the publicly available gate developed by researchers at the Swiss Federal Institute of Aquatic Science and Technology (Eawag gate; [147]) was first used and then results from Sperotech nano fluorescent size standard kit (Spherotech, Catalog # NFPPS-52-4K) were used to adjust the gate for the Canto (adjusted gate; Figure A.6). The Spherotech beads were all at a concentration of $1x10^6$ beads per mL. The Accuri was able to quantify the larger beads with under 10% error (Table A.6). The Canto with adjusted gate was most accurate for the largest bead (less than 1% error), but still had an error of 18.5% for the 0.88 μm beads, which improved from the standard error with the Eawag gate, 25.5%.

The beads that were 0.22 μm and 0.45 μm were not accurately quantified by either cytometer (Table A.6), but the small beads were detected outside of the gate by the Accuri and not by the Canto. This result might be evidence that the Accuri has a lower limit of quantificaiton than the Canto (Figure A.6), and the quantification limit was not determined specifically for the Canto. However, the Eawag method used in this study recommends working with cell counts of $10^2 - 10^7$ cells per mL [147]. If the detection limit for samples taken with the Canto was 10^2 cells per mL for both total cell counts and intact cell counts instead of the limits of 12 and 22 cells per mL respectively determined by Miller et al. with the Accuri [85], nothing would be impacted because the lowest Canto total cell count datapoint is 350 cells per mL and that of intact cell count is 304 cells per mL.

Bottled Evian water was used to verify that adjusting the Eawag gate led to comparable

cell counts of a microbial community from the same source. Three bottles of Evian water purchased from the same location were analyzed in biological triplicate with the Accuri on June 12, 2019 and in biological duplicate with the Canto on June 14, 2019. Adjusting the gate brought the Canto intact or total cell count value closer to that of the Accuri than the Eawag values in most cases (Figure A.7). This pattern did not hold for total cell count of bottle 1, which had an adjusted average greater than the Accuri average. However, this sample had the largest standard deviation (Table A.7), and the paired intact cell count measurement was brought much closer to that of the Accuri. Overall, the differences associated with cytometers following adjustment were minor as compared to differences associated even with the same site in a distribution system over time, which can range orders of magnitude (e.g., site_ut in Figure 2.1 A).

A.2 Supplemental Tables

Table A.1: Summary of sample locations and parameters measured. Each system was sampled in either 2016 and/or 2018 in the distribution system (where n is the number of sites sampled each year). The parameters measured were intact cell counts (ICC), total cell counts (TCC), residual disinfectant concentration, pH, temperature, adenosine triphosphate concentration (ATP), and/or heterotrophic plate counts (HPC).

system	distribution system	TCC and ICC	residual disinfectant	pH	temperature	ATP	HPC
A	2016	12	2016	2016	-	-	2016
	2018	12	2018	2018	2018	2018	2018
B	2016	12	2016	-	-	-	-
	2018	10	2018	2018	2018	2018	2018
C	2016	12	2016	2016	-	-	-
	-	-	-	-	-	-	-
D	2016	7	2016	2016	2016	-	-
	-	-	-	-	-	-	-
E	2016	5	2016	2016	2016	-	-
	-	-	-	-	-	-	-
F	-	-	-	-	-	-	-
	2018	24	2018	2018	2018	2018	2018

Table A.2: Ranges in parameter values for samples collected from all drinking water distribution systems sampled for this study by type of secondary disinfectant applied in the system, including intact cell counts (ICC), total cell counts (TCC), adenosine triphosphate concentration (ATP), and heterotrophic plate counts (HPC).

assay	secondary disinfectant	n	min	median	max	geometric mean	geometric standard deviation	arithmetic mean	arithmetic standard deviation
ICC (cells/mL)	Chloramine	112	118	2.42e+03	1.52e+05	3.62e+03	6.16	-	-
TCC (cells/mL)	Chloramine	112	350	9.76e+03	6.23e+05	1.32e+04	5.33	-	-
intracellular ATP (nM)	Chloramine	94	<1.83e-05	1.05e-04	0.029	2.10e-04	11.6	-	-
total ATP (nM)	Chloramine	94	1.85e-04	1.45e-03	0.031	1.69e-03	4.10	-	-
HPC (MPN/100 mL)	Chloramine	67	<1	24.7	2.42e+03	20.6	10	-	-
free chlorine (mg/L)	Chloramine	96	<0.02	0.05	0.54	-	-	0.084	0.095
total chlorine (mg/L)	Chloramine	109	<0.02	1.88	2.90	-	-	1.71	0.78
pH	Chloramine	84	7.67	8.05	8.45	-	-	8.03	0.14
temperature (°C)	Chloramine	82	13.7	18.6	28.8	-	-	20.0	3.99
ICC (cells/mL)	Chlorine	54	<22	3.53e+03	1.58e+05	2.58e+03	12.9	-	-
TCC (cells/mL)	Chlorine	54	31.7	7.13e+03	1.58e+05	4.97e+03	10.0	-	-
intracellular ATP (nM)	Chlorine	21	<1.83e-05	1.53e-03	0.013	9.13e-04	6.84	-	-
total ATP (nM)	Chlorine	21	3.08e-03	8.25e-03	0.015	7.41e-03	1.73	-	-
HPC (MPN/100 mL)	Chlorine	31	<1	2.03	230	3.26	4.02	-	-
free chlorine (mg/L)	Chlorine	54	0.1	0.73	2.14	-	-	0.79	0.47
total chlorine (mg/L)	Chlorine	32	0.24	0.71	1.22	-	-	0.72	0.28
pH	Chlorine	44	7.40	8.22	8.74	-	-	8.23	0.30
temperature (°C)	Chlorine	35	15.7	22.9	26.1	-	-	22.2	2.26

Table A.3: Corrected Akaike information criterion (AICc) values for backward stepwise model selection (all are generalized linear mixed models with site as a random intercept) shown in order of AICc.

model	int	free chlorine	pH	temp	total chlorine	free chlorine: pH	free chlorine: temp	total chlorine: pH	total chlorine: temp	df	AIC_c
2	8.63	-	0.40	0.35	-1.31	0.39	-	-	-0.24	8	1,526.38
12	8.46	-0.40	0.52	0.36	-1.30	0.53	-	-	-0.21	9	1,527.46
20	8.46	-0.40	0.52	0.36	-1.30	0.53	-	-	-0.21	9	1,527.46
11	8.24	-0.87	0.57	-	-1.23	0.59	-0.70	-	-0.13	9	1,527.57
18	8.47	-0.51	0.52	0.30	-1.33	0.74	-	-	-	8	1,527.97
10	8.64	-	0.42	0.40	-1.32	0.41	0.12	-	-0.24	9	1,528.81
13	8.29	-0.86	0.56	0.05	-1.26	0.71	-0.57	-	-	9	1,528.89
5	8.34	-0.65	0.55	5 0.19	-1.26	0.55	-0.36	-	-0.18	10	1,529.50
15	8.34	-0.65	0.55	0.19	-1.26	0.55	-0.36	-	-0.18	10	1,529.50
19	8.71	-0.003	0.34	0.39	-1.30	-	-	-	-0.33	8	1,529.63
22	8.71	-0.003	0.34	0.39	-1.30	-	-	-	-0.33	8	1,529.63
6	8.43	-0.40	0.48	0.33	-1.26	0.46	-	0.08	-0.21	10	1,529.83
4	8.24	-0.85	0.55	-	-1.21	0.56	-0.68	0.03	-0.13	10	1,530.16
3	8.61	-	0.37	0.39	-1.28	0.33	0.16	0.09	-0.24	10	1,531.09
7	8.29	-0.84	0.53	0.06	-1.24	0.67	-0.52	0.04	-	10	1,531.45
14	8.62	-0.19	0.35	0.26	-1.27	-	-0.28	-	-0.30	9	1,531.83
1	8.34	-0.62	0.52	0.20	-1.24	0.51	-0.31	0.04	-0.18	11	1,532.13
8	8.51	-0.24	0.30	0.27	-1.18	-	-0.08	0.21	-0.26	10	1,532.21
16	8.51	0.02	-	0.23	-1.14	0.24	-0.17	-	-0.20	9	1,534.46
21	8.51	0.02	-	0.23	-1.14	0.24	-0.17	-	-0.20	9	1,534.46
9	8.48	0.01	-	0.27	-1.09	0.08	0.06	0.23	-0.20	10	1,534.76
17	8.52	-0.33	0.40	-	-1.34	0.73	-	-	-0.05	8	1,537.39

Table A.4: Ranges in parameter values for samples collected from distribution system F, including intact cell counts (ICC), total cell counts (TCC), adenosine triphosphate concentration (ATP), and heterotrophic plate counts (HPC).

assay	n	min	median	max	geometric mean	geometric standard deviation	arithmetic mean	arithmetic standard deviation
ICC (cells/mL)	100	118	2.53e+03	1.53e+05	3.95e+03	5.59	-	-
TCC (cells/mL)	100	350	1.18e+04	6.23e+05	1.40e+04	5.29	-	-
intracellular ATP (nM)	94	2e-05	1e-04	0.029	2e-04	11.6	-	-
total ATP (nM)	94	2e-04	1e-03	0.031	2e-03	4.10	-	-
HPC (MPN/100 mL)	67	1.00	24.7	2.42e+03	20.6	10.0	-	-
free chlorine (mg/L)	96	<0.02	0.05	0.54	-	-	0.084	0.095
total chlorine (mg/L)	97	<0.02	1.88	2.90	-	-	1.70	0.77
pH	84	7.67	8.05	8.45	-	-	8.03	0.14
temperature (°C)	82	13.7	18.6	28.8	-	-	19.9	3.99

Table A.5: Number of samples (n) and percentage of those samples that were quantifiable by drinking water distribution system sampled, including intact cell counts (ICC), total cell counts (TCC), adenosine triphosphate concentration (ATP), and heterotrophic plate counts (HPC).

assay	DWDS A		DWDS B		DWDS C		DWDS D		DWDS E		DWDS F	
	n	percent quantifiable	n	percent quantifiable	n	percent quantifiable	n	percent quantifiable	n	percent quantifiable	n	percent quantifiable
ICC	22	100	20	100	12	100	7	85.7	5	40	100	100
TCC	22	100	20	100	12	100	7	100	5	100	100	100
intracellular ATP	11	90.9	10	90	0	-	0	-	0	-	94	64.9
total ATP	11	100	10	100	0	-	0	-	0	-	94	100
HPC	21	76.2	10	90	0	-	0	-	0	-	71	81.7

Table A.6: Result of calibration bead experiments with beads of four different diameters measured on Accuri flow cytometer with Eawag gate and Canto flow cytometer with Eawag gate and adjusted gate. Accuri results are biological triplicates of geometric averages from technical triplicates and Canto results are biological duplicates of geometric averages from technical triplicates.

flow cytometer and gate	measurement	0.22 μm	0.45 μm	0.88 μm	1.35 μm
Accuri Eawag gate	arithmetic mean (beads/mL)	7.8e+05	4.5e+03	1.1e+06	1.1e+06
	arithmetic standard deviation	1.7e+04	8.3e+02	2.2e+04	1.2e+04
	percent error (%)	22.3	99.6	6.20	9.82
Canto adjusted gate	arithmetic mean (beads/mL)	3.7e+03	2.4e+03	8.2e+05	9.9e+05
	arithmetic standard deviation	2.2e+03	1.6e+03	4.0e+04	2.4e+04
	percent error (%)	99.6	99.8	18.5	0.77
Canto Eawag gate	arithmetic mean (beads/mL)	1.2e+03	9.1e+02	7.5e+05	9.9e+05
	arithmetic standard deviation	8.1e+02	5.4e+02	6.1e+04	2.5e+04
	percent error (%)	99.9	99.9	25.5	0.96

Table A.7: Result of the same three bottles of Evian water measured on Accuri flow cytometer with Eawag gate and Canto flow cytometer with Eawag gate and adjusted gate. Accuri results are biological triplicates of geometric averages from technical triplicates and Canto results are biological duplicates of geometric averages from technical triplicates. Data for intact cell count assay (ICC) and total cell count assay (TCC) are shown.

flow cytometer gate	measurement	Evian bottle 1 TCC	Evian bottle 1 ICC	Evian bottle 2 TCC	Evian bottle 2 ICC	Evian bottle 3 TCC	Evian bottle 3 ICC
Accuri Eawag gate	arithmetic amean count (cells/mL)	1.9e+05	1.5e+05	1.6e+05	1.1e+05	1.2e+05	9.5e+04
	arithmetic standard deviation	2.5e+04	9.9e+03	6.2e+03	3.9e+03	3.8e+03	3.3e+03
Canto adjusted gate	arithmetic mean count (cells/mL)	2.7e+05	1.5e+05	1.5e+05	9.8e+04	1.1e+05	8.6e+04
	arithmetic standard deviation	1.2e+05	1.6e+04	8.2e+03	2.0e+04	4.7e+03	7.6e+03
Canto Eawag gate	arithmetic mean count (cells/mL)	2.1e+05	1.2e+05	1.2e+05	8.9e+04	9.8e+04	7.5e+04
	arithmetic standard deviation	8.8e+04	1.6e+04	9.6e+03	2.1e+04	2.3e+03	8.2e+03

A.3 Supplemental Figures

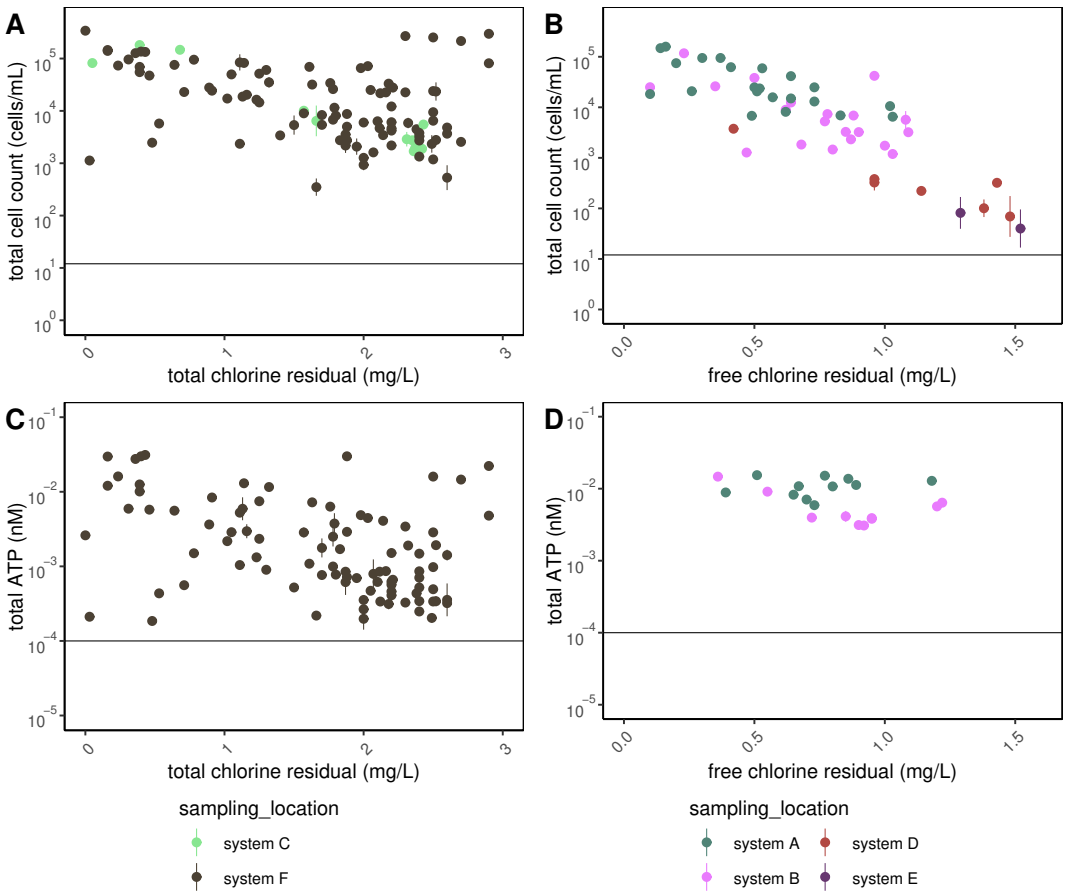

Figure A.1: Total cell counts (A-B) and total ATP (C-D) in drinking water distribution systems sampled in this study. Horizontal lines denote quantification limits. Points are the geometric mean of the technical replicates and error bars represent geometric standard deviation for technical triplicates.

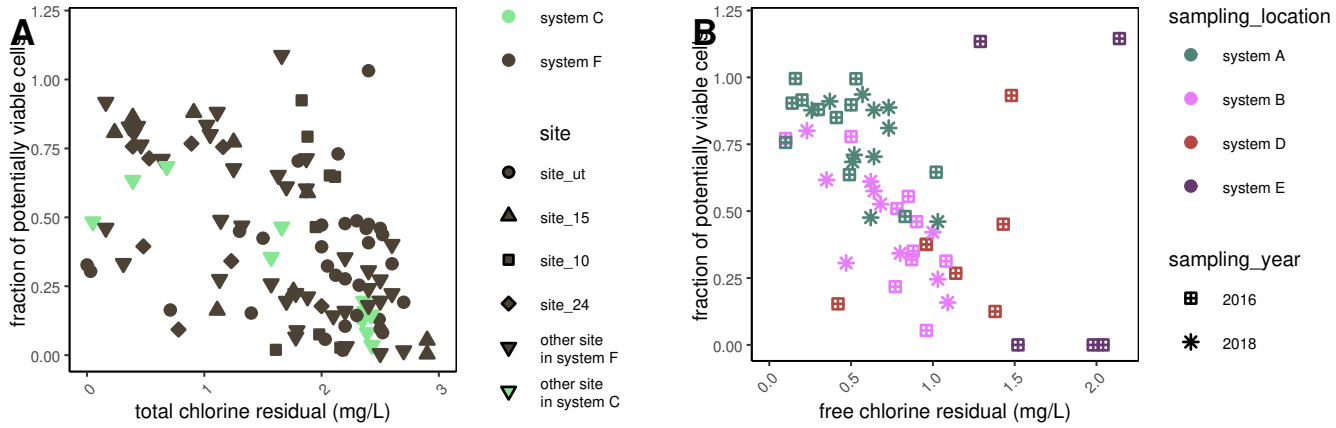

Figure A.2: Fraction of potentially viable cells (intact cell counts/total cell counts) in chloraminated (A) and chlorinated (B) drinking water distribution systems sampled in this study. Shapes in A denote locations in distribution system F that were sampled at least six times between August 2017 and April 2018. Shapes in B denote locations in distribution system A and distribution system B that were sampled once in 2016 and repeated in 2018.The four samples with intact cell counts/total cell counts > 1 had intact cell counts and total cell counts values within 15% of each other.

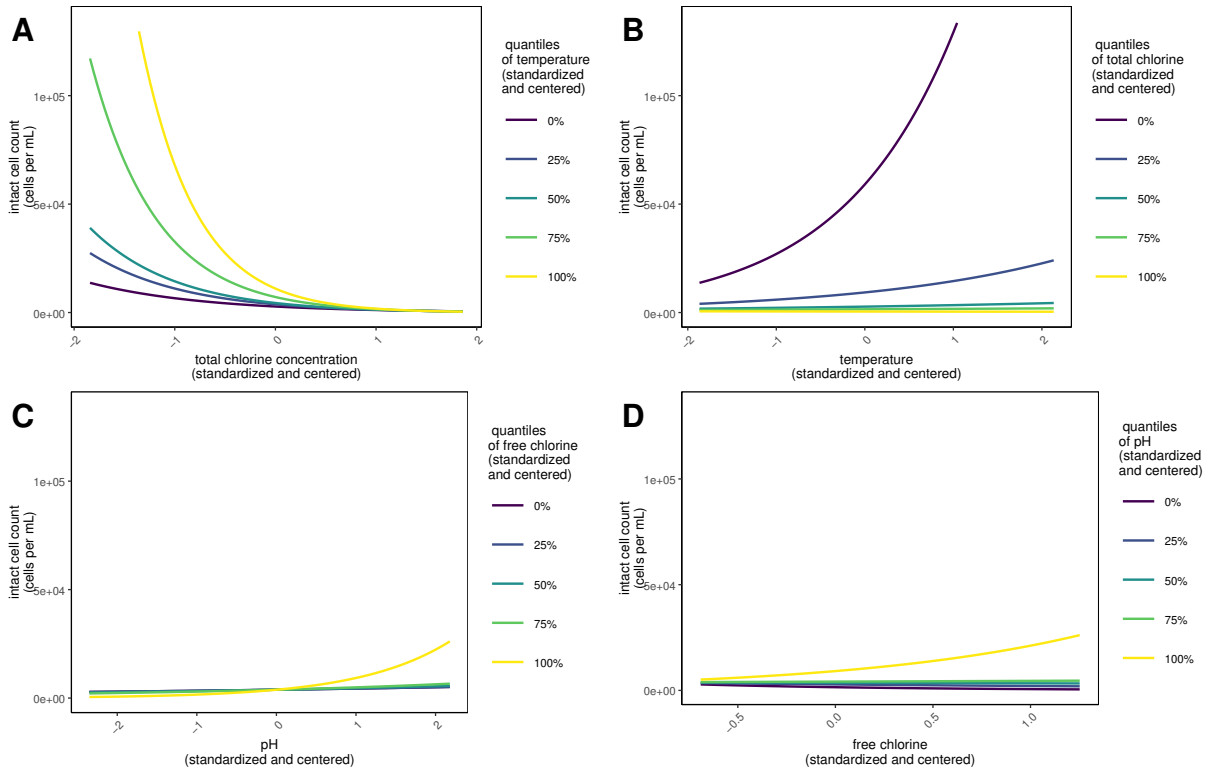

Figure A.3: Visual representation of the most optimal model (Equation 2.2).To generate lines, all fixed effects were held constant at its mean except (A) Figure 2.3 in the main text included for comparison: total chlorine is on the x-axis and temperature is varied in the model at each quantile value (-1.9, -0.10, -0.53, 0.87, and 2.1), (B) temperature is on the x-axis and total chlorine is varied in the model at each quantile value (-1.8, -0.43, 0.51, 0.96, and 1.9), (C) pH is on the x-axis and free chlorine is varied in the model at each quantile value (-0.69, -0.69, -0.58, -0.38, and 1.3), and (D) free chlorine is on the x-axis and pH is varied in the model at each quantile value (-2.3, -0.78, -0.17, -0.20, and 2.2).

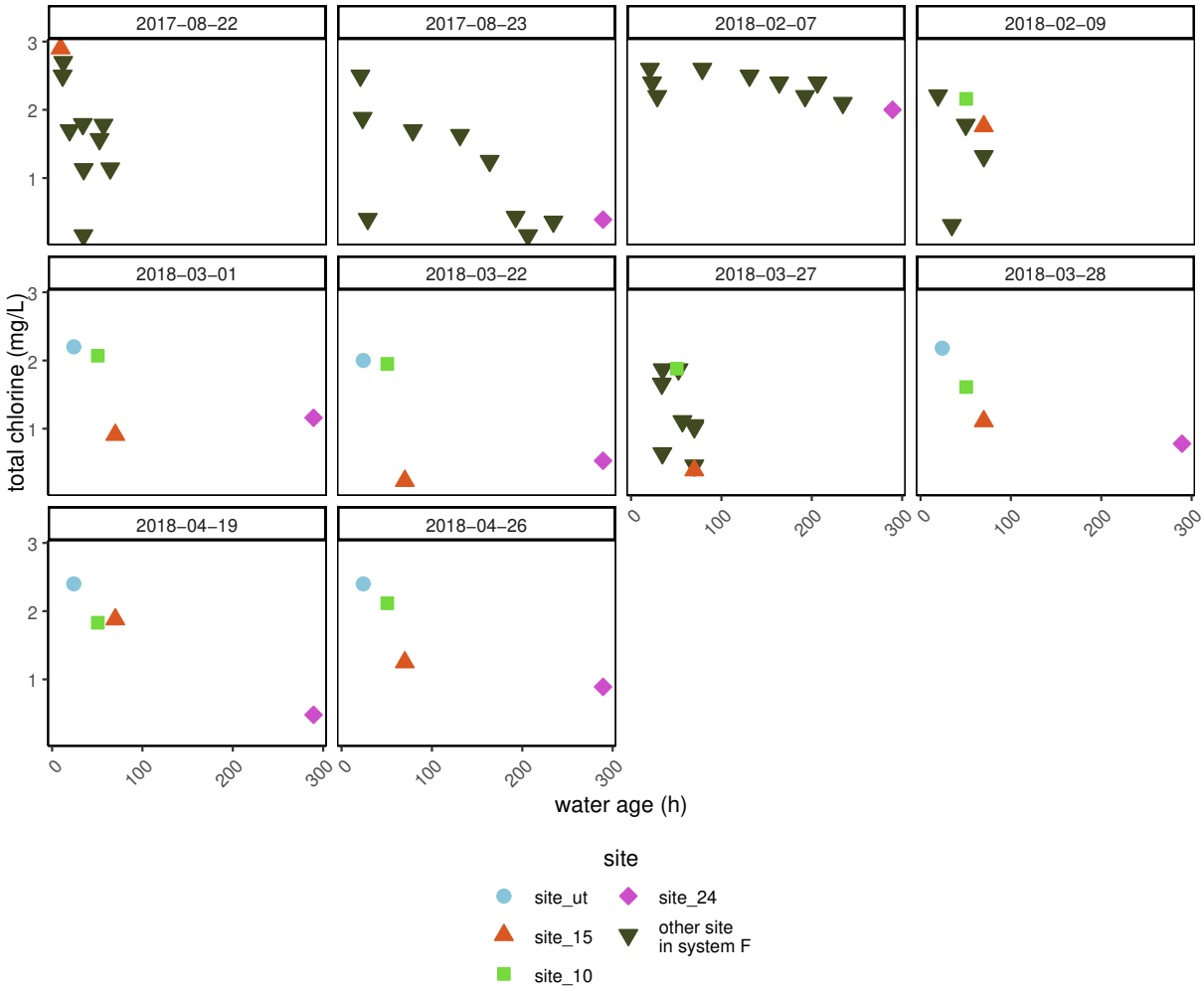

Figure A.4: Total chlorine concentration by water age (hours) in distribution system F for sampling dates with at least two samples collected. Shapes denote locations in distribution system F that were sampled at least six times between August 2017 and April 2018.

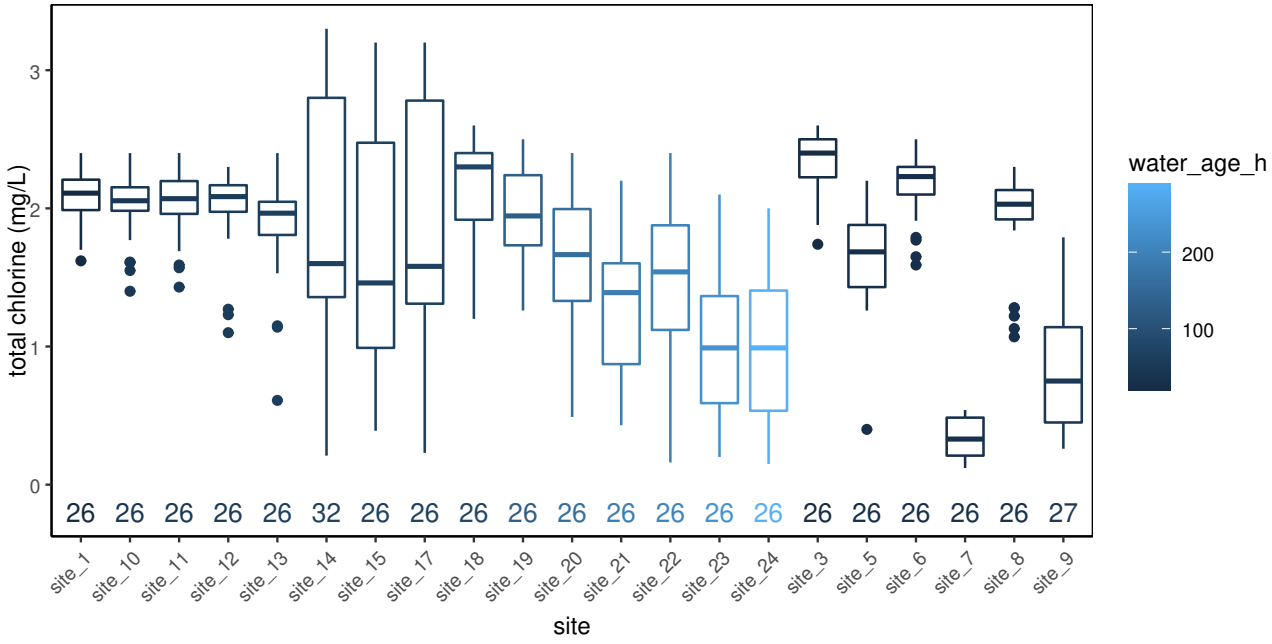

Figure A.5: Ranges in total chlorine concentration by location in distribution system F from July 2017 to July 2018. Numbers underneath each box represent the number of sample measurements for that site.

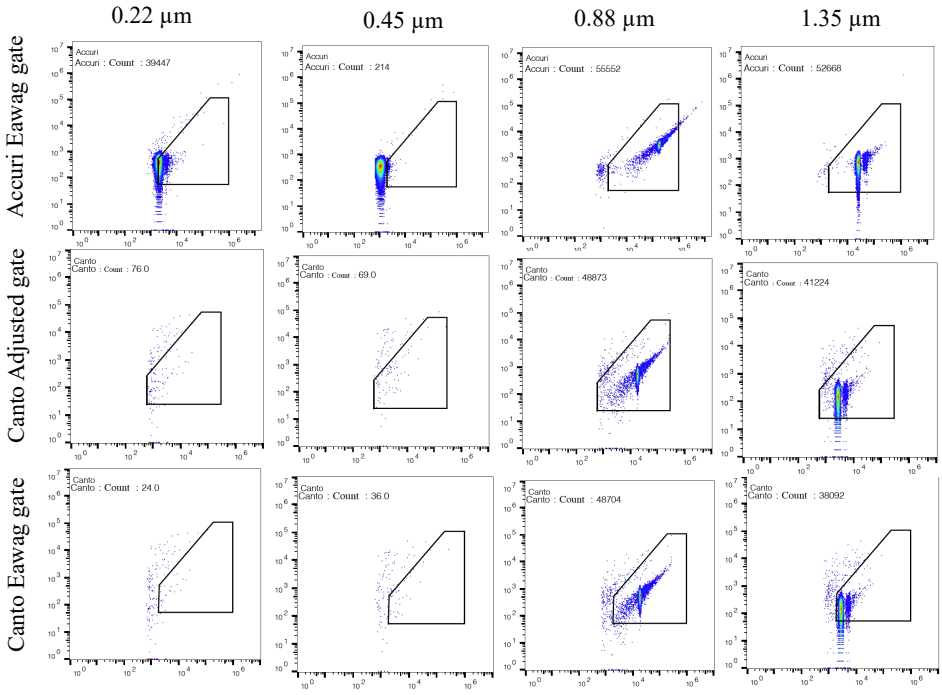

Figure A.6: Result of calibration bead experiments with beads of four different diameters measured on Accuri flow cytometer with Eawag gate and Canto flow cytometer with Eawag gate and adjusted gate. One technical replicate is shown for each particle size with green fluorescence on the y-axis and red fluorescence on the x-axis.

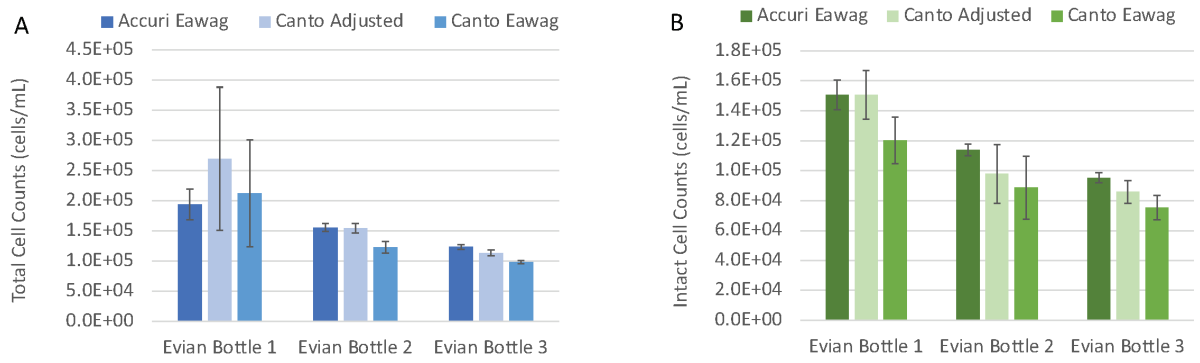

Figure A.7: Result of the same three bottles of Evian water measured on Accuri flow cytometer with Eawag gate and Canto flow cytometer with Eawag gate and adjusted gate. Accuri results are biological triplicates of geometric averages from technical triplicates and Canto results are biological duplicates of geometric averages from technical triplicates. Error bars represent spread associated with standard deviation of biological replicates. Data for total cell count assay (A) and intact cell count assay (B) are shown.

A.4 Author Contributions

- Lauren C. Kennedy: Experimental design, sampling, and lab work for systems A (2016 & 2018), B (2016 & 2018), C (2016), F (2018); data analysis; manuscript writing; manuscript editing
- Scott E. Miller: Experimental design, sampling, & lab work for systems A, B, C, D, E in 2016; manuscript editing
- Rose S. Kantor: Sampling and lab work for systems A and F in 2018; manuscript editing
- Kara L. Nelson: Experimental design, data analysis, manuscript writing, and manuscript editing

Appendix B

Supporting information for Chapter 3

No data shown.

Appendix C

Supporting information for Chapter 4

C.1 Supplemental Methods

Wastewater composite sample collection, continued

Immediately after collection at location K, wastewater was mixed and aliquoted in 1-L bottles that were frozen at -20°C. These samples were transported together on ice and processed within 48 hours, and biological triplicates were taken from each bottle, where biological replicates refer to wastewater subsamples. All location K samples were processed in triplicate. Samples were collected in 1-L bottles transported on ice within 48 hours of collection and then frozen at -80°C until processing. For location S, no samples had replication except 6/30 which was processed in triplicate. For location A, samples were processed in duplicate from 5/28/20 to 7/28/20 and with only one replicate from 8/4/20 to 9/9/20. For location N, no samples had biological replication. For location Q, no samples had replication except 7/1 which was processed in biological duplicate.

Wastewater Sample Processing via the 4S method, continued

Briefly, sodium chloride was added to 40-50 mL of wastewater to a final concentration of 4 M, Ethylenediaminetetraacetic acid was added to a final concentration of 1 mM, and the solution was buffered using 10mM tris(hydroxymethyl)aminomethane to pH 7.2. Samples were heated to 70°C for 45 minutes and prefiltered with a 5-μm PVDF filter using syringe filtration. The filtrate was mixed with 40 mL of 70% ethanol and vacuum filtered through a silica column (Zymo III-P), and the column was washed using 5 mL of wash buffer 1 and 10 mL of wash buffer 2. Genetic material was eluted from the column by adding 200 μL ZymoPURE elution buffer and heating to 50°C for 10 minutes, then centrifuging to collect the flowthrough. The eluent was stored in multiple tubes to minimize freeze-thaw at -80°C until qPCR.

Each extraction batch contained a negative control of 40 mL of phosphate buffered saline (PBS) solution, and each sample or control was spiked with 20 μL of a free RNA

control (SOC; stock solution of $1.33x10^9$ gene copies/μL) and 50 μL of a surrogate virus lysis/extraction control from the same bottle of Bovilis Coronavirus Calf Vaccine (Merck Animal Health, Merck & Co. Inc., Kenilworth, NJ, USA) resuspended in 20 mL of PBS to monitor recovery with and without lysis across batches. Because of challenges surrounding quantification of the surrogate spike without the influence of extraction efficiency [275], the controls in this study were used to assess consistency of extractions rather than recovery. Four representative samples were chosen from each location to assess SOC and BCoV recovery along with the batch PBS control, and Cts remained relatively consistent for SOC and varied considerably for BCoV. However, no signs that an extraction procedure failed were observed, and all samples were considered to pass this quality control screen.

RT-qPCR plate setup and controls, continued

To minimize qPCR contamination, sample processing and RT-qPCR plate assembly were performed in separate laboratories. Primers and probes were purchased as custom DNA oligos (Integrated DNA Technologies), except for the N1 assay (2019-nCoV CDC RUO Kit) and the Xeno assay (VetMAX™ Xeno^{TM} Internal Positive Control - VIC^{TM} Assay, ThermoFisher Scientific). Standard curves consisted of 10-fold serial dilutions of RNA standard from the same production batch of either synthetic RNA (Control 2- 102024, Twist Bioscience, San Francisco, CA) for the N1 assay, RNA from custom Ultramer RNA Oligonucleotides (Integrated DNA Technologies) for BCoV, geneBlocks DNA (Integrated DNA Technologies) for crAssphage, or RNA in-vitro transcribed from geneBlocks (Integrated DNA Technologies) with a HiScribe T7 Quick High Yield RNA Synthesis kit (New England Biolabs) for the SOC assay.

qPCR data processing

Raw Cq values were imported into a custom pipeline in python (v3.6.9) with key modules including Pandas (v1.1.5) and NumPy (v1.19.5). First, raw Cq values that did not amplify or that amplified below the limit of quantification were flagged. These Cq values were subbed with the Cq value corresponding to half the limit of detection (for N1) or half the bottom of the master standard curve (for all other assays) (Table C.5) so that unamplified values could be considered during outlier analysis. The N1 limit of detection (LoD) was calculated by analyzing all the RNA standard curves from the study as well as four additional triplicate standard curves that extended down to 0.3 gc/μL (Table C.8). The N1 LoD was set at 5 gc/rxn, at which point 67% of technical replicates were positive (Table C.8) The number of true unamplified values was also determined prior to substitution. For normalization purposes only, all samples that were below the detection limit for the N1 assay were divided by the upper quartile value for that biomarker within each location instead of the measured value, such that when N1 values below the detection limit were normalized, all values were equal. Next, outlier testing was performed using a two-sided Grubbs Test (alpha= 0.05; scikit-learn v0.22.post1). Raw Cq values that did not pass scikit-learn Grubbs test were

removed from further analysis. Next, Cq values were combined by calculating the average of the remaining values. Finally, the individual standard curve information was determined (Table C.4) for validation after outlier assessment, but Cq values were converted to quantities (gene copies per reaction) using the master standard curves (Table C.4). Individual standard curves ranged from 83.2% to 97.8% and R^2 ranged from 0.974 to 0.999 (Table C.4). NTCs only amplified for the SOC assay and they amplified far outside the range of the standard curve (Cq of the NTCs= 38 and Cq of the bottom of the standard curve = 29). qPCR quantities were converted to gene copies per mL using the weight-based volume of the wastewater samples and the elution volume after the 4S extraction. For samples with biological replicates (Table 4.1), the geometric mean and standard deviation of the biological replicates were calculated (SciPy v1.4.1) and used to plot points and error bars respectively.

Clinical testing and population data, continued

For daily new cases from locations S, K, A, and N, values below 11 new cases per day were masked by public health departments to maintain confidentiality of the contributing population and substituted at 5.5 cases for further analysis (Figure 4.3). For Location S, daily new case data (masked) and seven-day moving averages were provided (unmasked because all values were >11). For location K, daily new case data (masked) were provided, and seven-day moving averages of daily new cases were then calculated. Due to the low number of cases in locations A and N, most of the daily new case data were masked and are not shown. For location A, seven-day moving averages (masked) were provided and, for location N, fourteen-day moving averages (masked) were provided. These moving averages of new COVID-19 cases per day were divided by the sewershed population (daily per capita cases) (Table 4.1). Population data were provided by East Bay Municipal Utility District for locations S, A, and N. Population data for location K was provided by the Contra Costa County Public Health Department.

For San Quentin Prison (location Q), COVID-19 clinical data were obtained from the California Department of Corrections and Rehabilitation open data portal[1] (Table 4.1). These data included TotalConfirmed, defined as the cumulative number of patients with a positive COVID-19 result, and TotalActive, defined as the TotalConfirmed minus cases resolved due to death, release, or case resolution. A resolved case was defined on the open data portal as either 1. The case was closed as recovered or resolved, 2. The Public Health case surveillance system confirmed and documented that the patient was released from isolation in the past, and 3. The date the case was closed is in the past. The data provided correspond to the clinical reporting date. TotalConfirmed was used to calculate new cases reported each day. TotalActive was used to estimate the active cases on each day. Population and prison capacity data were found in population reports[2] and were divided by by population (estimated incidence and prevalence, respectively). No data were masked by the California Department

[1] https://data.ca.gov/dataset/cdcr-population-covid-19-tracking

[2] https://www.cdcr.ca.gov/research/population-reports-2/

of Corrections and Rehabilitation for location Q, but instances of 0 were subbed at half of 1 case for data analysis (to compare to masked data) and log-scale plotting (Figure 4.4).

C.2 Supplemental figures and tables

Table C.1: RT-qPCR reaction conditions for each assay. All reaction volumes were 20 μL.

reaction component	duplexed N1-Xeno (mM)	BCoV (mM)	SOC (mM)	crAss-phage (mM)
TaqMan Fast Virus 1-Step Master Mix	1x	1x	1x	1x
primer F	0.5	0.9	0.5	0.5
primer R	0.5	0.9	0.5	0.5
probe	0.125	0.25	0.125	0.125
Xeno assay	proprietary (0.8 μL/rxn)	-	-	-

Table C.2: RT-qPCR thermocycling conditions for SARS-CoV-2 N1, crAssphage, BCoV, and SOC assays.

reaction cycling step	temperature (°C)	time (minutes : seconds)
UNG incubation	25	2:00
RT step	50	15:00
polymearse activation	95	2:00
45 cycles	95	0:03
	55	0:30

Table C.3: qPCR assay information for the SARS-CoV-2 nucleocapsid N gene (N1), the bovine coronavirus transmembrane protein gene (BCoV), and crAssphage 056 (crAssphage)

gene target	type of sequence (length; accession)	sequence (5' -> 3')
SARS-CoV-2 N1	forward primer	GACCCCAAAATCAGCGAAAT
	reverse primer	TCTGGTTACTGCCAGTTGAATCTG
	probe	FAM-ACCCCGCATTACGTTTGGTGGACC- ZEN/IBFQ
	amplicon (72 bp; MN908947.3)	GACCCCAAAATCAGCGAAATGCACCCCGCATTACGT TTGGTGGACCCTCAGATTCAACTGGCAGTAACCAGA
VetMax^{TM} Xeno^{TM} internal positive control	forward primer	proprietary
	reverse primer	proprietary
	probe	proprietary
	amplicon	proprietary
BCoV	forward primer	CTGGAAGTTGGTGGAGTT
	reverse primer	ATTATCGGCCTAACATACATC
	probe	FAM-CCTTCATATCTATACACATCAAGTTGTT- ZEN/IBFQ
	amplicon (85 bp; AF39154)	CTGGAAGTTGGTGGAGTTTCAACCCAGAAA CAAACAACTTGATGTGTATAGATATGAAGGG AAGGATGTATGTTAGGCCGATAAT
crAssphage	forward primer 056F1	CAGAAGTACAAACTCCTAAAAAACGTAGAG
	reverse primer 056R1	GATGACCAATAAACAAGCCATTAGC
	probe 056P1	FAM-AATAACGATTTACGTGATGTAA-ZEN/IBFQ
	amplicon (126bp; MT006214.1)	CAGAAGTACAAACTCCTAAAAAACGTAGAGGTA GAGGTATTAATAACGATTTACGTGATGTAACTCG TAAAAAGTTTGATGAACATACTGATTGTAATAAAG CTAATGGCTTGTTTATTGGTCATC
SOC	forward primer	CCACCAAAGTGGGCGATAAA
	reverse primer	GGTGCCATTCGCCTCAATAA
	probe	FAM/TGGCGGTGAGGAAGTTTGGAAAGA/ZEN/IBFQ
	amplicon (89 bp, NA)	CCACCAAAGTGGGCGATAAAGGCAGCACCCGTTT ATTTGGCGGTGAGGAAGTTTGGAAAGATAGCCCG ATTATTGAGGCGAATGGCACC

Table C.4: All RT-qPCR plate-specific standard curves after outlier assessment for the N1 assay throughout the study.

plate id	linear dynamic range	slope	y-intercept	R^2	PCR efficiency	min Cq of NTC triplicates
87	6	-3.8	40.31	0.9928	0.832	negative
88	7	-3.4	39.21	0.9989	0.967	negative
92	7	-3.56	39.69	0.9921	0.91	negative
93	7	-3.42	40.47	0.9839	0.962	negative
94	7	-3.44	40.6	0.9968	0.954	negative
95	7	-3.42	38.91	0.9976	0.962	negative
96	7	-3.46	39.28	0.9992	0.945	negative
99	7	-3.54	40.09	0.9954	0.915	negative
100	7	-3.51	39.56	0.9944	0.927	negative
101	7	-3.57	40.49	0.9964	0.905	negative
102	7	-3.38	38.79	0.9919	0.978	negative
127	7	-3.65	40.35	0.993	0.879	negative

Table C.5: Master standard curve parameters (calculated after outlier assessment) and the values substituted for each assay for samples below the qPCR limit of detection.

target	slope	y-intercept	substitution for BLoD samples (gc/rxn, Cq)	min (gc/rxn; Cq)	max (gc/rxn; Cq)	PCR efficiency	R^2
N1	-3.48	39.78	2.5, 38.39	5, 37.35	1e+05, 22.4	0.94	0.986
SOC	-3.52	42.02	5000, 29.01	10000, 27.95	1e+10, 6.85	0.92	0.997
BCoV	-3.83	47.27	50, 40.76	100, 39.61	1e+08, 16.63	0.82	0.996
crAss-phage	-3.56	43.85	500, 34.24	1000, 33.17	1e+09, 11.81	0.91	0.996

Table C.6: Inhibition testing results from samples from locations Q, A,and N that had Xeno dCt> 2 after pre-screening.

sample location (date)	dilution factor	N1 mean quantity adjusted for dilution factor	N1 mean Ct	unamplified N1 replicates (%)	dCt N1 relative to 1x	expected dCt - actual dCt) N1 relative to 1x	dCt N1 relative to previous	expected dCt - actual dCt) N1 relative to previous	inhibited yes if subsequent dilution in previous column > 1	Xeno dCt relative to baseline (initial Xeno dCt)
Q 9/15/20	1*	-	-	100	-	-	-	-	-	1.62 (2.6)
	2	-	-	100	-	-	-	-	-	1.38
	5	-	-	100	-	-	-	-	-	0.76
	10	-	-	100	-	-	-	-	-	0.87
A 9/9/20	1	5.32	36.85	0	0	0	-	-	yes	2.58 (2.00)
	2	12.87	36.79	33	0.58	0.42	-0.06	1.06	yes	1.77
	5	26.34	36.96	33	0.75	1.55	0.17	1.13	yes	0.87
	10	81.24	36.22	0	-0.34	3.64	-0.74	1.74	-	0.48
A 9/9/20 rerun	1*	6.89	35.57	0	0	0	-	-	no	2.79 (2.00)
	2	6.40	36.62	0	1.05	-0.05	1.05	0.05	no	2.16
	4	10.73	37.10	0	1.53	0.47	0.48	0.82	no	1.63
	8	19.54	37.29	0	1.72	1.28	0.19	0.81	-	0.42
N 8/11/20	1	32.87	33.89	0	0	0	-	-	yes	1.52 (3.8)
	2*	111.73	33.18	0	-0.71	1.71	-0.71	1.71	no	1.98
	5	71.60	35.17	0	1.28	1.02	1.99	-0.69	no	0.47
	10	47.18	36.99	33	3.10	0.20	1.82	-0.82	-	0.73
N 9/1/20	1	5.67	37.02	0	0	0	-	-	yes	1.64 (2.1)
	2*	16.51	36.25	0	-0.77	1.77	-0.77	1.77	-	0.91
	5	-	-	66	-	-	-	-	-	0.85
	10	-	-	100	-	-	-	-	-	0.55

Table C.7: Inhibition testing results from samples from location S that had Xeno dCt> 2 relative to the baseline after the initial pre-screening.

sample location (date)	dilution factor	N1 mean quantity adjusted for dilution factor	N1 mean Ct	unamplified N1 replicates (%)	dCt N1 relative to 1x	expected dCt - actual dCt) N1 relative to 1x	dCt N1 relative to previous	expected dCt - actual dCt) N1 relative to previous	inhibited yes if subsequent dilution in previous column > 1	Xeno dCt relative to baseline (initial Xeno dCt)
S 6/2/20	1*	26.29	34.53	0	0	0	-	-	no	2.9 (3.4)
	2	32.45	35.26	33	0.72	0.28	0.72	0.28	no	1.89
	5	38.63	36.34	33	1.81	0.49	1.08	0.22	-	0.52
	10	-	-	66	-	-	-	-	-	0.43
S 6/9/20	1*	15.01	35.57	0	0	0	-	-	no	0.49 (2.8)
	2	31.46	35.78	0	0.21	0.79	0.21	0.79	no	0.34
	5	18.23	37.42	33	1.85	0.45	1.63	-0.33	-	0.43
	10	-	-	66	-	-	-	-	-	0.53
S 7/14/20	1*	42.68	33.56	0	0	0	-	-	no	1.5 (3.1)
	2	46.44	34.47	0	0.91	0.09	0.91	0.09	no	1.04
	5	43.04	35.98	0	2.42	-0.12	1.51	-0.21	no	0.88
	10	59.56	36.71	33	3.15	0.15	0.73	0.27	-	0.36
S 7/14/20 rerun	1	63.43	33.14	0	-	-	-	-	no	2.2 (3.1)
	2	70.92	34.01	0	0.87	0.13	0.87	0.13	no	1.46
	5	91.68	35.59	0	2.45	-0.15	1.58	-0.28	no	1.01
	10	105.94	35.89	0	2.75	0.55	0.30	0.70	-	0.55

Table C.8: Evidence for the qPCR limit of detection for the N1 assay which was chosen as 5 gene copies per reaction. This table includes all N1 standard curves run throughout the study and four additional extended standard curves with quantities below 5 gene copies per reaction. All standard curves were processed in triplicate.

standard curve quantity (gene copies per reaction)	fraction of positive replicates	total number of replicates
0.312	0.08	12
0.625	0.08	12
1.25	0.25	12
2.5	0.50	12
5	0.67	54
10	0.90	51
20	0.98	54
100	0.98	54
1000	1	54
10000	1	54
100000	0.98	54

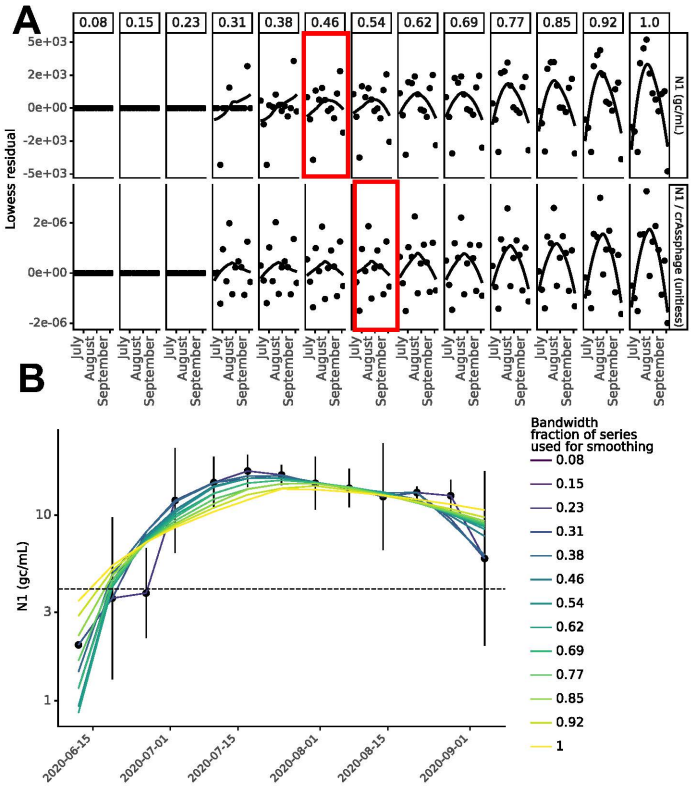

Figure C.1: (A) Residual plots for Lowess bandwidth parameter (α; column labels) determination for location K where the bandwidth parameter increases from inclusion of 1 data point (far left) to inclusion of all data points (far right) in each local regression for unnormalized N1 (top) and crAssphage-normalized N1 (bottom). The value of α that minimized the residual was selected (red boxes). (B) Visualization of how bandwidth parameter affected the Lowess trendline for location K.

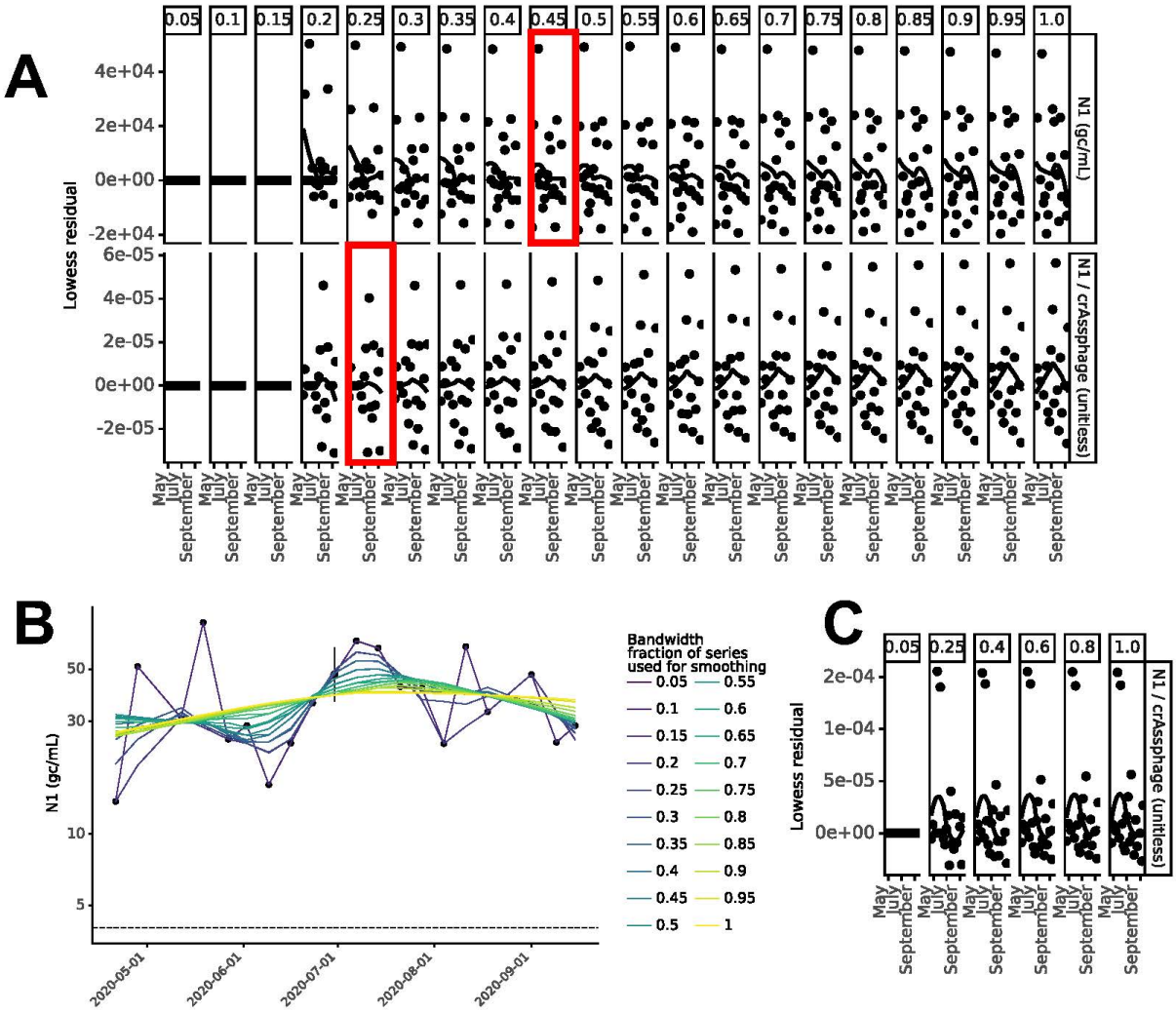

Figure C.2: (A) Residual plots for Lowess bandwidth parameter (α; column labels) determination for location S where the bandwidth parameter increases from inclusion of 1 data point (far left) to inclusion of all data points (far right) in each local regression for unnormalized N1 (top) and crAssphage-normalized N1 (bottom). The value of α that minimized the residual was selected (red boxes). (B) Visualization of how bandwidth parameter affected the Lowess trendline for location S. (C) The Lowess residual of two points for crAssphage-normalized N1 obscured trends and were removed for selection of the bandwidth parameter in part A.

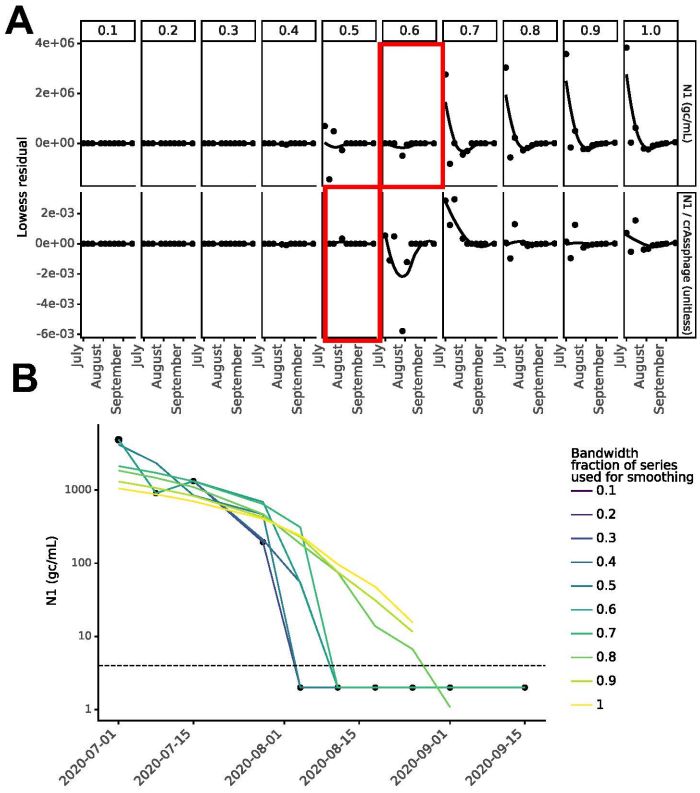

Figure C.3: (A) Residual plots for Lowess bandwidth parameter (α; column labels) determination for location Q where the bandwidth parameter increases from inclusion of 1 data point (far left) to inclusion of all data points (far right) in each local regression for unnormalized N1 (top) and crAssphage-normalized N1 (bottom). The value of α that minimized the residual was selected (red boxes). (B) Visualization of how bandwidth parameter affected the Lowess trendline for location Q.

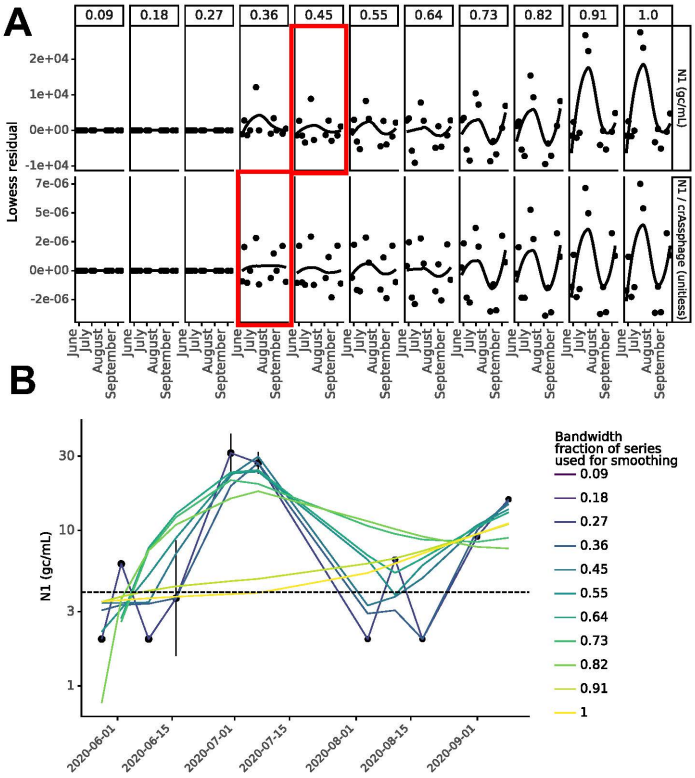

Figure C.4: (A) Residual plots for Lowess bandwidth parameter (α; column labels) determination for location A where the bandwidth parameter increases from inclusion of 1 data point (far left) to inclusion of all data points (far right) in each local regression for unnormalized N1 (top) and crAssphage-normalized N1 (bottom). The value of α that minimized the residual was selected (red boxes). (B) Visualization of how bandwidth parameter affected the Lowess trendline for location A.

Table C.9: By location, total number of biological replicates and detectable portion compared to the percent below the N1 limit of detection

location	total number of biological replicates	number of detectable biological replicates	percent of biological replicates below the limit of detection
A	17	10	41.2
K	39	32	17.9
N	18	14	22.2
Q	11	5	54.5
S	22	22	0
total	107	83	22.4

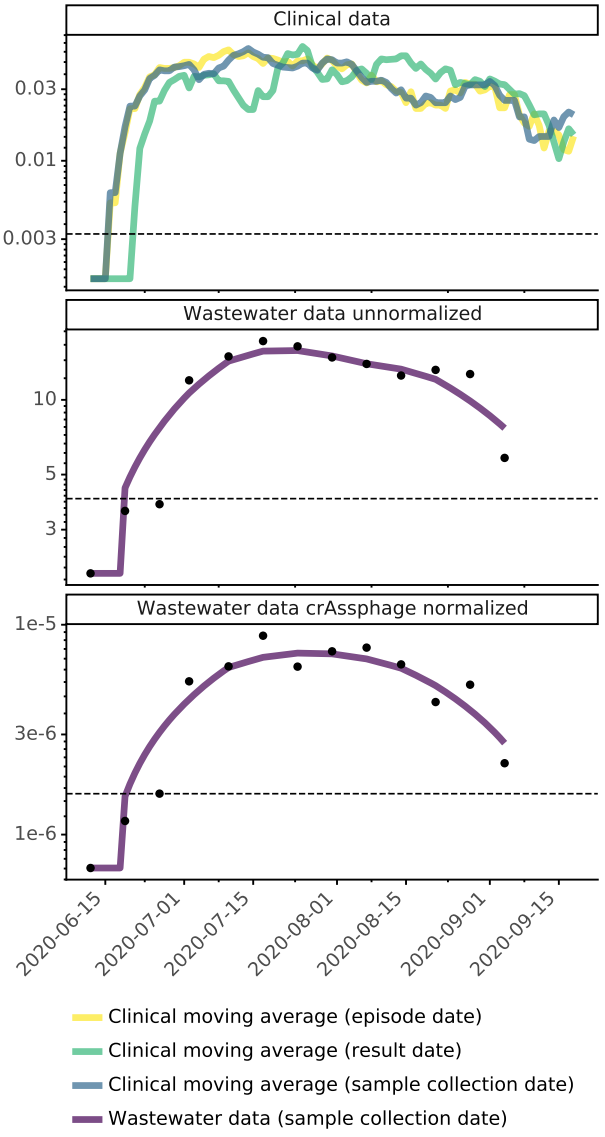

Figure C.5: Comparison of geocoded COVID-19 clinical testing results (top) to wastewater SARS-CoV-2 N1 signal (middle), and crAssphage-normalized signal (bottom) at location K from June to September 2020. COVID-19 clinical testing results are the seven-day moving averages of daily per capita cases with data aligned by episode date (yellow line), result date (green line), or sample collection date (blue line), with semi-transparency to visualize overlapping sections. Wastewater SARS-CoV-2 N1 signal is aligned by sample collection date (lines are the most optimal Lowess trendlines).

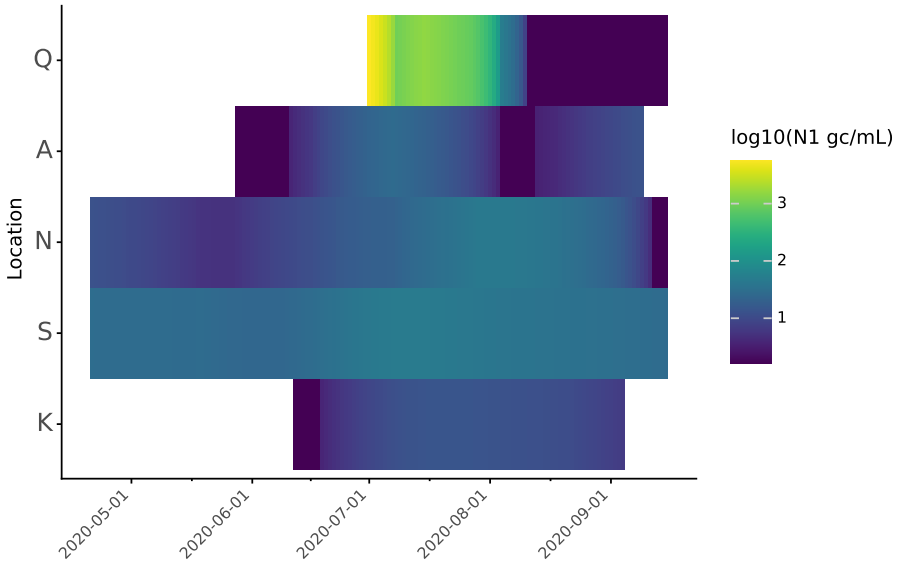

(a)

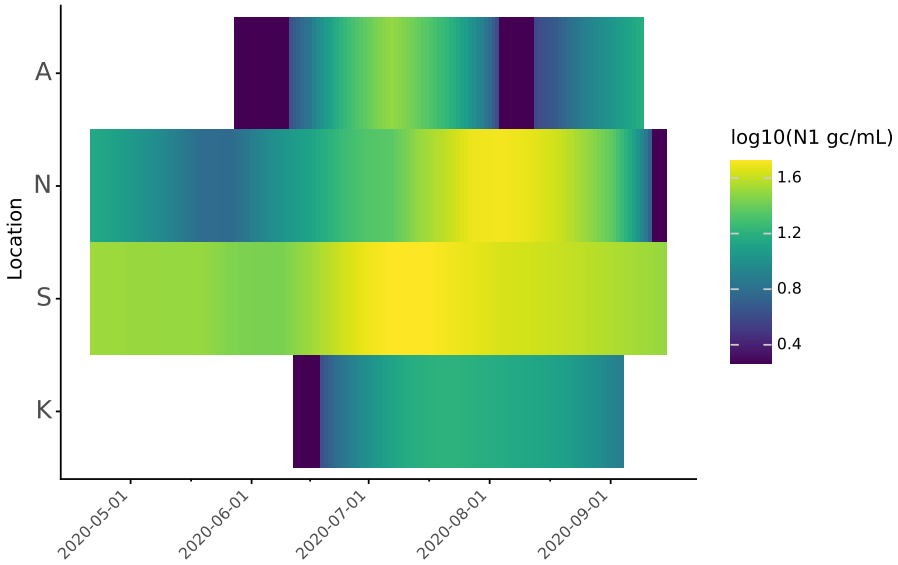

(b)

Figure C.6: Heatmap visualization of most optimal Lowess trendlines for SARS-CoV-2 N1 signal in wastewater by location (A) all locations (B) without location Q.

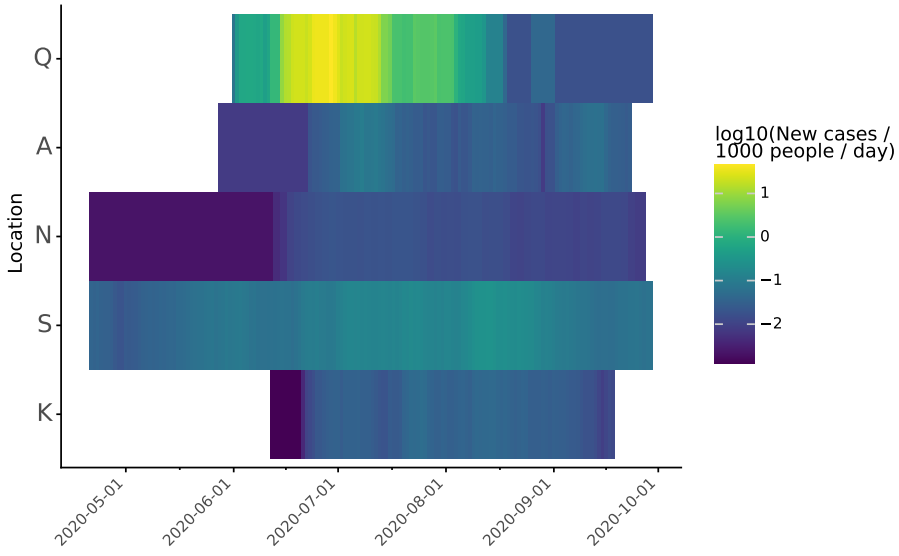

(a)

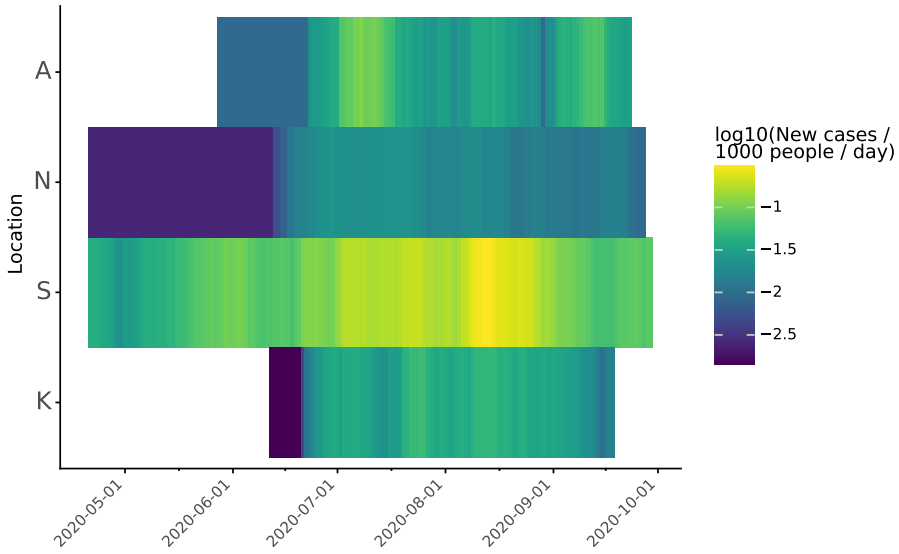

(b)

Figure C.7: Heatmap visualization of seven day moving average of COVID-19 daily per capita new cases by location (A) all locations (B) without location Q.

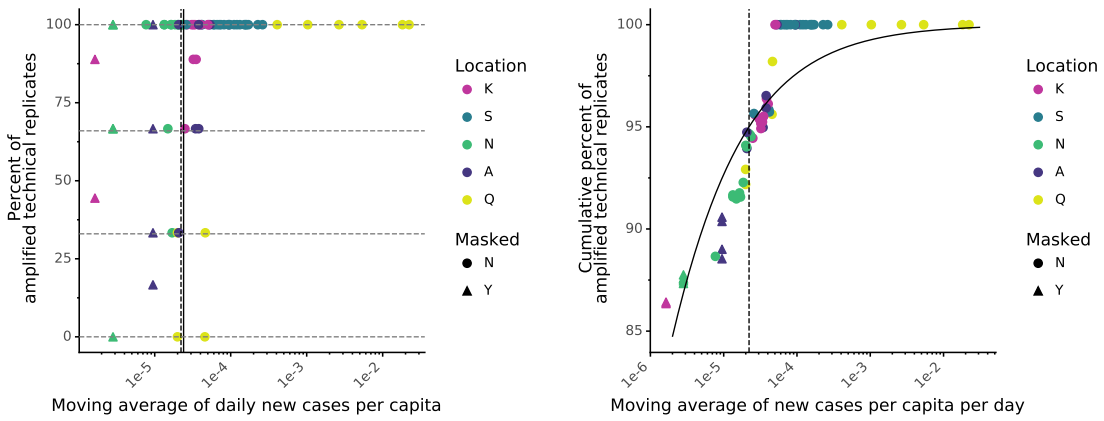

(a) (b)

Figure C.8: (A) The percent of amplified technical replicates for each value of the moving average of daily per capita cases (x-axis). Each biological replicate had three technical replicates, so the horizontal, dashed lines at 0%, 33%, 66%, and 100% show the range of values associated with each biological replicate that was associated with a unique x value. One or more biological replicates were associated with each moving average case value. The solid vertical line represents the estimated WBE clinical detection limit determined without masked data (2.4 cases in 100,000 people; Figure 4.5). (B) The cumulative percentage of amplified wastewater technical replicates was calculated by ranking the moving averages of daily per capita cases (including masked clinical case values; x-axis) from highest to lowest and calculating the fraction of qPCR replicates that amplified cumulatively (y-axis) for each value of x (same methodology as in Figure 4.5). In both plots, the dashed line represents the daily new cases per capita value above which 95% of wastewater technical replicates amplified (including masked values; 2.2 cases in 100,000 people), and shapes denote which daily per capita case values were masked.

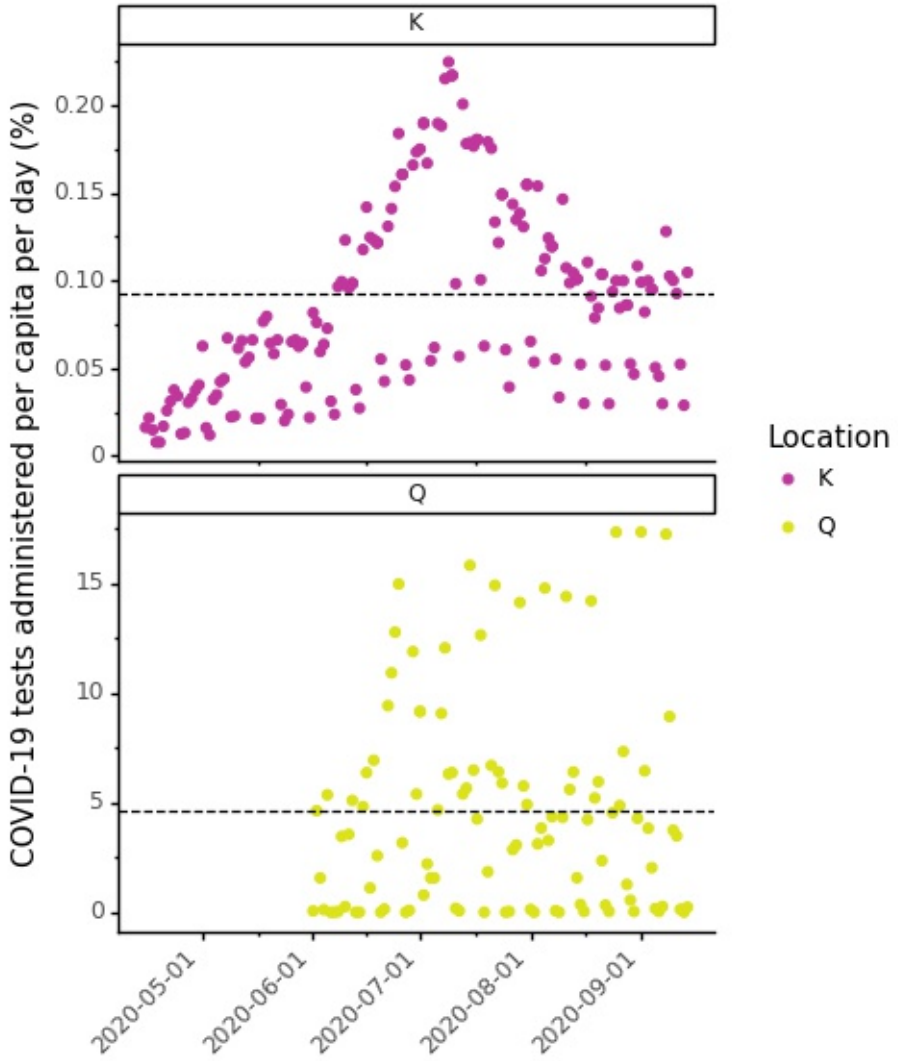

Figure C.9: COVID-19 tests administered per capita (%) during the sampling period for two locations: K and Q, where dashed lines are plotted at the mean percentage of the population tested for the sampling period.

C.3 Author Contributions

The following contributions apply to the full manuscript [267].

- Lauren C. Kennedy: conceptualization; data analysis; conducted half of the qPCR labwork; original manuscript writing

- Hannah D. Greenwald: conceptualization; data analysis; conducted half of the qPCR labwork; original manuscript writing
- Adrian Hinkle: conducted sample extractions, manuscript editing
- Vinson B. Fan: contributed to assay development (18S rRNA assay, optimization of RT-qPCR)
- Oscar N. Whitney: contributed to assay development (18S rRNA and crAssphage assays, optimization of extractions); manuscript editing
- Sasha Harris-Lovett: sample and data collection coordination with utilities, public health departments, and researchers; manuscript editing
- Alexander Crits-Christoph: contributed to assay development (optimization of extractions); manuscript editing
- Avi I. Flamholz: contributed to assay development (optimization of RT-qPCR); manuscript editing
- Basem Al-Shayeb: contributed to assay development (optimization of extractions)
- Lauren D. Liao: contributed to qPCR pipeline code development
- Dan Frost: coordinated wastewater sample and physicochemical data collection
- Daniel Brown: coordinated clinical data collection
- Chris Lynch: coordinated clinical data collection
- Jason Dow: coordinated wastewater sample and physicochemical data collection
- Mark Koekemoer: coordinated wastewater sample and physicochemical data collection
- Eileen White: coordinated wastewater sample and physicochemical data collection
- Alicia Chakrabati: coordinated wastewater sample and physicochemical data collection
- Matt Byers: coordinated clinical data collection
- Payal Sarkar: coordinated wastewater sample and physicochemical data collection
- Rose S. Kantor: conceptualization, data analysis, manuscript writing, and manuscript editing
- Kara L. Nelson: conceptualization, data analysis, manuscript writing, and manuscript editing